FINAL PROGRESS REPORT

Grant No.: N00014-95-1-1310

PRINCIPAL INVESTIGATOR: Jeffrey S. Berman, M.D.

INSTITUTION: Pulmonary Center, Boston University School of Medicine

GRANT TITLE: Regulation through CD4 of Adhesion Molecule Function by Lymphocyte Chemoattractant Factor (LCF/Interleukin-16)

AWARD PERIOD: 30 March 1996 - 30 March 1999

OBJECTIVE: The objective of this project is to characterize the effects of interleukin-16 (IL-16) on the adhesion of blood T cells to matrix proteins and to endothelial cells (EC), and determine the mechanisms behind this regulation.

APPROACH: The adhesion of T cells or T cell lines to matrix proteins or EC is assessed using a fluorescence-based assay. Recombinant IL-16 is produced and purified using standard methods. The effects of IL-16 on integrin subunit function is detected by the use of blocking antibodies. The role of CD4 is to be dissected using a murine T cell hybridoma transfected with wild type human CD4 or various CD4 mutants or chimeras, and by the use of inhibitors of signaling pathways. The interaction of IL-16 with heparin sulfate proteoglycans is assessed by binding to heparin, and by heparin- or antibody-inhibitable binding to endothelial cells (EC).

ACCOMPLISHMENTS : 1. IL-16 induced the adhesion of primary blood T cells to fibronectin. We have submitted for publication our previous findings showing the induction by IL-16 of primary blood T-cell adhesion to fibronectin, and the dependence of this adhesion on the activation of beta-1 integrin function. This last was shown using blocking studies using monoclonal antibodies to the alpha4 and alpha5 beta-1 integrins (these antibodies blocked all baseline and induced adhesion), and the demonstration that the cell surface levels of beta-1 integrins was not increased by short term treatment with IL-16. This effect was time dependent and decayed over two to four hours. This effect was also seen with the BY parent T cell line, a murine T cell hybridoma which expresses murine CD4 and which is sensitive to the migratory and the adhesive effects of IL-16, and which appears now to be the best experimental model of T cell signaling in response to IL-16. This cell line and a series of CD4 mutant transfected cell lines will be used to determine the signaling pathways used by IL-16 to induce adhesion. Initial experiments suggest that IL-16 induced adhesion is sensitive to the PI3 kinase inhibitor Wortmannin. We hypothesize that IL-16 may employ this signaling pathway to alter integrin function as has been previously hypothesized for other such stimuli.

2. We have performed similar experiments looking at the induction of adhesion of T cell adhesion to the RGD containing cytokine, osteopontin. This cytokine acts via numerous receptors, including the aVb3 integrin (the vitronectin receptor) and CD44. Using techniques developed for this grant, we are also looking at heparin and endothelial

REPORT DOCUMENTATION PAGE

Form Approved
OMB No. 0704-0188

1. AGENCY USE ONLY (Leave blank)	2. REPORT DATE	3. REPORT TYPE AND DATES COVERED
	9/01/95-6/30/99	Final Report

4. TITLE AND SUBTITLE

~~Cell Adhesion Molecule Research~~
See Doc.

5. FUNDING NUMBERS

G-
N00014-95-1-1310

6. AUTHOR(S)

Asthma and Allergy Foundation of America, Inc.

7. PERFORMING ORGANIZATION NAME(S) AND ADDRESS(ES)

Asthma and Allergy Foundation of America, Inc.
1233 20th Street, N.W., Suite 402
Washington, D.C. 20036

8. PERFORMING ORGANIZATION REPORT NUMBER

9. SPONSORING/MONITORING AGENCY NAME(S) AND ADDRESS(ES)

Office of Naval Research
800 North Quincy Street
Arlington, VA 22217-5660

10. SPONSORING/MONITORING AGENCY REPORT NUMBER

11. SUPPLEMENTARY NOTES

12a. DISTRIBUTION/AVAILABILITY STATEMENT

Distribution Unlimited

12b. DISTRIBUTION CODE

13. ABSTRACT (Maximum 200 words)

Critical progress has been made in the identification and characterization of cells and mediators involved in allergic inflammation. Accumulating evidence supports the importance of cell adhesion molecule expression as an initiating process in tissue inflammation. Despite progress made to date, much is still unknown about the exact mechanisms responsible for this inflammatory response. Scientists have been working to understand the selective cell recruitment operating in allergic disease with the hope of discovering therapeutic intervention strategies that will prevent the accumulation of unwanted cells in inflamed airways. Research has been directed at developing various approaches to generate specific antagonists. Some approaches under study interupt airway inflammation in its early stages during leukocyte-endothelial interactions. Other approaches inhibit cell recruitment at the endothelial wall. Many studies have been done, both in vivo and in vitro, and the advances that have been made suggest that these therapeutic interventions may be the keys to controlling and, possibly, curing asthma and allergic reactions.

14. SUBJECT TERMS

cell adhesion, allergic rhinitis, atopic allergic conditions, cell biology

15. NUMBER OF PAGES

16. PRICE CODE

17. SECURITY CLASSIFICATION OF REPORT	18. SECURITY CLASSIFICATION OF THIS PAGE	19. SECURITY CLASSIFICATION OF ABSTRACT	20. LIMITATION OF ABSTRACT
U	U	U	UL

cell binding of this novel cytokine which contains a consensus heparin binding site near the RGD sequence. In previous studies we had shown that osteopontin is produced early in numerous inflammatory lung diseases, by both mononuclear cells and by epithelial cells. Osteopontin is chemotactic for monocytes/macrophages and T cells, and co-stimulates the proliferation of T cells. Osteopontin also co-stimulates the production of cytokines by T cells, especially interferon-gamma and IL-12. We have not yet examined the effects of Osteopontin on IL-16 synthesis or release. The presence of the aVb3 integrin on a subset of osteopontin-responsive T cells is also a novel finding, and we are characterizing this subset of cells.

3. We have directly demonstrated binding of rIL-16 to heparin using heparin-sepharose or control columns and also to a heparin-inhibitable site on resting and activated endothelial cells. These are likely Heparan sulfate proteoglycans, as previously postulated. We also found that heparin inhibited the chemotactic function of IL-16 in a dose dependent manner. Unlike IP-10 and some other heparin binding chemokines, IL-16 did not appear to have either a proliferative or antiproliferative effect on endothelial or epithelial cells. We are proceding in two directions. First, we will determine if antibodies to other possible binding sites (for example, CD44) will inhibit endothelial cell binding. Of note, osteopontin is a putative CD44 ligand, and we are examining the role of CD44-osteopontin interactions on IL-16 binding. Second, we plan to determine the molecular interactions responsible for heparin binding. Using a model of the predicted primary structure of human IL-16, we found that the predicted isoelectric point was 5.2, much lower than the observed pI of 9.2-9.4. This suggests that positively charged amino acids (7 lysines and 4 arginines) which make up only 11/121 of the primary sequence contribute relatively highly to migratory behavior in solution isoelectric focusing. Interestingly, there is a stretch of four negatively charged residues (including the sequence RRK) in a region predicted to be highly hydrophilic and thus likely external in aqueous solution and available to interact with heparin. This stretch, from aa 105-111 is in the C-terminus, but does not appear to be in an alpha helical region, as has been found in the heparin binding C-terminal regions of some alpha chemokines. We have contructed deletion mutants, deleting part or all of this C-terminal sequence. These mutants were developed and expressed in our laboratory by our collaborators Hardy Kornfeld and John Nicoll. Finally, we have determined that at least some of the adhesion of recombinant IL-16 to endothelial cells and to the heparin matrix was due to processing artifacts caused by the processing of the recombinant protein, including the histidine tag. Because of these findings, we are re-engineering the synthesis and processing of IL-16 in this laboratory before finishing these studies. It is of interest that several publications from other laboratories which reported heparin and/or endothelial cell binding used histidine tagged recombinant molecules.

SIGNIFICANCE: IL-16 is a novel cytokine released early in antigen induced asthma, and produced by both T cells and epithelial cells. It is a potent chemoattractant for CD4+ T cells, monocytes and eosinophils. These experiments answer important questions about the basic biology of IL-16 and its mechanism of action.

PUBLICATIONS REPORTS AND ABSTRACTS:

1. Chupp GL, Kim S, Kornfeld H, Cruikshank WW, Wright EA, Berman JS. The

tissue and T cell distribution of precursor and mature Interleukin-16. J. Immunol. 161:3114-3119, 1998. .

2. Nau GJ, Guilfoile P, Chupp GL, Berman JS, Kim SJ, Kornfeld H, Young RA. A chemoattractant cytokine associated with granulomas in tuberculosis and silicosis. Proc Nat. Acad. Sci. 94:6114, 1997.

3. O'Regan A, Chupp GL, Lowry JA, Goetschkes M, Mulligan N, Berman JS. Osteopontin is associated with T cells in sarcoid granulomas and has cytokine-like properties that are modulated by thrombin cleavage. J Immunol, 1999; 162:1024-30.

4. Saukkonen JJ, Tantri A, Berman JS. Co-stimulation of CD28- T cells through CD3 and beta-1 integrins induces a limited Th1-cytokine response. Scand. J. Immunol. 1999, 50:145-150..

5. Nau GJ, Liaw L, Chupp GL, Berman JS, Hogan BLM, Young RA. Impaired host resistance against mycobacteria in mice lacking osteopontin. Infect. Immun. 1999; 67:4223-4230.

6. Wright EA, Lowry J, Berman JS. IL-16 is a heparin-binding cytokine and mediates increased adhesion of blood T cells to endothelial cells. Submitted.

7. O'Regan. A, Hayden J, Berman JS. Osteopontin induces IL-12 production by activating T cells to produce interferon-gamma and express CD40 ligand. Submitted.

8. O'Regan AW, Wright EA, Berman JS. Osteopontin, a novel early T cell associated cytokine in granulomatous disease, augments a Th1 cytokine response. Am J Respir Crit Care Med. 1999; 159:A214. (Oral presentation).

Tissue and T Cell Distribution of Precursor and Mature IL-16[1]

Geoffrey L. Chupp,[2]*† Eric A. Wright,* David Wu,* Margaret Vallen-Mashikian,* William W. Cruikshank,* David M. Center,* Hardy Kornfeld,* and Jeffrey S. Berman*‡

IL-16 is a novel cytokine, which is chemoattractant for $CD4^+$ T cells, macrophages, and eosinophils. Recently, it was reported that IL-16 is synthesized as an approximately 80-kDa precursor molecule, pro-IL-16. Since little is known about the processing and tissue distribution of IL-16 and pro-IL-16, we investigated the distribution of IL-16 mRNA and protein in human lymphoid tissue. Northern blotting identified IL-16 mRNA predominantly in normal lymphoid organs, including PBMC, spleen, and thymus. Immunohistochemistry of human lymph node localized IL-16 protein to lymphocyte cytoplasm within T cell zones and occasionally in lymphocytes in B cell zones. Flow cytometric detection of intracellular IL-16 showed that >70% of $CD4^+$ and $CD8^+$ T cells constitutively expressed IL-16 protein. Western blot analysis of PBMC revealed nearly all of this protein to be approximately 80-kDa pro-IL-16 in unstimulated PBMC, and upon cell activation, the amino terminus of pro-IL-16 is processed into multiple fragments. These results show that pro-IL-16 is widely and constitutively expressed and suggest that the amino terminus of the protein can be processed upon cell activation. *The Journal of Immunology,* **1998, 161: 3114–3119.**

Interleukin-16 is a multifunctional cytokine that induces its effects following interaction with CD4 (1–4). IL-16 is a chemotactic factor for $CD4^+$ T cells (5), monocytes (6), and eosinophils (7) and has been shown to up-regulate IL-2R (CD25) (1, 6) and induce the transient loss of responsiveness via the TCR (8, 9). Since these properties suggest that IL-16 may play an important role in migration and activation of $CD4^+$ T cells in vivo, we and others have attempted to identify the role of IL-16 in diseases characterized by $CD4^+$ T cell involvement, such as multiple sclerosis (10, 11), asthma (12–14), and AIDS (15–17). Most recently, IL-16 has been shown to inhibit HIV-1 replication by inuction of a repressor element that binds to the core enhancer of the HIV-1 long terminal repeat (16), but not inhibit viral entry (18).

Bioactivity ascribed to IL-16 was first identified in supernatants from Con A-stimulated PBMC that migrated at about 14 kDa in SDS-PAGE (5, 19). The full-length IL-16 cDNA, however, appears to code for a 631-amino acid protein with a predicted molecular mass of 67 kDa; the recombinant product of this cDNA migrated in SDS-PAGE near 80 kDa (20). Western blot analysis of the natural protein with Abs against bioactive 14-kDa IL-16 identified an approximately 80-kDa band in PBMC, which confirmed the existence of an approximately 80-kDa protein and suggested that IL-16 is first synthesized as a precursor, pro-IL-16[3] (20, 21). Processing appears to be by cleavage at aspartic acid residue 510, resulting in the secretion of a 121-amino acid C-terminal peptide, IL-16, which autoaggregates to form bioactive multimers (1, 19, 20).

Little is known about the expression and processing of pro-IL-16, however, work with T cell subsets suggests that pro-IL-16 processing may differ among cell types. IL-16 bioactivity is retrievable from unstimulated $CD8^+$ T cell lysates, and release of bioactivity is induced within 4 to 6 h following histamine or serotonin stimulation, indicating that bioactive IL-16 is constitutively expressed in $CD8^+$ T cells (22, 23). In contrast, $CD4^+$ T cells do not constitutively express or secrete IL-16 chemoattractant activity under these conditions (22, 24), but have been shown to constitutively express IL-16 mRNA. This discordance between $CD4^+$ and $CD8^+$ T cells would be explainable in part by the existence of a biologically inactive form of IL-16, possibly pro-IL-16 (22).

Given the potentially important role this cytokine plays in disease, defining the tissue and cellular distribution of IL-16 will advance the understanding of the factors governing its synthesis, processing, and secretion. In the current study, we sought to determine the tissue and cellular distribution of pro-IL-16 in human T cells. Widespread expression of pro-IL-16 was identified in lymphoid tissues and circulating lymphocytes by Northern blot analysis and immunohistochemistry. Using flow cytometry and intracytoplasmic staining of PBMC and Western analysis of T cell lysates, we characterized the expression of IL-16 in circulating lymphocytes, differentiated pro- from mature IL-16, and assessed the effect of cell activation on the expression of pro-IL-16.

Materials and Methods

Reagents

Recombinant IL-16 was generated as previously described (1). Briefly, a cDNA fragment corresponding to the IL-16 ORF plus nine additional NH4-terminal amino acids (GenBank accession no. M90391, nucleotides 787-1130) was ligated into the *Escherichia coli* expression vector pET-16b for the generation of a rIL-16-polyhistidine fusion protein that was purified by metal chelation chromatography. For the generation of Abs, the fusion

*Pulmonary Center, Boston University School of Medicine, Boston, MA 02118; †Pulmonary and Critical Care Medicine, Yale University School of Medicine, New Haven, CT 06520; and ‡Pulmonary and Critical Care Section, Boston Veterans Administration Medical Center, Boston, MA 02130

Received for publication September 18, 1997. Accepted for publication May 13, 1998.

The costs of publication of this article were defrayed in part by the payment of page charges. This article must therefore be hereby marked *advertisement* in accordance with 18 U.S.C. Section 1734 solely to indicate this fact.

[1] This work was supported in part by Grants HLP5056386, Specialized Center of Research in Pulmonary Fibrosis (to J.S.B. and D.M.C.), HL32802 (to D.M.C.), AI37368 (to W.W.C.), and a grant from the Asthma and Allergy Foundation of America (to J.S.B.). During this work G.L.C. received support from an American Lung Association Research Training Fellowship and a National Institutes of Health National Research Service Award training grant.

[2] Address correspondence and reprint requests to Dr. Geoffrey L. Chupp, Pulmonary and Critical Care Medicine, Yale University School of Medicine, 333 Cedar St., LCI 105, P.O. Box 208057, New Haven, CT 06520-8057. E-mail address: geoffrey.chupp@yale.edu

[3] Abbreviations used in this paper: pro-IL-16, approximately 80-kDa precursor IL-16; NWNT, nonadherent T cells.

0022-1767/98/$02.00

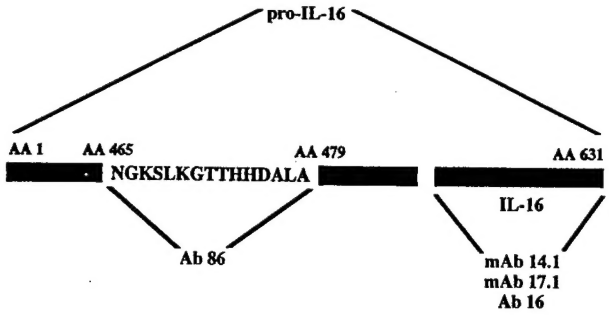

FIGURE 1. Structure and Ab recognition and current understanding of the IL-16 molecule. IL-16 is synthesized as a 631-amino acid precursor (pro-IL-16), and the secreted fragment (IL-16) autoaggregates to form bioactive multimers. mAbs 17.1, 14.1, and Ab 16 detect the secreted portion of IL-16, while Ab 86 detects a 15-amino acid peptide sequence in pro-IL-16.

protein was cleaved with factor Xa to remove the polyhistidine tag. Recombinant IL-16 was resuspended in PBS for use in blocking studies or, in the case of Western blotting, diluted SDS sample buffer, boiled for 5 min, and stored at −20°C. In vitro translated ^{35}S-labeled pro-IL-16 (derived from the full-length IL-16 cDNA, GenBank accession no. 90391, encoding a 631-amino acid protein) was synthesized using a rabbit reticulocyte lysate kit (Promega).

Antibodies

Rabbit polyclonal anti-pro-IL-16 Ab 86 was prepared by immunizing rabbits with the synthetic peptide 86 (5′-NGKSLKGTTHHDALA-3′). This peptide corresponds to amino acids 465 to 479 of the pro-IL-16 sequence, but is not included in mature IL-16 (Fig. 1). Sequence comparison of this 15-amino acid peptide against GenBank, EMBL, and PIR databases showed no homology with any known protein. Rabbit polyclonal anti-IL-16 Ab 16 was prepared from rIL-16-immunized rabbit sera as previously described (1). Murine anti-IL-16 mAbs 14.1 (isotype IgG2a, κ) and 17.1 (isotype IgG1, κ) were generated by Agmed (New Bedford, MA) and were screened based on their ability to specifically block bioactivity in vitro and recognize rIL-16 by Western blotting. All Abs were purified using protein A as previously described (1). FITC-conjugated mAb 17.1 was prepared using a FluoReporter kit (Molecular Probes, Eugene, OR) for intracellular cytokine staining. Isotype control mAb were purchased from BioSource (Camarillo, CA), PharMingen (San Diego, CA), or Zymed (San Francisco, CA), and anti-CD3 mAb was obtained from PharMingen. Anti-mouse and rabbit horseradish peroxidase-conjugated Ab for Western blots were purchased from Pierce (Rockford, IL).

Cell preparation

Blood was drawn from normal volunteers, aged 18 to 35 yr, into heparinized (100 U/ml) syringes. The blood was sedimented for 1 h at 37°C, and the leukocyte-rich plasma was aspirated, washed, pelleted, and resuspended in medium 199 plus 0.4% BSA. This suspension was layered on Ficoll-Hypaque cushions and centrifuged at 500 × *g* for 45 min. The subsequent PBMC-rich layers were aspirated and washed with medium three times and used or passed over nylon wool to acquire nonadherent T cells (NWNT). Pure $CD4^+$ or $CD8^+$ T cells were prepared by negative selection as previously described (22). Briefly, NWNT were incubated with 5 μg/1×10^6 cells with murine anti-human CD4 or CD8 mAb for 30 min at 4°C. Magnetic beads (BioMag, Advanced Magnetics, Cambridge, MA) conjugated with goat anti-mouse IgG were added for 30 min at 4°C, a magnet was taped to the bottom of the flask, and nonadherent cells were collected. This method routinely resulted in cell populations 95 to 98% depleted of labeled cells.

Northern blot analysis

A commercial multiple tissue Northern blot (Human MTN Blot II, Clontech, Palo Alto, CA) consisting of 2 μg poly(A)$^+$ RNA/lane from specific tissues transferred from a formaldehyde/1.2% agarose gel onto a positively charged nylon membrane was probed with a ^{32}P-labeled fragment of the human IL-16 cDNA corresponding to the C-terminal 393 bp of the coding sequence (1). The membrane was treated for 1 h with a prehybridization solution (QuikHybe, Stratagene, La Jolla, CA) containing 10 mg/ml salmon sperm DNA and subsequently hybridized with ^{32}P-labeled cDNA probe overnight at 68°C. After hybridization, the blot was washed twice at low stringency conditions of 2× SSC (300 mM NaCl, 30 mM sodium citrate, 0.5% sodium pyrophosphate, and 1% sodium lauryl sarkosine) at room temperature, followed by a wash at high stringency of 0.1× SSC at 60°C. Hybridization was visualized by autoradiography.

Immunohistochemistry

Two human lymph nodes acquired from excess tissue resected during surgical procedures and found to be normal reactive lymphoid tissue were embedded in optimal cutting temperature compound and snap-frozen at −70°C. Sections were fixed in cold methanol for 5 min and then washed with PBS. Immunohistochemistry was performed with a Vectastain ABC kit according to the manufacture's protocol (Vector Laboratories, Burlingame, CA). mAb 14.1 or isotype control Ab were diluted to identical concentrations in PBS, pipetted onto sections, and incubated overnight at 4°C. Secondary Abs were labeled with biotin, and detection was performed with a strepavidin-horseradish peroxidase conjugate and diaminobenzidine substrate. Slides were counterstained with hematoxylin, dehydrated in graded ethanol solutions, equilibrated with xylene, and coverslipped. Representative sections were photographed with Kodak Ektachrome 60T (Eastman Kodak, Rochester, NY). Images were prepared with Adobe Photoshop (Mountain View, CA).

Intracellular IL-16 staining and flow cytometry

Intracellular staining was accomplished using a protocol available from PharMingen based on work by Sander and colleagues (25, 26). Briefly, 10^6 PBMC were suspended in filtered staining buffer (PBS, 1% heat-inactivated FCS, and 0.1% (w/v) sodium azide, pH 7.4–7.5) at 2×10^6 cells/ml and incubated with phycoerythrin-conjugated Ab to the desired surface Ag for 30 min. The cells were washed once with staining buffer and centrifuged. The resulting pellet was resuspended in 100 μl of 4% paraformaldehyde and PBS, pH 7.4, for 20 min. After washing with staining buffer and centrifugation, the cells were resuspended in 50 μl of permeabilization buffer consisting of staining buffer and 0.1% saponin (w/v) and incubated with 0.3 μg of FITC-conjugated anti-IL-16 mAb 17.1 or isotype control for 30 min. The cells were then washed once with permeabilization buffer to remove unbound intracellular Ab, centrifuged, resuspended in 10% buffered formalin, and analyzed by flow cytometry using a FACScan (Becton Dickinson, Mountain View, CA). Analysis of 10,000 events within the lymphocyte gate was performed using LYSYS software (Becton Dickinson) and Microsoft Excel (Seattle, WA).

Surface staining control and blocking studies

To control for the possibility of anti-IL-16 mAb binding to the cell surface, cells were suspended as described above in staining buffer, incubated with FITC-conjugated mAb 17.1 or isotype control for 30 min, washed, fixed, and analyzed by FACS. Blocking with rIL-16 was accomplished by preincubating FITC-conjugated mAb17.1 or isotype control with 0.3 μg of rIL-16 for 30 min at 4°C. From this solution 0.3 μg of Ab was added to PBMC suspended in permeabilization buffer as described above. After washing with permeabilization buffer, the pellet was resuspended in buffered formalin and analyzed by FACS as described above.

Protein gel electrophoresis and Western blot analysis

Cell preparations prepared as described above were centrifuged at 250 × *g*, resuspended in 2× SDS sample buffer, boiled for 5 min, and stored at −20°C. Analysis by SDS-PAGE was performed with 3% stacking and 10% polyacrylamide gels according to the method of Laemmli. Western blotting was performed using standard protocols. Detection of specifically bound Ab was performed using a Super Signal detection kit (Pierce), or ^{125}I-labeled protein A.

Stimulation of T cell subsets with immobilized anti-CD3

T-25 tissue culture flasks (Costar) were precoated with anti-CD3 mAb at 1 μg/ml for 2 h at 37°C. After washing with sterile PBS, $CD4^+$ or $CD8^+$ T cells at 2×10^6/ml in medium 199/0.4% BSA were plated onto anti-CD3 or uncoated flasks and incubated at 37°C. After 6 and 24 h, cells were harvested and centrifuged, and the cell pellets were diluted in 2× SDS sample buffer.

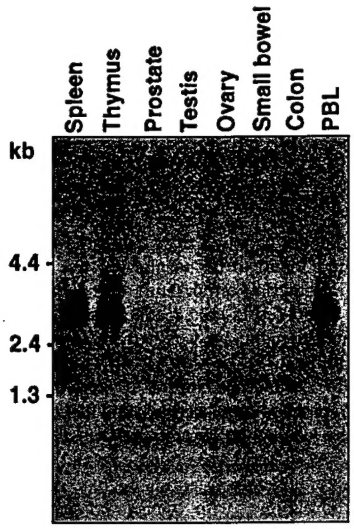

FIGURE 2. Tissue expression of IL-16 mRNA. A multiple tissue Northern blot consisting of 2 μg poly(A)$^+$ RNA/lane from human spleen, thymus, prostate, testis, ovary, small intestine, colon, and PBL was hybridized was a ^{32}P-labeled fragment of the human IL-16 cDNA. A single band of approximately 2.8 kb is present in the lanes of lymphoid tissues.

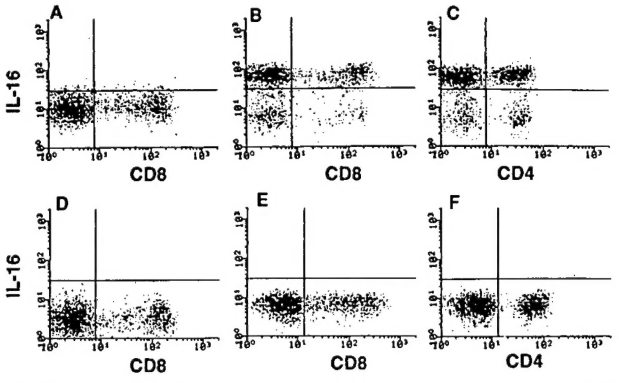

FIGURE 4. Cytoplasmic expression of IL-16 in unstimulated PBMC. Unstimulated PBMC were stained for CD4 or 8 vs IL-16 or control mAb and analyzed by FACS as described in *Materials and Methods*. *A*, Isotype control mAb vs CD8 shows background signal. *B* and *C*, Anti-IL-16 mAb vs CD8 or CD4 shows a majority of CD8$^+$ and CD4$^+$ T cells expressed IL-16. *D*, Staining for IL-16 vs CD8 in the absence of saponin shows that no IL-16 is expressed on the cell surface of CD8$^+$ or CD8$^-$ T cells within the lymphocyte gate. *E* and *F*, Preincubation of anti-IL-16 mAb with rIL-16 completely blocked the detection of intracellular IL-16 in both CD4$^+$ (*E*) and CD8$^+$ (*F*) T lymphocytes.

Results

IL-16 expression in multiple tissues

Tissue expression of IL-16 mRNA was evaluated by Northern blot analysis of poly(A)$^+$ RNA extracted from a variety of human organs and hybridized with a ^{32}P-labeled fragment of the human IL-16 cDNA (Fig. 2). A single band of approximately 2.8 kb was observed in lanes containing RNA from spleen, thymus, and peripheral blood leukocytes. Little or no signal was observed from prostate, testis, ovary, small bowel, or colon after prolonged autoradiograph exposure. In a separate Northern blot (not shown), a strong band at 2.8 kb was observed in poly(A)$^+$ RNA from pancreas, and very weak signals were observed in placenta, lung, liver, and brain. Thus, in the absence of disease, IL-16 mRNA expression was mainly restricted to the lymphoid compartment.

To determine whether IL-16 protein was detectable in peripheral lymphoid tissue, mAb 14.1 against IL-16 (see Fig. 1) was used for immunohistochemical staining of two human lymph nodes. A representative section is presented in Figure 3. In all specimens examined, IL-16 staining was observed in the majority of the cells in the mantle (T cell zone); staining of lymphocyte cytoplasm and lack of nuclear staining suggested that IL-16 was being identified in the cell cytoplasm. Conversely, relatively few cells expressed IL-16 within follicles (B cell zone). No signal was detectable in sections stained with isotype control mAb. These data corroborated the Northern blot findings and showed that IL-16 protein was expressed in the majority of lymphocytes in the T cell zones in lymph node.

Detection of IL-16 in unstimulated CD4$^+$ and CD8$^+$ T lymphocytes

Because CD8$^+$ T cells were previously found to constitutively express IL-16 bioactivity (22), we first characterized the expression of IL-16 protein in CD8$^+$ T cells. To accomplish this we used FITC-conjugated anti-IL-16 mAb 17.1, which recognizes an epitope on the C-terminal of the IL-16 molecule (see Fig. 1). A protocol employing saponin treatment was used to detect both surface and intracellular proteins. Two-color flow cytometry for CD8 vs IL-16 of unstimulated PBMC within the lymphocyte gate showed that 75% of CD8$^+$ cells expressed IL-16 protein (Fig. 4*B*) compared with isotype control mAb (Fig. 4*A*), with a mean fluorescence approximately 1 log greater than that of cells stained with control mAb. Surprisingly, when unstimulated PBMC were stained for CD4 vs IL-16, 73% of the CD4$^+$ cells also stained for

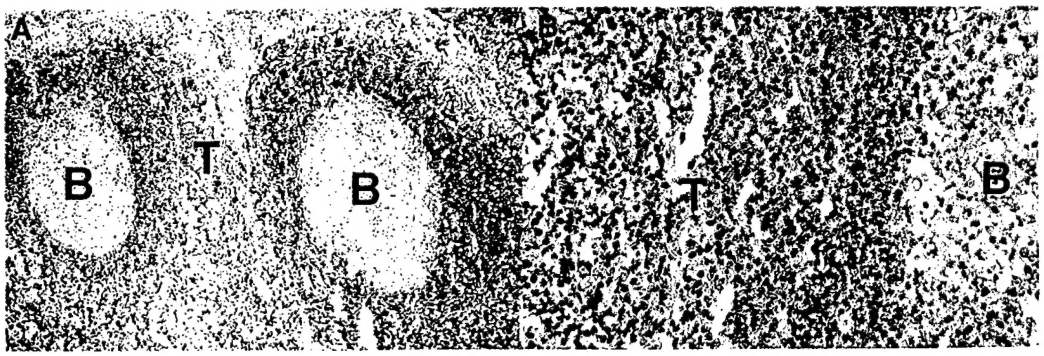

FIGURE 3. Expression of IL-16 protein in a human lymph node. Lymph node was snap-frozen and processed for IL-16 immunohistochemistry as described in *Materials and Methods*. *A*, Low power view of germinal centers rich in B cells (B) and surrounding mantle rich in T cells (T). *B*, High power view of the mantle zone showing cytoplasmic localization of IL-16 protein to most cells in the T cell zone and not in the B cell zone (germinal center). Brown diaminobenzidine staining localizes IL-16 protein to regions rich in T cells.

IL-16 (Fig. 4*C*). This finding was unexpected since $CD4^+$ T cells have not been shown to contain preformed bioactive protein. Similar percentages of $CD8^+$ (86 ± 8.98%) and $CD4^+$ (83 ± 8.18%) T cells stained for IL-16 in subsequent experiments using PBMC from different donors.

To confirm that mAb 17.1 was detecting intracellular protein and not binding to the cell surface, unstimulated PBMC were stained with FITC-conjugated mAb 17.1 in standard staining buffer in the absence of saponin. There was no detectable IL-16 on the surface of $CD8^+$ or $CD8^-$ lymphocytes, confirming that mAb 17.1 was detecting intracellular IL-16 (Fig. 4*D*). The specificity of this signal for IL-16 was confirmed by preincubating FITC-conjugated mAb 17.1 with rIL-16, which completely blocked the detection of intracellular IL-16 in both $CD4^+$ and $CD8^+$ lymphocytes (Fig. 4, *E* and *F*) These data indicated that the majority of resting unstimulated $CD4^+$ and $CD8^+$ T cells express IL-16 and that the antigenic portion of IL-16 resides in the intracellular compartment.

Identification of pro-IL-16 in unstimulated PBMC

To confirm the flow cytometry results, duplicate Western blots of rIL-16 and PBMC lysates were probed with the three anti-IL-16 Abs (Ab 16, and mAbs 14.1 and 17.1; see Fig. 1) and control Abs (Fig. 5*A*). Western blotting with secondary alone or control Ab detected no protein (not shown); however, probing with mAbs 17.1, 14.1, and Ab 16 recognized both 17-kDa rIL-16 and a prominent pro-IL-16 band at about 80 kDa. A third weak band migrating at about 60 kDa was detected when more protein was run per lane or with longer film exposure (not shown). The abundance of pro-IL-16 was evident, since the approximately 80-kDa band was prominent in lysate prepared from as few as 2.5×10^5 PBMC.

To verify that the approximately 80-kDa band recognized by Abs raised to rIL-16 was pro-IL-16, Ab 86 against pro-IL-16 (see Fig. 1) was used to probe a Western blot of rIL-16, PBMC lysate, and in vitro translated pro-IL-16 (Fig. 5*A*, blot 4). This Ab identified the approximately 80-kDa band in unstimulated PBMC with approximately equal intensity to that seen with Abs against IL-16, but did not recognize rIL-16.

To substantiate that the approximately 80-kDa band detected by mAb 17.1 was pro-IL-16, we probed a Western blot of rIL-16, unstimulated PBMC and in vitro translated pro-IL-16 with mAb 17.1 and identified comigrating bands in both the PBMC and in vitro translated pro-IL-16 lanes (Fig. 5*B*). These data validated that mAbs against rIL-16 recognize native pro-IL-16 and show that pro-IL-16 is abundant in $CD4^+$ and $CD8^+$ T cells, and that the majority of IL-16 protein identified by flow cytometry is in the form of pro-IL-16.

In contrast to the abundant presence of pro-IL-16, IL-16 was not abundant in unstimulated PBMC and was only intermittently detectable on immunoblots of cell lysates. Figure 5*C* is a representative Western blot using Ab 16 as a primary Ab and [^{125}I]protein A for detection of PBMC before and after magnetic bead depletion of $CD4^+$ T cells. In this donor, pro-IL-16 and th1e mature form of IL-16 were detectable in NWNT before depletion (*lane d*) and in purified $CD8^+$ T cells after magnetic bead depletion (*lane e*). The 121-amino acid bioactive form of IL-16 has not been detectable by Western blot in purified $CD4^+$ T cells (not shown).

Processing of pro-IL-16 in $CD4^+$ and $CD8^+$ T cells after anti-CD3 stimulation

The data presented show that pro-IL-16 is abundant and constitutively expressed in $CD4^+$ and $CD8^+$ T cells. We hypothesized that upon stimulation with immobilized anti-CD3, pro-IL-16 would be processed releasing IL-16. Purified $CD4^+$ or $CD8^+$ T cells were incubated with plate-bound anti-CD3 and harvested after 6 and 24 h (Fig. 6). Western blotting of harvested cell lysates revealed a prominent pro-IL-16 band at about 80 kDa of equal intensity in unstimulated $CD4^+$ and $CD8^+$ T cell lysates (*lanes a* and *b*, respectively). After 6 h the pro-IL-16 band was preserved, and several lower m.w. bands appeared in both $CD4^+$ (*lane c*) and $CD8^+$ (*lane d*) T cells, which at 24 h were less prominent (*lane e*, $CD4^+$ at 24 h; *lane f*, $CD8^+$ at 24 h). These data suggested that pro-IL-16 may be processed upon cell stimulation. The hypothesis that mature IL-16 is released by processing of pro-IL-16 is further supported by the observation that native secreted IL-16 is weakly, if at all, detectable in low amounts on Western blots of cell lysates with the Abs used in these experiments (for example, Fig. 5*C*). Although we did find IL-16 chemoattractant bioactivity in culture supernatants that was specifically inhibited by anti-IL-16 Abs, there was insufficient IL-16 protein in the supernatants to detect an

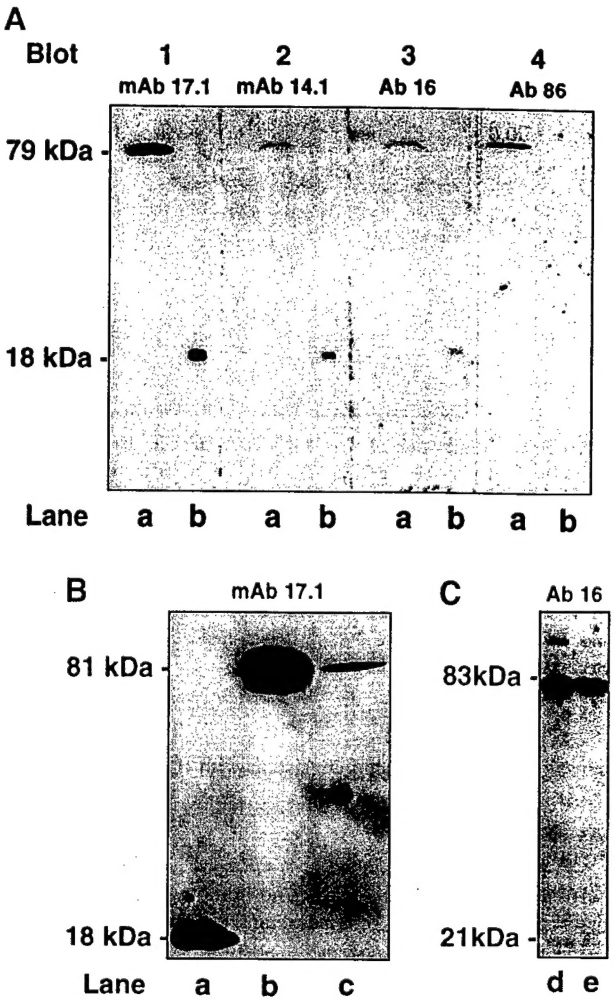

FIGURE 5. · SDS-PAGE and Western blot analysis for IL-16. Western blots of 5.0×10^5 unstimulated PBMC (*lanes a*) and 10 ng of rIL-16 (*lanes b*) and in vitro translated pro-IL-16 (*B, lane c*) were probed with Abs against IL-16 (mAbs 17.1 and 14.1 and Ab 16, blots 1, 2, and 3, respectively) and pro-IL-16 (Ab 86, blot 4). *A*, All three Abs against IL-16 recognized rIL-16 as well as a prominent band at about 80 kDa in PBMC lysates, whereas Ab 86 against pro-IL-16 recognized the approximately 80-kDa band, but not rIL-16. *B*, mAb 17.1 identified comigrating approximately 80-kDa native pro-IL-16 and in vitro translated pro-IL-16. *C*, Lysate of 1.25×10^6 NWNT before (*lane d*) and after (*lane e*) depletion of CD4 cells, showing in this blood donor a weakly detectable, 17-kDa IL-16 and prominent, approximately 80-kDa pro-IL-16 bands.

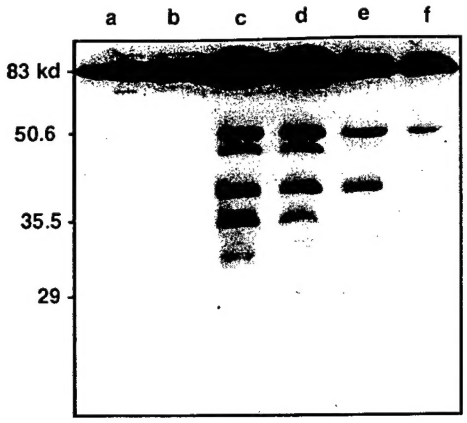

FIGURE 6. Stimulation of T cell subsets results in the processing of pro-IL-16. Purified $CD4^+$ or $CD8^+$ T cells (1.25×10^6) were incubated in the presence of anti-CD3 as described in *Materials and Methods*, harvested, and analyzed by Western blot using Ab 14.1. At time zero (*lanes a* and *b*), a prominent, approximately 80-kDa band was visible in both $CD4^+$ and $CD8^+$ T cells (*lanes a* and *b*, respectively). After 6 h (*lanes c* and *d*) or 24 h (*lanes e* and *f*) of stimulation, the approximately 80-kDa band was still present, and multiple lower molecular mass bands were detectable in both $CD4^+$ and $CD8^+$ T cells.

approximately 17-kDa band consistent with IL-16 in these experiments (not shown).

Discussion

IL-16 is a novel cytokine bearing no homology to other proteins possessing lymphocyte chemoattractant activity (27). Specifically, IL-16 contains a single cysteine at position 22, the IL-16 gene is not located on the chemokine cluster, and it lacks a signal peptide typical of proteins secreted via the Golgi apparatus. The recent identification of pro-IL-16, however, suggests that IL-16 has similarities without structural homology to IL-1, being proteolytically cleaved by an IL-converting enzyme-like protein upon cell activation (20, 28). The current investigations show that pro-IL-16 is constituitively distributed in abundance in circulating human T cells, spleen, and thymus, and suggest that pro-IL-16 is proteolytically processed at several sites upon cell activation.

The initial experiments identifying IL-16 mRNA primarily in lymphoid organs (Fig. 1) suggest that under normal conditions IL-16 may participate in immune system homeostasis in nondiseased states. This hypothesis is further supported by the finding of widespread expression of IL-16 protein in the T cell zone in human lymphoid tissue (Fig. 2). It is also likely that IL-16 has alternative functions in pathologic states (29), where IL-16 expression is not restricted to lymphoid cells. For example, in asthmatic lung, in which there is $CD4^+$ T cell accumulation, the bronchial epithelium can be an alternate source of IL-16 (14).

The experiments aimed at the FACS detection of IL-16 in unstimulated PBMC were based on previous data showing IL-16 bioactivity in unstimulated $CD8^+$ T cell lysates (22). We hypothesized that flow cytometry would detect IL-16 in a subset of unstimulated $CD8^+$ T cells, but found that nearly all unstimulated $CD8^+$ T cells stained for IL-16 (Fig. 4). Further, we detected IL-16 in nearly all unstimulated $CD4^+$ T cells. This was unexpected, as $CD4^+$ T cell lysates have not been shown to contain IL-16 chemoattractant activity, and required that we confirm that the abundant protein in $CD4^+$ and $CD8^+$ T cells detected by flow cytometry signal was IL-16. Western blotting with three Ab against secreted IL-16 peptide and one Ab against pro-IL-16 showed that the abundant protein identified by flow cytometry was the approximately 80-kDa pro-IL-16 (Fig. 5, *A* and *B*).

Taken together with the fact that $CD4^+$ T cells express IL-16 mRNA (22) and that IL-16 chemoattractant activity is detectable in supernatants of $CD4^+$ T cell cultures after 6 h of stimulation with immobilized anti-CD3 (D. Wu, manuscript in preparation), these data suggest that the processing of pro-IL-16 leading to the secretion of mature IL-16 differs between $CD8^+$ and $CD4^+$ T cells. While both cell types constitutively express pro-IL-16, however, $CD8^+$ T cells also constitutively express a significant pool of mature IL-16 peptide, while $CD4^+$ T cells constitutively express little or no mature IL-16, requiring cell activation to secrete mature IL-16.

Western blotting also suggested that upon stimulation with Ag, pro-IL-16 is cleaved at alternative sites (Fig. 6). Since the Ab used for Western blotting in this experiment detects the carboxyl terminus of IL-16, these data suggest that the amino terminus of pro-IL-16 is processed. Recently, caspase-3, an IL-1β-converting enzyme family member, has been shown in vitro to cleave a 50-kDa pro-IL-16 peptide releasing an approximately 20-kDa fragment possessing IL-16 bioactivity (30). Our studies suggest that other IL-16 cleavage sites are also likely to exist (Fig. 5*C*). The physiologic relevance of these cleavage fragments to IL-16 function or degradation is not yet known. We have also noted that when protein is extracted from resting T cells with nonionic detergent rather than SDS, similar bands are detectable. Although it is possible that pro-IL-16 is susceptible to degradation by nonionic detergent, a more plausible explanation is that during nonionic detergent solubilization, pro-IL-16 processing enzymes resistant to standard protease inhibitors (but inactivated by SDS) may be able to cleave pro-IL-16. This explanation is further supported by the finding that similar bands were detected by Western blot analysis of anti-CD3-stimulated T cell lysates extracted in SDS sample buffer (Fig. 6) and may explain why we detect a predominant approximately 80-kDa band in unstimulated PBMC rather than processed fragments identified by others (20).

To determine the effect of cell activation on pro-IL-16 expression, we stimulated T cells with immobilized anti-CD3. Since previous studies showed that release of bioactive IL-16 from serotonin-stimulated $CD8^+$ T cells does not require new protein synthesis (23), we hypothesized that TCR ligation would result in the processing of pro-IL-16 and the release of mature IL-16. We were unable to detect mature IL-16 in stimulated cell lysates, but found that the amino terminus of pro-IL-16 was cleaved upon cell activation (Fig. 6). The significance of these activation-induced cleavage products is unknown. Pro-IL-16 also remained abundant following cell stimulation, suggesting that only a small proportion of pro-IL-16 is processed at the carboxyl terminus to release mature IL-16 and, since native mature IL-16 is weakly, if at all, detectable in low amounts on Western blots with the Abs used in these experiments (Fig. 5*C*), that the preformed pool of pro-IL-16 is large compared with the amount of processed secreted IL-16.

It is unlikely that pro-IL-16 has bioactivity ascribed to IL-16, such as chemoattractant activity or inhibition of HIV replication. Pro-IL-16 is abundant in peripheral blood $CD4^+$ T cells, yet there is a lack of chemoattractant activity in unstimulated $CD4^+$ T cell lysates (22), and peripheral blood $CD4^+$ T cells support HIV replication.

This study shows that pro-IL-16 is a substantial component of the majority of unstimulated blood T cells. The pathway of IL-16 synthesis and secretion remains largely obscure and continues to be actively investigated. It is not known whether mature IL-16 can

be secreted by a subset of lymphocytes capable of cleaving pro-IL-16 or if all pro-IL-16-expressing cells have the capacity to secrete mature IL-16. It is also unknown whether the amino terminal processed products of cell activation represent intermediate forms of IL-16 before the release of mature IL-16, or if these proteins represent processing products with alternative intra- or extracellular functions. Further investigations will be required to detect other functional roles for this protein.

Acknowledgments

We thank Dr. John Hayes and Margo Goetschkes for their technical assistance with immunohistochemistry.

References

1. Cruikshank, W. W., D. M. Center, N. Nisar, M. Wu, B. Natke, A. C. Theodore, and H. Kornfeld. 1994. Molecular and functional analysis of a lymphocyte chemoattractant factor: association of biologic function with CD4 expression. *Proc. Natl. Acad. Sci. USA 91:5109.*
2. Center, D. M., H. Kornfeld, and W. W. Cruikshank. 1996. Interleukin 16 and its function as a CD4 ligand. *Immunol. Today 17:476.*
3. Center, D. M., J. S. Berman, H. Kornfeld, A. C. Theodore, and W. W. Cruikshank. 1995. The lymphocyte chemoattractant factor. *J. Lab. Clin. Med. 125:167.*
4. Cruikshank, W. W., J. L. Greenstein, A. C. Theodore, and D. M. Center. 1991. Lymphocyte chemoattractant factor induces CD4-dependent intracytoplasmic signaling in lymphocytes. *J. Immunol. 146:2928.*
5. Center, D. M., and W. Cruikshank. 1982. Modulation of lymphocyte migration by human lymphokines. I. Identification and characterization of chemoattractant activity for lymphocytes from mitogen-stimulated mononuclear cells. *J. Immunol. 128:2563.*
6. Cruikshank, W. W., J. S. Berman, A. C. Theodore, J. Bernardo, and D. M. Center. 1987. Lymphokine activation of $T4^+$ T lymphocytes and monocytes. *J. Immunol. 138:3817.*
7. Rand, T. H., W. W. Cruikshank, D. M. Center, and P. F. Weller. 1991. CD4-mediated stimulation of human eosinophils: lymphocyte chemoattractant factor and other CD4-binding ligands elicit eosinophil migration. *J. Exp. Med. 173: 1521.*
8. Cruikshank, W. W., K. Lim, A. C. Theodore, J. Cook, G. Fine, P. F. Weller, and D. M. Center. 1996. IL-16 inhibition of CD3-dependent lymphocyte activation and proliferation. *J. Immunol. 157:5240.*
9. Theodore, A. C., D. M. Center, J. Nicoll, G. Fine, H. Kornfeld, and W. W. Cruikshank. 1996. CD4 ligand IL-16 inhibits the mixed lymphocyte reaction. *J. Immunol. 157:1958.*
10. Biddison, W. E., D. D. Taub, W. W. Cruikshank, D. M. Center, E. W. Connor, and K. Honma. 1997. Chemokine and matrix metalloproteinase secretion by myelin proteolipid protein-specific $CD8^+$ T cells: potential roles in inflammation. *J. Immunol. 158:3046.*
11. Schluesener, H. J., K. Seid, J. Kretzschmar, and R. Meyermann. 1996. Leukocyte chemotactic factor, a natural ligand to CD4, is expressed by lymphocytes and microglial cells of the MS plaque. *J. Neurosci. Res. 44:606.*
12. Cruikshank, W. W., A. Long, R. E. Tarpy, H. Kornfeld, M. P. Carroll, L. Teran, S. T. Holgate, and D. M. Center. 1995. Early identification of interleukin-16 (lymphocyte chemoattractant factor) and macrophage inflammatory protein 1α (MIP1α) in bronchoalveolar lavage fluid of antigen-challenged asthmatics. *Am. J. Respir. Cell Mol. Biol. 13:738.*
13. Center, D. M., H. Kornfeld, M. J. Wu, M. Falvo, A. C. Theodore, J. Bernardo, J. S. Berman, W. W. Cruikshank, R. Djukanovic, L. Teran, et al. 1994. Cytokine binding to $CD4^+$ inflammatory cells: implications for asthma. *Am. J. Respir. Crit. Care Med. 150:S59.*
14. Laberge, S., P. Ernst, O. Ghaffar, W. Cruikshank, H. Kornfeld, D. M. Center, and Q. Hamid. 1997. Increased expression of interleukin-16 in bronchial mucosa of subjects with atopic asthma. *Am. J. Respir. Cell Mol. Biol. 17:193.*
15. Baier, M., A. Werner, N. Bannert, K. Metzner, and R. Kurth. 1995. HIV suppression by interleukin-16. *Nature 378:563.*
16. Maciaszek, J. W., N. A. Parada, W. W. Cruikshank, D. M. Center, H. Kornfeld, and G. A. Viglianti. 1997. IL-16 represses HIV-1 promoter activity. *J. Immunol. 158:5.*
17. Scala, E., D. O. G. R. Rosso, O. Turriziani, R. Ferrara, A. M. Mazzone, G. Antonelli, F. Aiuti, and R. Paganelli. 1997. C-C chemokines, IL-16, and soluble antiviral factor activity are increased in cloned T cells from subjects with long-term nonprogressive HIV infection. *J. Immunol. 158:4485.*
18. Zhou, P., S. Goldstein, K. Devadas, D. Tewari, and A. L. Notkins. 1997. Human $CD4^+$ cells transfected with IL-16 cDNA are resistent to HIV-1 infection: inhibition of mRNA expression. *Nat. Med. 3:659.*
19. Cruikshank, W. W., and D. M. Center. 1982. Modulation of lymphocyte migration by human lymphokines. II. Purification of a lymphotactic factor. *J. Immunol. 128:2569.*
20. Baier, M., N. Bannert, A. Werner, K. Lang, and R. Kurth. 1997. Molecular cloning, sequence, expression, and processing of the interleukin 16 precursor. *Proc. Natl. Acad. Sci. USA 94:5273.*
21. Chupp, G. L., Y. Zhang, E. A. Wright, W. W. Cruikshank, H. Kornfeld, D. M. Center, and J. S. Berman. 1997. Pro-IL-16 is an 80 kDa cytoplasmic protein expressed in blood T-lymphocytes. *J. Allergy Clin. Immunol. 99:S54.*
22. Laberge, S., W. W. Cruikshank, H. Kornfeld, and D. M. Center. 1995. Histamine-induced secretion of lymphocyte chemoattractant factor from $CD8^+$ T cells is independent of transcription and translation: Evidence for constitutive protein synthesis and storage. *J. Immunol. 155:2902.*
23. Laberge, S., W. W. Cruikshank, D. J. Beer, and D. M. Center. 1996. Secretion of IL-16 (lymphocyte chemoattractant factor) from serotonin-stimulated $CD8^+$ T cells in vitro. *J. Immunol. 156:310.*
24. Berman, J. S., W. W. Cruikshank, D. M. Center, A. C. Theodore, and D. J. Beer. 1985. Chemoattractant lymphokines specific for the helper/inducer T-lymphocyte subset. *Cell. Immunol. 95:105.*
25. Sander, B., J. Andersson, and U. Andersson. 1991. Assessement of cytokines by immunofluorescence and the paraformaldehyde-saponin procedure. *Immunol. Rev. 119:65.*
26. Jung, T., U. Schauer, C. Heusser, C. Newmann, and C. Rieger. 1993. Detection of intracellular cytokines by flow cytometry. *J. Immunol. Methods 159:197.*
27. Schall, T. 1994. The chemokines. In *The Cytokine Handbook.* A. Thomson, ed. Academic Press, New York, p. 419.
28. Thornberry, N., A., H. Bull, G. J. Calaycay, R. K. Chapman, T. A. Howard, D. M. Kostura, J. D. Miller, K. S. Molineaux, M. J. Weidner, R. J. Aunins, et al. 1992. A novel heterodimeric cysteine protease is required for interleukin-1β processing in monocytes. *Nature 356:768.*
29. Shimada, M., T. Matsumata, A. Taketomi, K. Shirabe, K. Yamamoto, K. Takenaka, and K. Sugimachi. 1995. The role of interleukin-6, interleukin-16, tumor necrosis factor-alpha and endotoxin in hepatic resection. *Hepatogastroenterology 42:691.*
30. Zhang, Y., D. M. Center, D. M. H. Wu, W. W. Cruikshank, J. Yuan, D. W. Andrews, and H. Kornfeld. 1998. Processing and activation of pro-interleukin-16 by caspase-3. *J. Biol. Chem. 273:1144.*

INFECTION AND IMMUNITY, Aug. 1999, p. 4223–4230
0019-9567/99/$04.00+0

Vol. 67, No. 8

Attenuated Host Resistance against *Mycobacterium bovis* BCG Infection in Mice Lacking Osteopontin

GERARD J. NAU,[1,2] LUCY LIAW,[3]† GEOFFREY L. CHUPP,[4]‡ JEFFREY S. BERMAN,[4,5] BRIGID L. M. HOGAN,[3] AND RICHARD A. YOUNG[1]*

Whitehead Institute for Biomedical Research and Department of Biology, Massachusetts Institute of Technology, Cambridge, Massachusetts 02142[1]; Infectious Disease Unit, Massachusetts General Hospital, Boston, Massachusetts 02114[2]; Howard Hughes Medical Institute and Department of Cell Biology, Vanderbilt University Medical Center, Nashville, Tennessee 37232[3]; Pulmonary Center, Boston University School of Medicine, Boston, Massachusetts 02188[4]; and Boston VA Medical Center, Boston, Massachusetts 02130[5]

Received 24 February 1999/Returned for modification 14 April 1999/Accepted 22 April 1999

Expression of the cytokine osteopontin (OPN) is elevated in granulomas caused by *Mycobacterium tuberculosis*. We tested the hypothesis that OPN contributes to host protection in a mouse model of mycobacterial infection. When infected with *Mycobacterium bovis* BCG, mice lacking a functional OPN gene had more severe infections characterized by heavier bacterial loads and a delayed clearance of the bacteria. The OPN-null mice had greater granuloma burdens consistent with the elevated bacterial load. The ability of osteopontin to facilitate the clearance of mycobacteria was most pronounced early after infection and appeared to be independent of known mediators of resistance to infection by mycobacteria: antigen-specific T-cell immunity, gamma interferon production, and nitric oxide production. BCG grew more rapidly in macrophages derived from OPN-null mice than in those from wild-type mice, demonstrating that the null phenotype was due to an intrinsic macrophage defect. These results indicate that osteopontin augments the host response against a mycobacterial infection and that it acts independently from other antimycobacterial resistance mechanisms.

Tuberculosis is a pandemic infection that involves much of the world's population and is caused by *Mycobacterium tuberculosis*. The World Health Organization has raised concern over the epidemic potential of this organism because of increasing antimicrobial resistance (36). Recently, an isolate of *M. tuberculosis* with an extraordinary growth rate and with increased rates of transmission was isolated (46). These findings have generated interest in understanding the unique interactions of host cells and mycobacteria: *M. tuberculosis* can elude host immune responses and persist in a latent state for years. The granuloma is a feature of this host-pathogen interaction. Granulomas are characterized by a mononuclear cell infiltration of macrophages and lymphocytes, by the formation of giant cells and epithelioid cells, and by fibrosis, sometimes with calcification (2, 12). The public health concerns and the unusual pathology of tuberculosis led us to question what is normally involved in the host macrophage response after infection by mycobacteria.

We have undertaken a study of macrophage gene expression changes after infection by mycobacteria. By differential screening of a cDNA library and probes derived from a murine macrophage cell line, one gene isolate, osteopontin (OPN), was identified repeatedly in cells infected by mycobacteria compared with cells infected by *Escherichia coli* (35). We found that osteopontin gene expression in human pulmonary macrophages increased after infection with virulent *M. tuberculosis* and that OPN protein expression was widespread in human tuberculosis pathology (35).

OPN is a secreted, phosphorylated, glycoprotein that is associated with several host inflammatory states. The gene encoding OPN, known as *spp1*, cosegregates with resistance to lethal infection by *Orientia* (*Rickettsia*) *tsutsugamushi* in mice (16, 23). The protein stimulates the migration of macrophages (22, 34, 42) and of smooth muscle cells (29, 51). OPN is found in the inflammatory macrophages of rat myocardium after cryoinjury (33), in arterial atherosclerosis (21, 24), and in several granulomatous conditions (3, 35). OPN has been labeled a cytokine based on its proinflammatory properties (38, 45) and is a likely candidate for mediating or modulating mononuclear cell infiltration and chronic inflammation.

We and others have identified genes whose expression changes in mammalian cells after infection (35, 52). These findings merit further studies to determine the roles of these genes in infection. The work detailed here describes the use of OPN knockout mice (28) to investigate whether OPN influences the host response against infection by mycobacteria. Animals lacking OPN had more severe infections and were delayed in eliminating the mycobacteria after infection. The findings identify a novel role for OPN as an accessory molecule to activate macrophages and to augment the clearance of inflammatory stimuli.

MATERIALS AND METHODS

Animals. OPN mutant mice (*spp1*^{tm1}) and wild-type controls 5 to 8 weeks old and matched for age and sex were used for experiments. The generation of the OPN mutant mice has been described elsewhere (28). The experiments described herein were done with wild-type and mutant animals on a (129 × Black Swiss) hybrid background as was used previously (28). Genotyping was confirmed on all breeding pairs with a PCR analysis. All animal procedures were performed according to the guidelines of the Massachusetts Institute of Technology Committee on Animal Care.

Infections. *Mycobacterium bovis* bacillus Calmette-Guérin (BCG) (ATCC 35734; Trudeau mycobacterial culture collection no. 1011, "BCG Pasteur") was grown from a frozen stock for 6 to 7 days (to an optical density at 600 nm of

* Corresponding author. Mailing address: Whitehead Institute for Biomedical Research, 9 Cambridge Center, Cambridge, MA 02142. Phone: (617) 258-5218. Fax: (617) 258-0376. E-mail: young@wi.mit.edu.

† Present address: Center for Molecular Medicine, Maine Medical Center Research Institute, South Portland, ME 04106.

‡ Present address: Section of Pulmonary and Critical Care Medicine, Yale University School of Medicine, New Haven, CT 06520.

~1.4) in Middlebrook 7H9 broth with 0.5% glycerol, 0.05% Tween 80, and ADC enrichment (Difco, Detroit, Mich.). On the day of infection, bacteria were resuspended in phosphate-buffered saline (PBS), and an inoculum of approximately 10^7 CFU was delivered intraperitoneally. This route of inoculation was selected because of previous studies of OPN and infection (23, 37) and because intraperitoneal infections can successfully generate systemic mycobacterial infections (32). At various times after infection, organs were harvested for analysis. For CFU analysis, liver sections were weighed and disrupted in PBS with an electric homogenizer (Polytron PT 1200B; Kinimatica). Serial dilutions were made in 7H9 medium, and aliquots were spread on 7H10 plates. CFU were enumerated 3 to 4 weeks later.

Immunohistochemistry. Organs were harvested for histologic analysis at the times indicated after infection. Tissues were fixed in buffered formalin and processed by standard histologic techniques. For immunohistochemistry, paraffin-embedded tissue sections were deparaffinized in HistoClear (National Diagnostics, Atlanta, Ga.), rehydrated in graded ethanol washes, and washed in PBS. The F4/80 antibody (Harlan Bioproducts, Indianapolis, Ind.) was used according to the manufacturer's recommendations. Rabbit antiserum against holo-NOS2 (49) was a gift from Qiao-wen Xie and Carl Nathan and was used as described previously (30), except that a 1:750 dilution was incubated with specimens at room temperature for 2 h. Biotinylated secondary antibodies, avidin-biotin-horseradish peroxidase conjugates, and substrates (Vector Labs, Burlingame, Calif.) were used according to the manufacturer's directions. Slides were counterstained with hematoxylin (Dako, Carpinteria, Calif.). After the completion of staining, specimens were dehydrated in graded ethanol and ClearRite 3 (Richard-Allan Scientific, Kalamazoo, Mich.) before being mounted with Permount (Fisher, Fair Lawn, N.J.).

Quantitation of granuloma burden. The percent granuloma burden, the total percentage of liver surface area covered by granulomas, was measured by macrophage immunostaining and a Bioquant image analysis system (Nashville, Tenn.) (26, 27). The Bioquant system is an operator-interactive image analysis device linked to stage x-y encoders, utilizing a Dage MTI CCD72 video camera system with a Leitz Aristoplan microscope. A systematically random sampling scheme was used to select fields for measurement of granuloma burden: a grid was overlaid over the liver section, and from a random start point, every eighth 500-μm by 500-μm field was captured by video under a ×16 objective with the fluorescein cube. The counting chamber consisted of a 500-μm by 500-μm sampling box with extended exclusion lines. For each field, a threshold optical density was obtained, which discriminated staining from background. Manual editing of each field eliminated artifacts, as well as excluding granulomas touching the lower and left borders of the counting chamber, while including granulomas touching the upper and right borders. Granulomas were defined as areas of immunoreactivity greater than 150 μm^2, or greater than approximately two to three macrophages. The total number of granulomas, the area of each granuloma, and the sum of the areas of the granulomas divided by the total area sampled (granuloma burden) were determined over four to five liver sections for each animal. Some background counts could be attributed to the confluence of Kupffer cells that registered above the threshold filter. Statistical analysis was by *t* test comparing homozygous *spp1*^{tm1} and wild-type mice. The appropriateness of the sampling scheme was evaluated by calculating the precision of the estimates, expressed as the coefficient of error (CE) (48). The CE was <0.10, suggesting that a minimal amount of variance in the granuloma burden measurement was from the sampling technique and that measured differences reflected true biological variability. All measurements were performed by a single examiner (G.N.) blinded to treatment group.

In vitro cell stimulation. Spleens were harvested at the times indicated after infection and were crushed through nylon mesh to obtain single-cell suspensions. Cells were washed and resuspended to 4×10^6 cells/ml, and 1 ml was plated per well of a Falcon 24-well plate (Becton Dickinson, Lincoln Park, N.J.) with various antigens or concanavalin A (ConA). The purified protein derivative (PPD) from *M. tuberculosis* was generously donated by Lederle Laboratories (Pearl River, N.Y.). Supernatants were harvested 72 h later. The gamma interferon (IFN-γ) MiniKit from Endogen (Woburn, Mass.) was used to assay the culture supernatants.

NO measurement. Peritoneal exudate cells (PEC) were isolated 5 to 7 days after intraperitoneal inoculation of 1 ml of 3% thioglycolate. In some instances, macrophages were purified by adherence and recovered by dispase treatment and scraping (7). The production of nitric oxide (NO) by the PEC was assessed by measuring the accumulation of nitrite in culture supernatants. Griess reagents were used as described previously (25).

In vitro assay of BCG growth. The measurement of BCG growth in macrophages was performed by using a [^{3}H]uracil assay that has been widely used to measure the growth of mycobacteria (5, 17, 18, 40); uptake closely correlates with CFU (17). Thioglycolate-derived PEC (2×10^5) and BCG (multiplicity of infection, 5 to 10 bacteria per 1 macrophage) were cocultured with RPMI (Life Technologies, Gaithersburg, Md.) with 1% heat-inactivated fetal calf serum in U-bottom plates (ICN Biomedicals, Inc., Aurora, Ohio). After 4 h of coincubation, the wells were washed with warm Hank's balanced salt solution (Life Technologies) to remove extracellular BCG and nonadherent cells and RPMI medium–1% fetal calf serum was added. At various times after the infection, [^{3}H]uracil was added to the wells, and after 18 h, the contents of the wells were harvested with a cell harvester (Skatron, Inc., Sterling, Md.) by using Triton X-100 for macrophage lysis and trichloroacetic acid.

RESULTS

Reduced clearance of *M. bovis* BCG in OPN-deficient mice. Wild-type and OPN-null mice were infected with BCG, and the bacterial load in liver sections was assessed over 12 weeks by using standard tissue staining for acid-fast bacilli. Four independent experiments were performed, and representative results are shown in Fig. 1. When sections of liver and spleen obtained 4 weeks after infection from wild-type mice were stained for acid-fast organisms, few bacilli were detected (Fig. 1A and C). In contrast, the mycobacteria were easily identified in the livers and spleens of OPN-null animals (Fig. 1B and D). Similar results were seen in lung sections (data not shown).

The burden of mycobacteria in infected tissue was measured by serial dilutions of homogenized liver samples from the wild-type and OPN-null mice (Fig. 1E). Similar numbers of bacilli were found in wild-type and *spp1*^{tm1} mice immediately after infection. However, there was a significant difference in the mycobacterial burden 4 weeks after infection. In three independent experiments, OPN-null mice had 10- to 40-fold more bacteria per gram of liver tissue than wild-type mice. The *spp1*^{tm1} animals were, however, capable of reducing the mycobacterial burden by 12 weeks. These results show that the OPN-null mice have impaired clearance of BCG early after infection compared to that in wild-type mice.

Increase in granuloma number and size in OPN mutants. Several biological activities have been attributed to OPN that suggested it would be involved in granuloma formation: OPN is known to activate macrophage migration in vitro and in vivo (22, 34, 42), and it can bind calcium (6). However, histologic analyses of tissues after infection showed that granulomas were present in OPN-null animals; immunohistochemical analyses showed that these granulomas were comprised of both macrophages and T cells similar to those of the wild type (data not shown). The macrophage staining did indicate a difference in the total amount of hepatic tissue involved with granulomas. This difference was quantitated by measuring the granuloma burden. Liver sections stained for macrophages with the F4/80 monoclonal antibody and the Vector red alkaline phosphate substrate were subjected to a stereologic evaluation to measure the granuloma burden. The fluorescent emissions from the Vector red substrate clearly demonstrated that the OPN-null mice had more macrophages within the liver and overall a greater burden of granulomas (Fig. 2A). The granuloma burdens of liver specimens from 20 animals were systematically measured as described in Materials and Methods. The wild-type animals had an estimated 1.1% of the liver tissue area involved with granulomas (Fig. 2B). In contrast, the OPN-null mice had 3.1% of the liver tissue area involved with granulomas. Statistically significant differences were also observed when the sections were analyzed for the number of granulomas and the average granuloma size (Fig. 2B). The inability of OPN-null mice to clear BCG was reflected in more extensive granulomatous inflammation.

Macrophage recruitment in OPN-null mice. OPN induces inflammatory infiltrates when administered in vivo (42), and it is expressed rapidly after intraperitoneal administration of inflammatory stimuli (37). Because we used an intraperitoneal route of infection, it was possible that the elevated bacterial counts in *spp1*^{tm1} mice were a result of an early defect in inflammatory cell accumulation after inoculation. To test this possibility, we quantitated the acute inflammatory response after infection. Seventy-two hours is sufficient time to allow

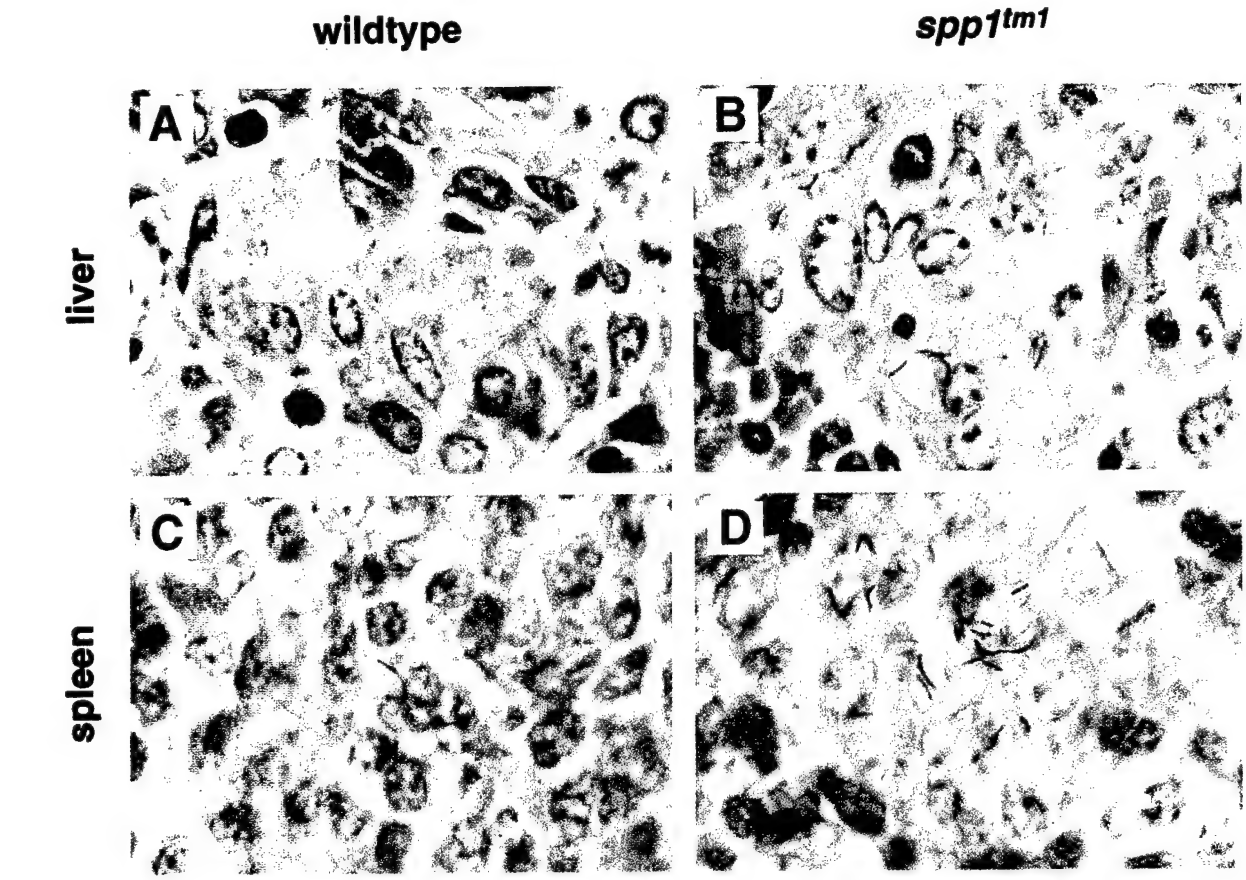

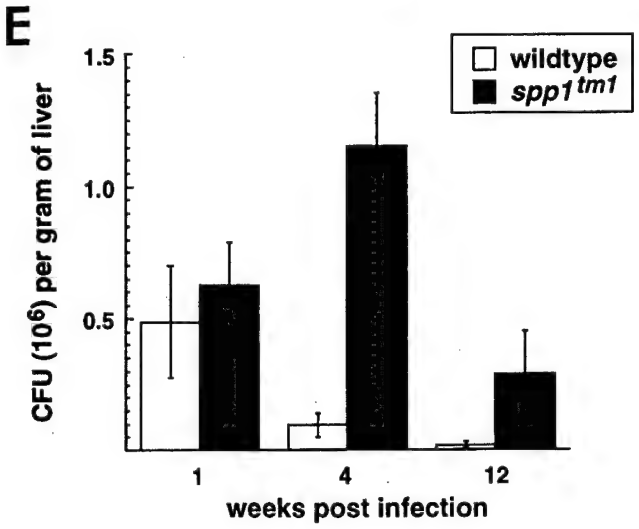

FIG. 1. Mycobacterial organism burden in tissues of OPN-null mice after intraperitoneal infection with BCG. (A to D) Ziehl-Nielson stains of liver (A and B) and spleen (C and D) from wild-type (A and C) and *spp1*^{tm1} (B and D) animals. The mycobacteria stain red. Similar findings were observed in 15 animals per genotype from four different experiments. Original magnification, ×500. (E) CFU determination from liver samples of animals infected intraperitoneally at time 0 weeks. Symbols represent means ± standard errors for three to four animals per group. A 10- to 40-fold difference in CFU between wild-type and *spp1*^{tm1} animals at 4 weeks was observed in three different experiments. $P < 0.05$ at 4 weeks postinfection. A similar 10-fold difference in CFU was also observed in these animals' spleens at the 12-week time point.

peak OPN gene expression after instillation of a peritoneal irritant (37). At this time after BCG inoculation, OPN-null mice unexpectedly had more cellular exudates than wild-type mice (Fig. 3A). To assess the specificity of this response, intraperitoneal injection of thioglycolate was used to elicit inflammatory cells. In repeated experiments, the PEC from *spp1*^{tm1} mice outnumbered those from wild-type mice (Fig. 3B). Cytospin and fluorescence-activated cell sorter analyses of the inflammatory exudates demonstrated there was an abundance of macrophages in PEC from both genotypes (data not shown). These results indicate that *spp1*^{tm1} mice did not have a defect in macrophage recruitment; in fact, these animals had a exaggerated inflammatory responses to peritoneal irritants.

IFN-γ production and NO metabolism are normal in OPN-null mice. The production of IFN-γ (9, 19) and reactive nitrogen intermediates (RNI) (4, 5, 13, 30) is crucial to the successful eradication of *M. tuberculosis* infections. It was possible that the OPN-null mice were deficient in producing one or both of these important factors after infection by BCG.

We analyzed the induction of antigen-specific immunity in *spp1*^{tm1} versus that in wild-type animals. Splenocytes from animals infected 4 weeks earlier were stimulated in vitro with ConA, an irrelevant antigen (ovalbumin [OVA]), the relevant mycobacterial antigen (purified protein derivative [PPD]), or culture medium only. The results in Fig. 4A demonstrate that splenocytes from OPN-null animals were capable of producing IFN-γ specifically after stimulation with the relevant antigen, PPD. The level of IFN-γ produced by splenocytes from null animals was comparable to that produced by splenocytes from

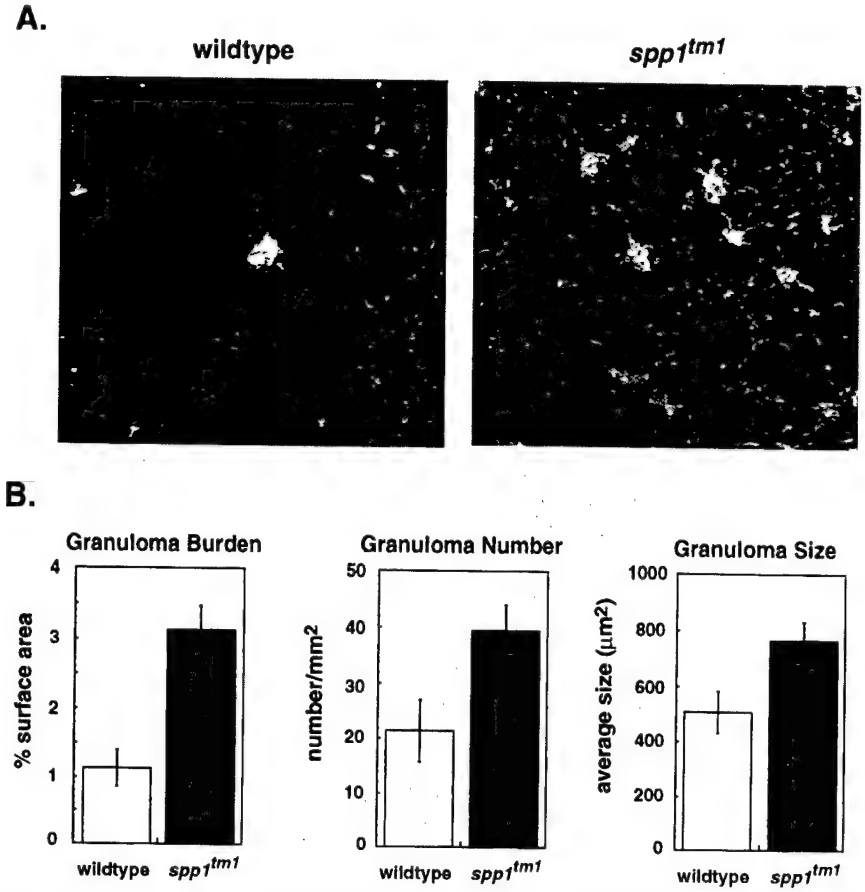

FIG. 2. Assessment of granuloma burden after infection with BCG. (A) Fluorescent images of liver sections from mice of each genotype captured in the BioQuant system. A low-power-view of granuloma burden in OPN-null and wild-type mice viewed by fluorescent microscopy under a fluorescein cube is shown. The original images were captured with a ×16 objective lens. (B) Comparison of granuloma burden, granuloma number, and average granuloma size of wild-type versus *spp1*^{tm1} animals. Measurements were performed with 10 OPN-null and 10 wild-type animals from four separate experiments. OPN-null animals had more extensive hepatic inflammation by all measures. Values are ± standard error. $P < 0.05$ for each comparison. Livers from uninfected control animals of each genotype showed granuloma burdens of <0.05%.

wild-type animals; this occurred when the difference between the CFU was the greatest. There was no difference in the kinetics of induction of T-cell immunity, because splenocytes of both genotypes produced similar levels of IFN-γ 1 week after infection (Fig. 4B). In addition, splenocytes from wild-type and OPN-null mice did not differ in their production of interleukin-4 (IL-4) or IL-10 after stimulation (data not shown). Therefore, the OPN mutant mice mounted appropriate T-cell responses after infection. In addition, there was not a defect in antigen presentation.

We next tested macrophages for RNI production by measuring the surrogate marker for NO, NO_2^- (14). Figure 5A shows the production of RNI by PEC from wild-type and *spp1*^{tm1} mice treated with inflammatory stimuli. Cells from both strains of mice produced comparable RNI after stimulation by IFN-γ plus lipopolysaccharide (LPS) or plus tumor necrosis factor alpha (TNF-α).

Because the requirements of NO production in vivo may differ from the conditions used in the in vitro culture system, the expression of NOS2 was assessed in vivo. Immunohistochemical staining of liver sections revealed widespread NOS2 protein in the granulomas of both wild-type and OPN mutant animals 4 weeks after infection (Fig. 5B). Macrophages infiltrating the livers of both wild-type and mutant animals 1 week after infection also stained faintly for NOS2 (data not shown).

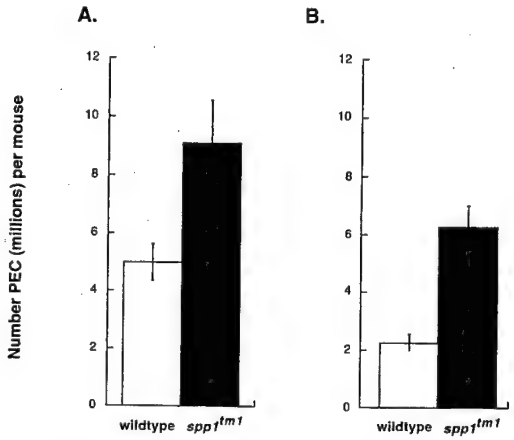

FIG. 3. Exaggerated inflammatory response of *spp1*^{tm1} mice compared to wild-type animals after exposure to thioglycolate or BCG. (A) A total of 10^7 BCG organisms were inoculated intraperitoneally, and PEC were harvested 3 days later. Viable cells were counted on a hemocytometer by trypan blue exclusion. Results are means ± standard errors of 10 animals per group from two separate experiments. $P < 0.05$ for the significance of differences. (B) PEC accumulation 3 days after intraperitoneal injection of thioglycolate. Results are means ± standard errors for five animals per group. $P < 0.05$ for the significance of differences. Significant differences in cell counts were observed in five other experiments in which PEC pooled from OPN-null mice outnumbered those from wild-type mice by 1.6- to 6-fold 5 to 7 days after administration of thioglycolate.

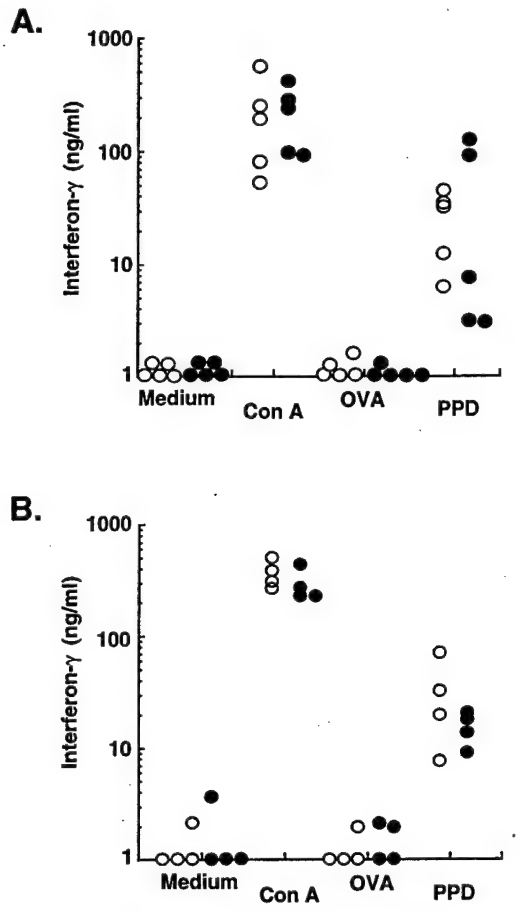

FIG. 4. OPN-null animals are capable of developing antigen-specific immunity comparable to wild-type animals. Splenocytes were stimulated in vitro 4 weeks after infection (A) or 1 week after infection (B). IFN-γ secretion was measured in supernatants harvested after 72 h of incubation with culture medium only, ConA (5 μg/ml), OVA (10 μg/ml), or PPD (10 μg/ml). Each symbol represents an individual animal: solid symbols are *spp1*^{tm1} animals, and open symbols are wild-type animals. Those symbols on the *x* axis represent cytokine levels below the smallest *y* axis value or that were undetectable in the enzyme-linked immunosorbent assay.

As was observed with the T-cell activity (Fig. 4A), the NOS2 was present in tissues at the time of the greatest difference in CFU between the genotypes.

Macrophages from OPN-null mice are defective in killing BCG. The presence of specific T-cell immunity (Fig. 4) and the apparently normal induction of NOS2 (Fig. 5) were consistent with the fact that OPN-null animals eventually reduce the numbers of BCG (Fig. 1E). It was possible, however, that there was a difference in the ability of the macrophages from *spp1*^{tm1} mice to limit the growth of the BCG in the absence of antigen-specific immunity. We tested the antimycobacterial activity of macrophages from naïve wild-type and null mice by infecting them with BCG in vitro. As shown in Fig. 6, [^{3}H]uracil incorporation by BCG, which correlates directly with CFU (17), increased exponentially in macrophages derived from OPN-null mice. In contrast, the incorporation of [^{3}H]uracil by BCG cultured with wild-type macrophages was linear throughout the experiment (Fig. 6). Thus, the OPN-null mice have an intrinsic defect in their macrophages that renders them more susceptible to BCG growth.

DISCUSSION

Resistance to tuberculosis in humans involves a complex network of activation signals and effector responses. The more primitive innate immune system relies on pattern recognition of a microorganism to initiate containment of a pathogen (15). Subsequently, initiation of the adaptive immune response enhances the eradication of *M. tuberculosis* via effector mechanisms such as macrophage activation (10) or direct cytotoxicity (44). The macrophage is a key participant in the innate response and in the effector phase of the adaptive response. Thus, understanding the interaction between macrophages and mycobacteria should help to identify novel host factors that influence resistance to this disease. Our previous analysis of changes in gene expression in macrophages after BCG infection identified one protein, OPN, whose expression was closely linked to tuberculosis infection. Our current studies with an OPN-null mouse demonstrate that OPN enhances host defenses against a mycobacterial infection.

Mice lacking a functional OPN gene suffered from more severe infections by *M. bovis* BCG than wild-type controls. The OPN-null animals had delayed eradication of live bacilli and exaggerated peritoneal inflammation. The *spp1*^{tm1} mice also had a greater hepatic granuloma burden, consistent with persistence of the bacilli and delayed resolution of the inflammation. The defect of the OPN-null mice is intrinsic to the macrophage and the cells' inability to control the growth of the mycobacteria.

Although it has been labeled a chemoattractant cytokine, OPN's role in the immune and inflammatory system has been the subject of much speculation. Intradermal injection of the protein can cause inflammation (22, 34, 42). Previous studies have shown that animals treated with anti-OPN serum have a macrophage migration defect (22, 50). In contrast, we found that OPN-null mice had more macrophages accumulate in response to thioglycolate or to an acute or a chronic mycobacterial infection. Similarly, there was no apparent difference in macrophage accumulation between wild-type and *spp1*^{tm1} animals after skin incision (28). While these findings do not exclude OPN as a chemoattractant molecule, it appears some stimuli, such as BCG, elicit signals that compensate for the absence of OPN and promote macrophage accumulation.

Rollo and colleagues have demonstrated an inhibitory activity of OPN on NO production and cytotoxicity by macrophages in vitro (39). The production of nitrite after stimulation with LPS and IFN-γ was delayed, a result of failed NOS2 mRNA induction (39). Our studies of the OPN-null mice have not shown a gross abnormality of NO metabolism. While OPN may inhibit NO production under certain conditions, our data indicate that, overall, OPN enhances the eradication of mycobacteria in vivo.

The data presented here, together with those of other studies (41), implicate OPN and its receptor, CD44, as cofactors in granulomatous inflammation. CD44 is believed to be one of several receptors for OPN (47). Mice deficient in CD44 have an exaggerated granulomatous response to intravenous *Corynebacterium parvum* (41). Likewise, the *spp1*^{tm1} mice had an increased granuloma burden after BCG infection. Thus, the phenotypes of the two mutant mice are similar: a 1.5- to 2-fold increase in granuloma size and number was observed in both null animals after a challenge with an agent that induces granuloma formation. A physiologic interaction of OPN with CD44 in granulomatous inflammation would explain the comparable phenotypes observed in both null mice.

The current data support a model in which the OPN-null mice have a defect in an important effector response of mac-

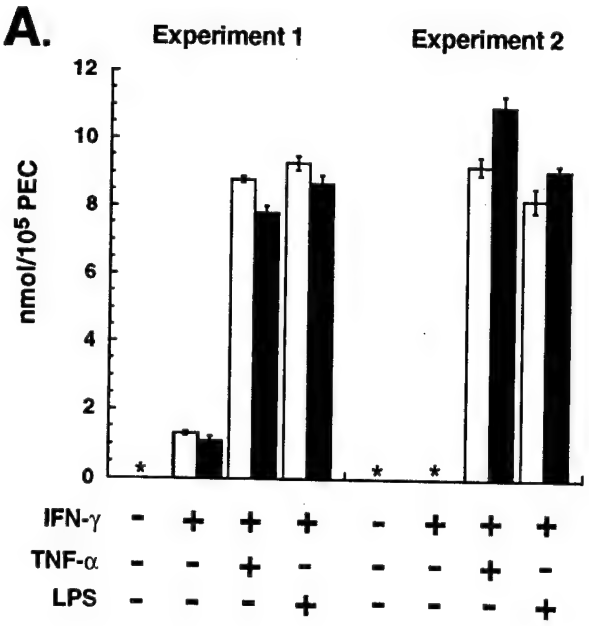

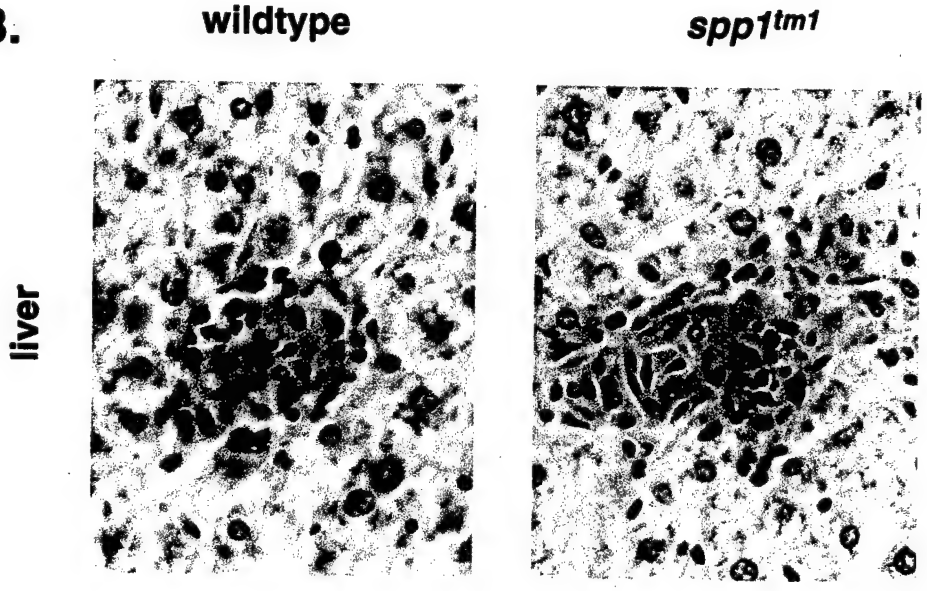

FIG. 5. Macrophages from OPN-null and wild-type animals produce similar amounts of NO in vitro and NOS2 in vivo. (A) Nitrite production from PEC stimulated in vitro. Thioglycolate-elicited PEC were stimulated with IFN-γ (100 ng/ml) for 6 (experiment 1) or 16 (experiment 2) h followed by addition of TNF-α (10 ng/ml [experiment 1] or 100 ng/ml [experiment 2]) or LPS (5 μg/ml) for 48 h. Values are means ± standard errors of quadruplicate cultures; open bars and solid bars are PEC from wild-type and *spp1*^{tm1} animals, respectively. *, none detected. There was no detectable nitrite produced by cells stimulated with either TNF-α or LPS alone. (B) Immunohistochemical stain for NOS2 4 weeks after infection with BCG. Representative animals are shown for each genotype. Similar results were observed with 14 animals in three separate experiments. The resident macrophages of control, uninfected animals did not stain for NOS2. Original magnification, ×200.

rophages during a mycobacterial infection. OPN expression by macrophages is increased soon after a mycobacterial infection (35). We have now demonstrated that an OPN-null mutation creates an early defect in the eradication of mycobacteria in vivo and a defect in controlling BCG growth in vitro. These results are consistent with findings of reduced debridement of tissue wounds in the OPN-null mouse, probably due to poor macrophage function (28). Together with the observations with the CD44-null mouse described above, these data suggest that OPN enhances macrophage activity to degrade material taken up after phagocytosis, which would eradicate mycobacteria more efficiently.

Multiple factors, such as the production of inflammatory cytokines (10, 11, 19, 20) and the production of NO (4, 30), are involved in host resistance to tuberculosis. Our present results indicate that OPN has a costimulatory role in macrophage activation to enhance the killing of mycobacteria by macrophages. A similar model of accessory molecule stimulation of monocytes has been suggested previously (31). Activation of human monocytes by IFN-γ is enhanced when the cells are cultured on fibronectin (31). In addition, interactions between several cell types and the extracellular matrix can significantly increase the expression of chemokines (43). OPN, like fibronectin, contains an arginine-glycine-aspartic acid (RGD) domain and may act as a soluble protein (42) or may be cross-linked to extracellular matrix proteins (1).

The goal of our initial investigation was to identify macrophage genes whose expression was altered after infection by mycobacteria. The current work confirms the biological relevance of the findings of the genetic screen by identifying an active role of OPN in the clearance of mycobacteria after infection. Further delineation of OPN's effects on macrophages may lead to new strategies to treat infections, similar to using IFN-γ in patients with multidrug-resistant tuberculosis (8).

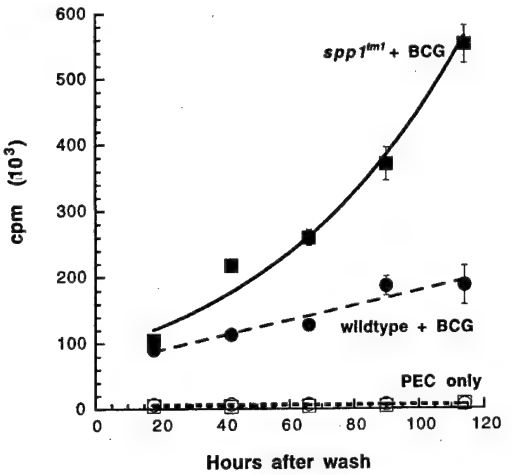

FIG. 6. Macrophages from OPN-null mice are more permissive to the viability and growth of BCG in vitro. Infections were performed as described in Materials and Methods. The data are mean counts per minute ± standard errors of quadruplicate cultures; error bars that are not visible are smaller than the symbol for that data point. Time 0 represents the time that the wells were washed after the 4-h infection, the time of the first tritium pulse. The BCG cultured with *spp1*^{tm1} PEC grew exponentially (solid squares) ($R^2 = 0.98$). The BCG cultured with wild-type PEC grew linearly (solid circles) ($R^2 = 0.92$). The 95% confidence limits for the best fit lines did not overlap beyond 60 h. No significant [^{3}H]uracil incorporation was observed with wild-type PEC (open circles) or *spp1*^{tm1} PEC (open squares) in the absence of BCG. Similar results were seen in two independent experiments.

ACKNOWLEDGMENTS

This work was supported by Public Health Service grants AI37869 (to R.A.Y.) and AI01305 (to G.J.N.). B.L.M.H., in whose laboratory the *spp1*-null mice were generated by L.L., is an Investigator of The Howard Hughes Medical Institute.

We thank Qiao-wen Xie and Carl F. Nathan (Cornell University Medical College, Department of Medicine) for providing the anti-holo-NOS2 reagent. The PPD was kindly provided by Patricia Van Zandt at Lederle Laboratories. We thank Michael C. Irizarry and Bradley T. Hyman (Massachusetts General Hospital, Department of Neurology) for assistance with the immunohistochemistry and stereologic procedures. We thank Sven Holder (Massachusetts General Hospital) and Margo Goetschkes (Boston VA Medical Center) for assistance with histology.

REFERENCES

1. **Beninati, S., D. R. Senger, E. Cordella-Miele, A. B. Mukherjee, I. Chackalaparampil, V. Shanmugam, K. Singh, and B. B. Mukherjee.** 1994. Osteopontin: its transglutaminase-catalyzed posttranslational modifications and cross-linking to fibronectin. J. Biochem. **115**:675–682.
2. **Boros, D.** 1978. Granulomatous inflammations. Prog. Allergy **24**:183–267.
3. **Carlson, I., K. Tognazzi, E. J. Manseau, H. F. Dvorak, and L. F. Brown.** 1997. Osteopontin is strongly expressed by histiocytes in granulomas of diverse etiology. Lab. Investig. **77**:103–108.
4. **Chan, J., K. Tanaka, D. Carroll, J. Flynn, and B. R. Bloom.** 1995. Effects of nitric oxide synthase inhibitors on murine infection with *Mycobacterium tuberculosis*. Infect. Immun. **63**:736–740.
5. **Chan, J., Y. Xing, R. S. Magliozzo, and B. R. Bloom.** 1992. Killing of virulent Mycobacterium tuberculosis by reactive nitrogen intermediates produced by activated murine macrophages. J. Exp. Med. **175**:1111–1122.
6. **Chen, Y., B. S. Bal, and J. P. Gorski.** 1992. Calcium and collagen binding properties of osteopontin, bone sialoprotein, and bone acidic glycoprotein-75 from bone. J. Biol. Chem. **267**:24871–24878.
7. **Coligan, J. E., A. M. Kruisbeek, D. H. Margulies, E. M. Shevach, and W. Strober (ed.).** 1994. Current protocols in immunology, 2nd ed., vol. 2. John Wiley & Sons, Inc., New York, N.Y.
8. **Condos, R., W. N. Rom, and N. W. Schluger.** 1997. Treatment of multidrug-resistant pulmonary tuberculosis with interferon-gamma via aerosol. Lancet **349**:1513–1515.
9. **Cooper, A. M., D. K. Dalton, T. A. Stewart, J. P. Griffin, D. G. Russell, and I. M. Orme.** 1993. Disseminated tuberculosis in interferon gamma gene-disrupted mice. J. Exp. Med. **178**:2243–2247.
10. **Cooper, A. M., and J. L. Flynn.** 1995. The protective immune response to Mycobacterium tuberculosis. Curr. Opin. Immunol. **7**:512–516.
11. **Cooper, A. M., J. Magram, J. Ferrante, and I. M. Orme.** 1997. Interleukin 12 (IL-12) is crucial to the development of protective immunity in mice intravenously infected with Mycobacterium tuberculosis. J. Exp. Med. **186**:39–45.
12. **Dannenberg, A. M., Jr., and G. A. W. Rook.** 1994. Pathogenesis of pulmonary tuberculosis: an interplay of tissue-damaging and macrophage-activating immune responses—dual mechanisms that control bacillary multiplication. p. 459–484. *In* B. R. Bloom (ed.), Tuberculosis: pathogenesis, protection, and control. ASM Press, Washington, D.C.
13. **Denis, M.** 1991. Tumor necrosis factor and granulocyte macrophage-colony stimulating factor stimulate human macrophages to restrict growth of virulent Mycobacterium avium and to kill avirulent M. avium: killing effector mechanism depends on the generation of reactive nitrogen intermediates. J. Leukoc. Biol. **49**:380–387.
14. **Ding, A. H., C. F. Nathan, and D. J. Stuehr.** 1988. Release of reactive nitrogen intermediates and reactive oxygen intermediates from mouse peritoneal macrophages. Comparison of activating cytokines and evidence for independent production. J. Immunol. **141**:2407–2412.
15. **Fearon, D. T., and R. M. Locksley.** 1996. The instructive role of innate immunity in the acquired immune response. Science **272**:50–53.
16. **Fet, V., M. E. Dickinson, and B. L. Hogan.** 1989. Localization of the mouse gene for secreted phosphoprotein 1 (Spp-1) (2ar, osteopontin, bone sialoprotein 1, 44-kDa bone phosphoprotein, tumor-secreted phosphoprotein) to chromosome 5, closely linked to Ric (Rickettsia resistance). Genomics **5**:375–377.
17. **Flesch, I., and S. H. Kaufmann.** 1987. Mycobacterial growth inhibition by interferon-gamma-activated bone marrow macrophages and differential susceptibility among strains of Mycobacterium tuberculosis. J. Immunol. **138**: 4408–4413.
18. **Flesch, I. E., J. H. Hess, I. P. Oswald, and S. H. Kaufmann.** 1994. Growth inhibition of Mycobacterium bovis by IFN-gamma stimulated macrophages: regulation by endogenous tumor necrosis factor-alpha and by IL-10. Int. Immunol. **6**:693–700.
19. **Flynn, J. L., J. Chan, K. J. Triebold, D. K. Dalton, T. A. Stewart, and B. R. Bloom.** 1993. An essential role for interferon gamma in resistance to Mycobacterium tuberculosis infection. J. Exp. Med. **178**:2249–2254.
20. **Flynn, J. L., M. M. Goldstein, J. Chan, K. J. Triebold, K. Pfeffer, C. J. Lowenstein, R. Schreiber, T. W. Mak, and B. R. Bloom.** 1995. Tumor necrosis factor-alpha is required in the protective immune response against Mycobacterium tuberculosis in mice. Immunity **2**:561–572.
21. **Giachelli, C. M., N. Bae, M. Almeida, D. T. Denhardt, C. E. Alpers, and S. M. Schwartz.** 1993. Osteopontin is elevated during neointima formation in rat arteries and is a novel component of human atherosclerotic plaques. J. Clin. Investig. **92**:1686–1696.
22. **Giachelli, C. M., D. Lombardi, R. J. Johnson, C. E. Murry, and M. Almeida.** 1998. Evidence for a role of osteopontin in macrophage infiltration in response to pathological stimuli in vivo. Am. J. Pathol. **152**:353–358.
23. **Groves, M. G., D. L. Rosenstreich, B. A. Taylor, and J. V. Osterman.** 1980. Host defenses in experimental scrub typhus: mapping the gene that controls natural resistance in mice. J. Immunol. **125**:1395–1399.
24. **Hirota, S., M. Imakita, K. Kohri, A. Ito, E. Morii, S. Adachi, H. M. Kim, Y. Kitamura, C. Yutani, and S. Nomura.** 1993. Expression of osteopontin messenger RNA by macrophages in atherosclerotic plaques. A possible association with calcification. Am. J. Pathol. **143**:1003–1008.
25. **Hwang, S. M., C. A. Lopez, D. E. Heck, C. R. Gardner, D. L. Laskin, J. D. Laskin, and D. T. Denhardt.** 1994. Osteopontin inhibits induction of nitric oxide synthase gene expression by inflammatory mediators in mouse kidney epithelial cells. J. Biol. Chem. **269**:711–715.
26. **Hyman, B. T., K. Marzloff, and P. V. Arriagada.** 1993. The lack of accumulation of senile plaques or amyloid burden in Alzheimer's disease suggests a dynamic balance between amyloid deposition and resolution. J. Neuropathol. Exp. Neurol. **52**:594–600.
27. **Irizarry, M. C., F. Soriano, M. McNamara, K. J. Page, D. Schenk, D. Games, and B. T. Hyman.** 1997. Aβ deposition is associated with neuropil changes, but not with overt neuronal loss in the human amyloid precursor protein V717F (PDAPP) transgenic mouse. J. Neurosci. **17**:7053–7059.
28. **Liaw, L., D. E. Birk, C. B. Ballas, J. S. Whitsitt, J. M. Davidson, and B. L. M. Hogan.** 1998. Altered wound healing in mice lacking a functional osteopontin gene (spp1). J. Clin. Investig. **101**:1468–1478.
29. **Liaw, L., M. P. Skinner, E. W. Raines, R. Ross, D. A. Cheresh, S. M. Schwartz, and C. M. Giachelli.** 1995. The adhesive and migratory effects of osteopontin are mediated via distinct cell surface integrins. Role of alpha v beta 3 in smooth muscle cell migration to osteopontin in vitro. J. Clin. Investig. **95**:713–724.
30. **MacMicking, J. D., R. J. North, R. La Course, J. S. Mudgett, S. K. Shah, and C. F. Nathan.** 1997. Identification of nitric oxide synthase as a protective locus against tuberculosis. Proc. Natl. Acad. Sci. USA **94**:5243–5248.
31. **McCarthy, J. B., B. V. Vachhani, S. M. Wahl, D. S. Finbloom, and G. M. Feldman.** 1997. Human monocyte binding to fibronectin enhances IFN-gamma-induced early signaling events. J. Immunol. **159**:2424–2430.
32. **Murray, P. J., L. Wang, C. Onufryk, R. I. Tepper, and R. A. Young.** 1997. T

cell-derived IL-10 antagonizes macrophage function in mycobacterial infection. J. Immunol. **158**:315–321.
33. **Murry, C. E., C. M. Giachelli, S. M. Schwartz, and R. Vracko.** 1994. Macrophages express osteopontin during repair of myocardial necrosis. Am. J. Pathol. **145**:1450–1462.
34. **Nasu, K., T. Ishida, M. Setoguchi, Y. Higuchi, S. Akizuki, and S. Yamamoto.** 1995. Expression of wild-type and mutated rabbit osteopontin in Escherichia coli, and their effects on adhesion and migration of P388D1 cells. Biochem. J. **307**:257–265.
35. **Nau, G. J., P. Guilfoile, G. L. Chupp, J. S. Berman, S. J. Kim, H. Kornfeld, and R. A. Young.** 1997. A chemoattractant cytokine associated with granulomas in tuberculosis and silicosis. Proc. Natl. Acad. Sci. USA **94**:6414–6419.
36. **Pablos-Mendez, A., A. Laszlo, F. Bustreo, N. Binkin, D. L. Cohn, C. S. B. Lambregts-van Weezenbeek, S. J. Kim, P. Chaulet, P. Nunn, and M. C. Raviglione.** 1997. Anti-tuberculosis drug resistance in the world. WHO/TB/97.229. World Health Organization, Geneva, Switzerland.
37. **Patarca, R., G. J. Freeman, R. P. Singh, F. Y. Wei, T. Durfee, F. Blattner, D. C. Regnier, C. A. Kozak, B. A. Mock, H. D. Morse, et al.** 1989. Structural and functional studies of the early T lymphocyte activation 1 (Eta-1) gene. Definition of a novel T cell-dependent response associated with genetic resistance to bacterial infection. J. Exp. Med. **170**:145–161.
38. **Patarca, R., R. A. Saavedra, and H. Cantor.** 1993. Molecular and cellular basis of genetic resistance to bacterial infection: the role of the early T-lymphocyte activation-1/osteopontin gene. Crit. Rev. Immunol. **13**:225–246.
39. **Rollo, E. E., D. L. Laskin, and D. T. Denhardt.** 1996. Osteopontin inhibits nitric oxide production and cytotoxicity by activated RAW264.7 macrophages. J. Leukoc. Biol. **60**:397–404.
40. **Rook, G. A., J. Steele, L. Fraher, S. Barker, R. Karmali, J. O'Riordan, and J. Stanford.** 1986. Vitamin D3, gamma interferon, and control of proliferation of Mycobacterium tuberculosis by human monocytes. Immunology **57**: 159–163.
41. **Schmits, R., J. Filmus, N. Gerwin, G. Senaldi, F. Kiefer, T. Kundig, A. Wakeham, A. Shahinian, C. Catzavelos, J. Rak, C. Furlonger, A. Zakarian, J. J. Simard, P. S. Ohashi, C. J. Paige, J. C. Gutierrez-Ramos, and T. W. Mak.** 1997. CD44 regulates hematopoietic progenitor distribution, granuloma formation, and tumorigenicity. Blood **90**:2217–2233.
42. **Singh, R. P., R. Patarca, J. Schwartz, P. Singh, and H. Cantor.** 1990. Definition of a specific interaction between the early T lymphocyte activation 1 (Eta-1) protein and murine macrophages in vitro and its effect upon macrophages in vivo. J. Exp. Med. **171**:1931–1942.
43. **Smith, R. E., C. M. Hogaboam, R. M. Strieter, N. W. Lukacs, and S. L. Kunkel.** 1997. Cell-to-cell and cell-to-matrix interactions mediate chemokine expression: an important component of the inflammatory lesion. J. Leukoc. Biol. **62**:612–619.
44. **Stenger, S., and R. L. Modlin.** 1998. Cytotoxic T cell responses to intracellular pathogens. Curr. Opin. Immunol. **10**:471–477.
45. **Uede, T., Y. Katagiri, J. Iizuka, and M. Murakami.** 1997. Osteopontin, a coordinator of host defense system: a cytokine or an extracellular adhesive protein? Microbiol. Immunol. **41**:641–648.
46. **Valway, S. E., M. P. C. Sanchez, T. F. Shinnick, I. Orme, T. Agerton, D. Hoy, J. S. Jones, H. Westmoreland, and I. M. Onorato.** 1998. An outbreak involving extensive transmission of a virulent strain of *Mycobacterium tuberculosis*. N. Engl. J. Med. **338**:633–639.
47. **Weber, G. F., S. Ashkar, M. J. Glimcher, and H. Cantor.** 1996. Receptor-ligand interaction between CD44 and osteopontin (Eta-1). Science **271**:509–512.
48. **West, M. J.** 1993. New stereological methods for counting neurons. Neurobiol. Aging **14**:275–285.
49. **Xie, Q. W., H. J. Cho, J. Calaycay, R. A. Mumford, K. M. Swiderek, T. D. Lee, A. Ding, T. Troso, and C. Nathan.** 1992. Cloning and characterization of inducible nitric oxide synthase from mouse macrophages. Science **256**:225–228.
50. **Yu, X. Q., D. J. Nikolic-Paterson, W. Mu, C. M. Giachelli, R. C. Atkins, R. J. Johnson, and H. Y. Lan.** 1998. A functional role for osteopontin in experimental crescentic glomerulonephritis in the rat. Proc. Assoc. Am. Physicians **110**:50–64.
51. **Yue, T. L., P. J. McKenna, E. H. Ohlstein, M. C. Farach-Carson, W. T. Butler, K. Johanson, P. McDevitt, G. Z. Feuerstein, and J. M. Stadel.** 1994. Osteopontin-stimulated vascular smooth muscle cell migration is mediated by beta 3 integrin. Exp. Cell Res. **214**:459–464.
52. **Zhu, H., J. P. Cong, G. Mamtora, T. Gingeras, and T. Shenk.** 1998. Cellular gene expression altered by human cytomegalovirus: global monitoring with oligonucleotide arrays. Proc. Natl. Acad. Sci. USA **95**:14470–14475.

Editor: S. H. E. Kaufmann

Scand. J. Immunol. **50**, 145–149, 1999

Costimulation of $CD28^-$ T Cells Through CD3 and β_1-Integrins Induces a Limited Th1 Cytokine Response

J. J. SAUKKONEN, A. TANTRI & J. BERMAN

The Pulmonary Center, Boston University Medical School, Boston, MA, USA

(Received 1 September 1998; Accepted in revised form 3 March 1999)

Saukkonen JJ, Tantri A, Berman J. Costimulation of $CD28^-$ T Cells Through CD3 and β_1-Integrins Induces a Limited Th1 Cytokine Response. Scand J Immunol 1999;50:145–149

The costimulatory molecule CD28 regulates antigen-specific T-cell proliferation and the synthesis of multiple cytokines. The absence of CD28 on a subset of $CD8^{bright+}$ T cells suggests that these cells may utilize alternative costimulatory pathways or have a limited cytokine response to presented antigen. We used fibronectin, a ligand for the β_1-integrins $\alpha_4\beta_1$ and $\alpha_5\beta_1$, as an alternate costimulatory ligand to assess the functional phenotype of $CD8^{bright+}CD28^-$ T cells. CD25 expression was significantly up-regulated in $CD8^{bright+}CD28^-$ T cells by immobilized anti-$CD3_i$ with fibronectin. Costimulation with fibronectin also significantly augmented anti-$CD3_i$-induced IFN-γ production only among $CD8^{bright+}CD28^-$ T cells. The $CD8^{bright+}CD28^-$ T cells did not produce significant IL-2 and IL-10 even in response to maximal stimulation with phorbol myristate acetate and ionomycin. These data support a costimulatory role for β_1-integrins in $CD8^{bright+}CD28^-$ T cells and indicate that $CD8^{bright+}$ $CD28^-$ T cells have a restricted Th1 cytokine repertoire.

J. J. Saukkonen, Pulmonary Center, Boston University School of Medicine, 80 East Concord Street, R-304, Boston, MA 02118, USA

INTRODUCTION

CD28 is a critical costimulatory molecule, markedly augmenting both anti-CD3-induced T-cell proliferation [1–4] and the secretion of multiple cytokines [5, 6]. CD28 is expressed by the majority of circulating T cells, while $CD28^-$ lymphocytes are found among $CD8^{bright+}$ T cells and $CD8^{dim+}$ natural killer (NK) cells [7–10]. However, large $CD28^-$ T-cell populations are found in normal lung and in progressive HIV infection [11–16]. Functionally, T cells lacking CD28 display limited proliferation in response to anti-CD3 [10, 15–18]. In particular, $CD28^-$ T cells may have a restricted ability to produce the array of cytokines normally regulated through the CD28 pathway. We tested the hypothesis that $CD8^{bright+}CD28^-$ T cells could utilize β_1-integrins as alternative costimulatory molecules. To assess the feasibility of costimulating $CD8^{bright+}CD28^-$ T cells through β_1-integrins, we first determined the surface expression of $\alpha_4\beta_1$ and $\alpha_5\beta_1$ on these cells. Subsequently, we assessed the induction of both CD25 and the cytokines interferon (IFN)-γ, interleukin (IL-2) and IL-10 in $CD8^{bright+}CD28^-$ T cells following costimulation with fibronectin (FN) and anti-$CD3_i$.

MATERIALS AND METHODS

T-cell isolation. Peripheral blood mononuclear cells (PBMC) were prepared by Ficoll-Paque (Pharmacia Biotech, Uppsala, Sweden) centrifugation at 500 *g* for 45 min. T cells were subsequently isolated by nylon wool nonadherence.

Monoclonal antibodies. The following monoclonal antibodies (MoAbs) were used for extracellular antigen staining: anti-CD8 (Biosource, Camarillo, CA, USA), RED613-conjugated goat anti-mouse (Gibco BRL, Gaithersburg, MD, USA), anti-CD25-fluorescein isothiocyanate (FITC; Becton-Dickinson, Mountain View, CA, USA), anti-CD28-phycoerythrin (PE; Pharmingen, San Diego, CA, USA) or -FITC (Immunotech, Westbrook, ME, USA), and anti-VLA4 ($\alpha_4\beta_1$) and anti-VLA5 ($\alpha_5\beta_1$, Immunotech). Intracellular MoAbs (Pharmingen) used included: anti-IFN-γ-FITC, anti-IL-2-PE, and IL-10-PE. Negative isotype-specific controls (Pharmingen) in the appropriate concentrations were used to determine the limits of nonspecific fluorescence.

T-cell stimulation. T cells were added to plastic 48-well plates (Costar, Cambridge, MA, USA) with or without anti-$CD3_i$ (150 ng/well, Biosource) and FN (10 μg/well), or phorbol myristate acetate (PMA; 3 μM, Sigma, St. Louis, MO, USA) with ionomycin (I; 0.5 μM, Sigma). Cells were cultured in RPMI (Mediatech) with 10% fetal calf serum (FCS; Sigma) plus monensin (3 μM, Pharmingen) for 24–48 h, periods that were found to be optimal for these studies.

Surface antigen and intracellular cytokine staining. The method of Sander *et al.* was modified for surface antigen staining followed by intracellular cytokine staining [19–22]. T cells (0.5×10^6) in 500 μl of staining buffer (phosphate-buffered saline, PBS, 0.1% sodium azide and 1% FBS; pH 7.5) were stained with extracellular MoAbs at 4 °C for 25 min, washed and fixed in 100 μl 4% paraformaldehyde (Baker, Phillipsburg, NJ). Cells were permeabilized in 50 μl of 0.1% saponin (Sigma) in PBS with 1% heat-inactivated FCS and 0.1% sodium azide, then stained with intracellular cytokine antibody (Ab) or control Ab for 30 min at 4 °C. Cells were washed in permeabilization buffer and resuspended in 150 μl of 10% formalin (Fisher Scientific, Fair Lawn, NJ, USA) and 550 μl of staining buffer.

Flow cytometric analysis of extracellular and intracellular antigen staining. Cells were analysed on a Becton-Dickinson FACScan flow cytometer. Data were gated on $CD8^{bright+}$ cells and controls were used to determine the 95% confidence interval of nonspecific staining.

Statistical analysis. The Wilcoxon signed rank test was used to identify differences between paired groups, where appropriate the Student's *t*-test was used for smaller numbers.

RESULTS

Both $CD8^{bright+}CD28^-$ and $CD8^{bright+}CD28^+$ T cells express β_1 integrins

The data given in Fig. 1 and Table 1 show that a substantial number of $CD8^{bright+}CD28^-$ T cells expressed $\alpha_4\beta_1$ and $\alpha_5\beta_1$ ligands for FN. These data indicate that ≈ 30% of $CD8^{bright+}CD28^-$ T cells should be responsive to FN costimulation.

FN costimulation induced comparable CD25 expression in $CD8^{bright+}CD28^-$ and $CD8^{bright+}CD28^+$ T cells

CD25 expression was increased significantly on $CD8^{bright+}CD28^-$ T cells by costimulation with anti-$CD3_i$ and FN ($P=0.045$) for 24 h but not by anti-CD3 alone, when compared with unstimulated cells (Fig. 2). Costimulation with anti-$CD3_i$ and FN tended to increase CD25 expression beyond that achieved by anti-$CD3_i$ alone, but this augmentation did not achieve statistical significance for either the $CD8^{bright+}CD28^+$ or $CD28^-$ T-cell subset. Addition of a neutralizing antibody to IL-2 failed to block CD25 up-regulation on either $CD8^{bright+}CD28^-$ or $CD8^{bright+}CD28^+$ T cells (data not shown), suggesting that CD25 up-regulation in this system was not dependent on paracrine IL-2 secreted by activated T cells.

Table 1. Percentage of $CD^{bright+}$ T cells expressing β_1-integrins

	$CD28^-$		$CD28^+$	
Donor	α4β1	α5β1	α4β1	α5β1
1	16.1	10.7	44.8	31
2	39.1	55.7	45.1	56.2
3	41	23.7	56.2	43.3
4	59.5	6.3	75.8	23.7
5	15.5	5.8	34.1	14.8
6	24.2	49.1	49.2	56.9
Mean	32.6	25.2	50.9*	37.7†
SEM	7.0	9.0	5.8	7.1

*$P=0.003$; †$P=0.012$, compared with $CD28^-$.

β_1-Integrin costimulation induced significant intracellular IFN-γ only in $CD8^{bright+}CD28^-$ T cells

Activation of $CD8^{bright+}CD28^-$ T cells with CD3 and FN induced significant IFN-γ production beyond that achieved through CD3 alone (Fig. 3, mean percentage cells positive ± SEM 22.6 ± 6.8 versus 13.7 ± 6, respectively, $P=0.018$). However, $CD8^{bright+}CD28^+$ T cells failed to display a significant increase in intracellular IFN-γ in response to either anti-$CD3_i$ alone or with FN. The production of IFN-γ, following anti-$CD3_i$ + FN costimulation, tended to be higher among $CD8^{bright+}CD28^-$ T cells than among $CD8^{bright+}CD28^+$ T cells, a finding which approached statistical significance (mean percentage cells positive ± SEM 22.6 ± 6.8 versus 2.5 ± 1.2, respectively, $P=0.067$).

Intracellular IL-2 and IL-10 production by $CD8^{bright+}CD28^-$ and $CD8^{bright+}CD28^+$ T cells

Maximal stimulation with PMA-I significantly increased, over unstimulated controls, the production of IL-2 (mean percentage cells positive ± SEM 22.2 ± 5.2 versus 6.4 ± 0.7, $P=0.0309$) and IL-10 (14.6 ± 2.4 versus 7.9 ± 0.5, $P=0.042$) only by $CD8^{bright+}CD28^+$ T cells (Figs 4 and 5). This suggested that $CD8^{bright+}CD28^-$ T cells have a restricted cytokine repertoire compared with $CD8^{bright+}CD28^+$ T cells. Submaximal stimuli, such as anti-$CD3_i$, with or without FN, failed to induce a significant increase in IL-2 or IL-10 for either group of T cells.

DISCUSSION

We examined the functional capabilities of a unique subset of $CD8^+$ T cells that lack CD28, a predominant population which we identified previously in normal lung and in HIV-infected patients. This paper reports two findings regarding $CD8^{bright+}CD28^-$ T cells [1]: they can be costimulated through the β_1-integrins $\alpha_4\beta_1$ and $\alpha_5\beta_1$, and [2] they are potent producers of IFN-γ, but not of IL-2 or IL-10.

Whole T-cell populations have been successfully costimulated through β_1-integrins, inducing proliferation and increasing IL-2 and IFN-γ production beyond that induced by anti-$CD3_i$ alone [23–27]. We found that 25–30% of $CD8^{bright+}CD28^-$ T cells expressed $\alpha_4\beta_1$ and $\alpha_5\beta_1$ integrins, constituting a substantial subset capable of binding FN. Costimulation with anti-$CD3_i$ and FN increased surface expression of the activation marker CD25, and induced intracellular IFN-γ production beyond that induced by anti-$CD3_i$ alone. A neutralizing antibody to IL-2 failed to block CD25 up-regulation on costimulated $CD8^{bright+}CD28^-$ and $CD8^{bright+}CD28^+$ T cells. Thus, CD25 up-regulation on

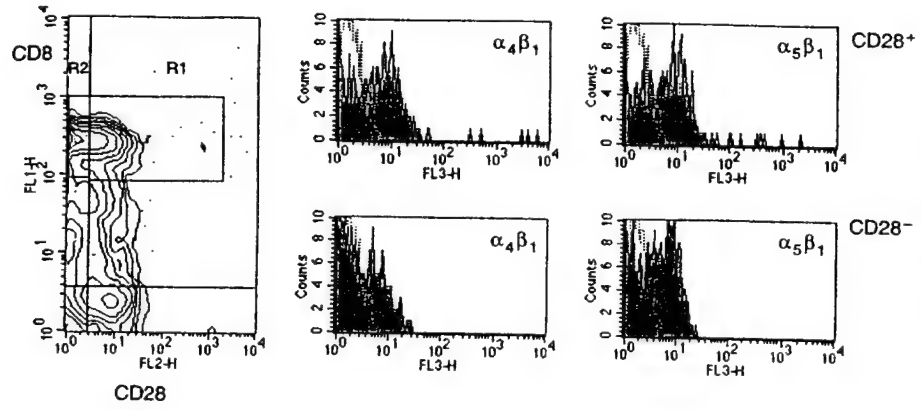

Fig. 1. CD8$^{bright+}$CD28$^-$ and CD8$^{bright+}$CD28$^+$ T cells express $\alpha_4\beta_1$ and $\alpha_5\beta_1$ integrins. Three-colour flow cytometry was used to first identify CD8$^{bright+}$CD28$^+$ and CD8$^{bright+}$CD28$^-$ T cells, shown here as R1 and R2, respectively, on a two-dimensional contour plot. Histograms were then constructed for $\alpha_4\beta_1$ and $\alpha_5\beta_1$ integrin expression for each of these populations. Staining from the isotype control is represented by the dotted lines.

CD8$^{bright+}$CD28$^-$ T cells was not related to paracrine IL-2 secreted by CD28$^+$ T cells also activated by the same stimuli. CD8$^{bright+}$CD28$^-$ T cells, unlike CD8$^{bright+}$CD28$^+$ T cells, failed to produce significant IL-2 and IL-10 despite maximal activation with PMA-I. These data indicate that CD8$^{bright+}$CD28$^-$ T cells may be costimulated through β_1-integrins and indicate that CD8$^{bright+}$CD28$^-$ T cells have a restricted T-helper (Th)1 cytokine repertoire.

The β_1-integrin-mediated activation of CD28$^-$CD8$^{bright+}$ T cells was remarkable for the magnitude and specificity of the cytokine response. Since 25–30% of CD8$^{bright+}$CD28$^-$ T cells expressed $\alpha_4\beta_1$ and $\alpha_5\beta_1$, approximately one-half of the cells capable of responding did so. The method of intracellular staining with monensin typically yields positive signals in the 5% range for T cells [19–22], much lower than the response elicited here. Stimulation of CD8$^{bright+}$CD28$^-$ T cells induced only IFN-γ, even in response to PMA-I. Significant IL-2 and IL-10 production was seen only among CD8$^{bright+}$CD28$^+$ T cells and only in response to PMA-I. T cells from the CD28-deficient mouse and human CD28$^-$ blood T cells have also been reported to be incapable of producing IL-2 [12, 22]. The CD28 pathway stabilizes IL-2 mRNA [5, 29] thus, IL-2 gene expression may be short lived in CD28$^-$ T cells [12]. The inability of CD8$^{bright+}$CD28$^-$ T cells to produce IL-2 may hinder the production of IL-2-dependent cytokines [30]. In contrast, the production of IFN-γ may be enhanced by, but does not require, CD28 costimulation [5, 29, 30]. Thus, CD8$^{bright+}$CD28$^-$ T cells, despite activation eliciting CD25 expression, are restricted in their cytokine repertoire, suggesting that these T cells have differentiated.

The CD28$^-$ T-cell subset consists of effector cells with limited replicative ability. These cells express markers associated with cytotoxic T-lymphocytes (CTL) [11, 15], are capable of anti-CD3-redirected cytolysis and of major histocompatibilty complex (MHC)-restricted cytotoxicity [10]. Early data regarding CD28$^-$ T cells indicated that they were capable of acting as suppressor cells [17, 18, 31]. Clonally expanded CD28$^-$CD8$^+$ T cells have shortened telomeres compared with CD28$^+$CD8$^+$ T cells, suggesting that the former have undergone more rounds of replication than the latter and are limited in future replicative ability [32]. We previously reported that 70% of normal alveolar

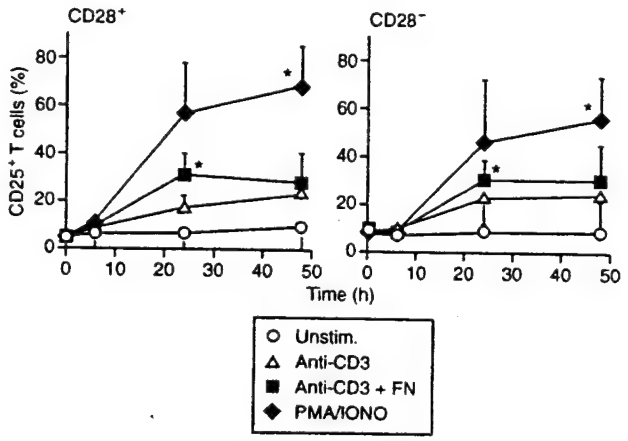

Fig. 2. Costimulated CD8$^{bright+}$CD28$^-$ and CD8$^{bright+}$CD28$^+$ T cells express CD25. Three-colour flow cytometry was used to assess CD25 surface expression on CD8$^{bright+}$CD28$^-$ and CD8$^{bright+}$CD28$^+$ T cells in response to stimuli ($n = 6$). Costimulation for 24 h with anti-CD3$_i$ and FN, but not anti-CD3$_i$ alone, significantly increased CD25 surface expression on both T-cell subtypes compared with unstimulated T cells.

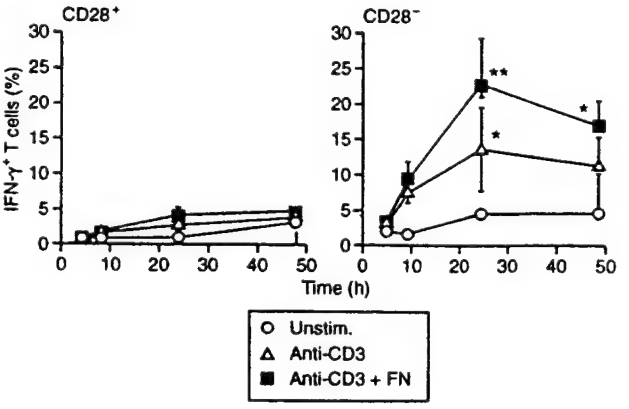

Fig. 3. β_1-integrin costimulated CD8$^{bright+}$CD28$^-$ T cells produce intracellular IFN-γ. T cells were cultured in the presence of monensin, stained for surface expression of CD8 and CD28, fixed, permeabilized with saponin, and stained with antibody to IFN-γ ($n = 7$). Anti-CD3$_i$ plus FN significantly augmented intracellular IFN-γ production beyond that induced by anti-CD3$_i$ alone at 24 h.

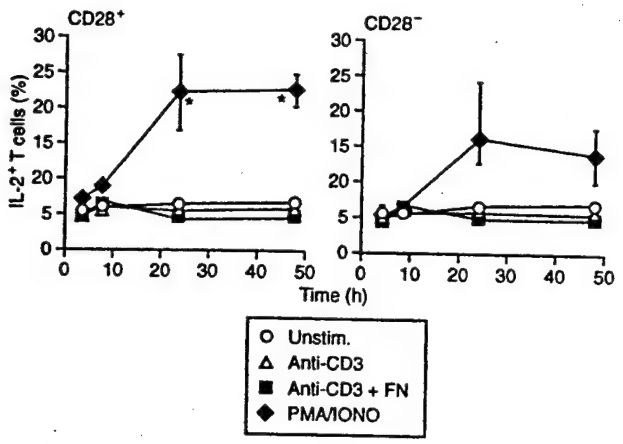

Fig. 4. Intracellular IL-2 production induced by activation of $CD8^{bright+}CD28^+$, but not $CD8^{bright+}CD28^-$, T cells. T cells were cultured and stimulated as in Fig. 3 and stained with antibody to IL-2 ($n = 6$). Three-colour flow cytometry demonstrated that intracellular IL-2 was signficantly increased by PMA-I only in $CD8^{bright+}CD28^+$ T cells.

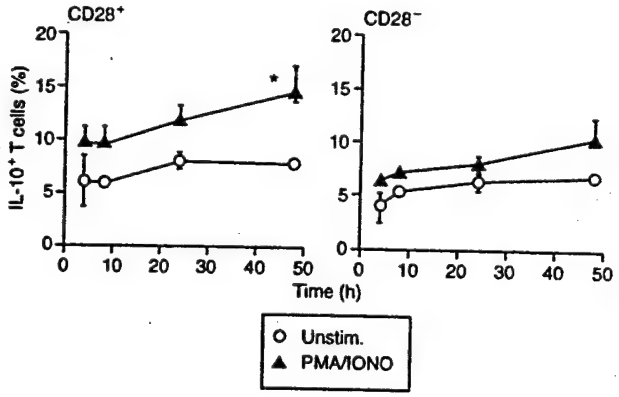

Fig. 5. Intracellular IL-10 production induced by activation of $CD8^{bright+}CD28^+$, but not $CD8^{bright+}CD28^-$, T cells. T cells were cultured and stimulated as described in Fig. 3 and intracellular cytokine detection performed to detect IL-10. Only $CD28^+CD8^{bright+}$ T cells produced significant intracellular IL-10 in response to PMA-I ($n = 5$).

$CD8^+$ T cells express CD28 [11], a significant population to have limited replicative ability. The mucosa of the lung is a site of chronic and diverse antigenic exposure, where a restricted and regulated immune response is desirable. Alveolar macrophages do not normally express B7 costimulatory molecules, ligands for CD28 [33], limiting the generation of antigen-specific T-cell responses. The majority of alveolar $CD8^{bright+}$ T cells are likely to be activated through alternative costimulatory pathways such as the β_1-integrins, leading to a restrained immune response.

ACKNOWLEDGEMENTS

We would like to thank Dr Geoffrey Chupp and Mr Eric Wright for their technical assistance. This work was supported by the Edward Welch Research Fund of the Massachusetts Thoracic Society, the Parker B. Francis Foundation and the National Heart, Lung and Blood Institute #1 R29 HL53249 02 (J.J.S.). J.S.B. is supported by SCOR #P50HL56386.

REFERENCES

1 Azuma M, Cayabyab M, Buck D, Phillips J, Lanier L. CD28 interaction with B7 costimulates primary allogeneic proliferative response and cytotoxicity mediated by small resting T lymphocytes. J Exp Med 1992;175:353–60.

2 Cerdan C, Martin Y, Courcol M, Mawas C, Birg F, Olive D. CD28 costimulation up-regulates long-term IL-2R beta expression in human T cells through combined transcriptional and post-transcriptional regulation. J Immunol 1995;154:1007–13.

3 Harding F, Allison J. CD28–B7 interactions allow the induction of CD8+ cytotoxic T lymphocytes in the absence of exogenous help. J Exp Med 1993;177:1791–6.

4 Harding F, McArthur J, Gross J, Raulet D, Allison J. CD28-mediated signalling co-stimulates murine T cells and prevents induction of anergy in T-cell clones. Nature 1992;356:607–9.

5 Thompson C, Lindsten T, Ledbetter J, Kunkel S, Young H, Emerson S, Leiden J, June C. CD28 activation pathway regulates the production of multiple T-cell-derived lymphokines/cytokines. Proc Natl Acad Sci USA 1989;86:1333–7.

6 Walter H, Schepens S, Van Wauwe J, deBoer M. Ligation of CD28 on resting T cells by its ligand B7 results in the induction of both Th1- and Th2-type cytokines. Eur Cytokine Network 1994;5:13–21.

7 Yamada H, Martin P, Braun M, Beatty P, Sadamoto K, Hansen J. Monoclonal antibody 9.3 and anti-CD11 antibodies define reciprocal subsets of lymphocytes. Eur J Immunol 1985;15:1164–8.

8 Linsley P, Ledbetter J. The role of the CD28 receptor during T cell responses to antigen. Annu Rev Immunol 1993;11:191–212.

9 Martin P, Ledbetter J, Morishita Y, June C, Beatty P, Hansen J. A 44 kilodalton cell surface homodimer regulates interleukin-2 production by activated human T lymphocytes. J Immunol 1986;136:3282–7.

10 Azuma M, Phillips J, Lanier L. CD28-T lymphocytes: antigenic and functional properties. J Immunol 1993;150:1147–59.

11 Saukkonen J, Kornfeld H, Berman J. Expansion of a $CD8^+CD28^-$ T cell population in blood and lungs of HIV^+ patients. J Acquired Immunodeficiency Syndrome 1993;6:1194–203.

12 Hoshino T, Yamada A, Honda J *et al.* Tissue-specific distribution and age-dependent increase of human $CD11b^+$ T cells. J Immunol 1993;151:2237–46.

13 Brinchman J, Dobloug J, Heger B, Haaheim L, Sannes M, Egelund T. Expression of costimulatory molecule CD28 on T cells in human immunodeficiency virus type 1 infection: functional and clinical correlations. J Infect Dis 1994; 169:730–8.

14 Choremi-Papadopoulo H, Viglis V, Gargalianos P, Kordossis T, Iniotaki-Theodoraki A, Kosmidis J. Downregulation of CD28 surface antigen on $CD4^+$ and $CD8^+$ T lymphocytes during HIV-1 infection. J Acquired Immunodeficiency Syndromes 1994;7:245–53.

15 Borthwick N, Bofill M, Gombert W, Akbar A, Medina E, Sagawa K, Lipman M, Johnson M, Janossy G. Lymphocyte activation in HIV-1 infection. II. Functional defects of $CD28^-$ T cells. AIDS 1994;8:431–41.

16 Vingerhoets J, Vanham G, Kestens L *et al.* Increased cytolytic T lymphocyte activity and decreased B7 responsiveness are associated

with CD28 down-regulation on CD8$^+$ T cells from HIV-infected subjects. Clin Exp Immunol 1995;100:425–33.

17 Damle N, Mohagheghpour N, Hansen J, Engleman E. Alloantigen-specific cytotoxic and suppressor T lymphocytes are derived from phenotypically distinct precursors. J Immunol 1983;131:2296–9.

18 Li S, Ottenhof T, Van den Elsen P *et al.* Human suppressor T cell clones lack CD28. Eur J Immunol 1990;20:1281–8.

19 Sander B, Andersson J, Andersson U. Assessment of cytokines by immunofluorescence and the paraformaldehyde-saponin procedure. Immunol Rev 1991;119:65–93.

20 Assenmacher M, Scmilz J, Radbruch A. Flow cytometric determination of cytokines in activated murine T-helper lymphocytes. Eur J Immunol 1994;24:1097–101.

21 Jung T, Schauer U, Heusser C, Neumann C, Rieger C. Detection of intracellular cytokines by flow cytometry. J Immunol Methods 1993;159:197–207.

22 Prussin C, Metcalf D. Detection of intracytoplasmic cytokine using flow cytometry and directly conjugated anti-cytokine antibodies. J Immunol Methods 1995;188:117–28.

23 Shimizu Y, van Seventer G, Horgan K, Shaw S. Co-stimulation of proliferative response of resting CD4:$^+$ T cells by the interaction of VLA-4 and VLA-5 with fibronectin. J Immunol 1990;145:59.

24 Udagawa T, McIntyre B. A VLA-4 alpha-chain specific monoclonal antibody enhances CD3-induced IL-2/Il-2 receptor-dependent T-cell proliferation. Lymphokine Cytokine Res 1992;11:193–9.

25 Yamada A, Nojima Y, Sugita K, Dang N, Schlossman S, Morimoto C. Crosslinking of VLA/CD29 moleclue has a co-mitogenic effect with anti-CD3 on CD4 cell activation in serum-free culture system. Eur J Immunol 1991;21:319–25.

26 Yamada A, Nikaido T, Nojima Y, Schlossman S, Morimoto C. Activation of human CD4 T lymphocytes: interaction of fibronectin with VLA-5 receptor on CD4 cells induces AP-1 transcription factor. J Immunol 1991;146:53–6.

27 Ofosu-Appiah W, Warrington R, Morgan K, Wilkins J. Lymphocyte extracellular matrix interactions: induction of interferon by connective tissue components. Scand J Immunol 1989;29:517–25.

28 Lucas P, Negishi I, Nakayama K, Fields L, Loh D. Naive CD28 deficient T cells can initiate but not sustain an *in vitro* antigen–specific immune response. J Immunol 1995;154:5757–68.

29 Morvan P, Picot C, Dejour R, Genetet B, Genetet N. Distinct pattern of IL-2 and IFN-γ gene expression in CD4 and CD8 T cells: cytofluorometric analysis at a single cell level using non-radioactive probes. Cell Mol Biol 1995;41:945–57.

30 Kuiper H, de Jong R, Brouwer M, Lammers K, Wijdenes J, van Lier R. Influence of CD28 costimulation on cytokine production is mainly regulated via interleukin 2. Immunology 1994;83:38–44.

31 Lum L, Orcutt-Thordarson N, Seigneuret M, Hansen J. *In vitro* regulation of immunoglobulin synthesis by T cell subpopulations defined by a new human T cell antigen (9.3). Cell Immunol 1982;72:122–9.

32 Monteiro J, Batliwalla F, Ostrer H, Gregersen P. Shortened telomeres in clonally expanded CD28–CD8$^+$ T cells imply a replicative history that is distinct from their CD28$^+$–CD8$^+$ counterparts. J Immunol 1996;156:3587–90.

33 Chelen C, Fang Y, Freeman G *et al.* Human alveolar macrophages present antigen ineffectively due to defective expression of B7 costimulatory cell surface molecules. J Clin Invest 1995; 95:1415–21.

Proc. Natl. Acad. Sci. USA
Vol. 94, pp. 6414–6419, June 1997
Medical Sciences

A chemoattractant cytokine associated with granulomas in tuberculosis and silicosis

GERARD J. NAU*†, PATRICK GUILFOILE*‡, GEOFFREY L. CHUPP§, JEFFREY S. BERMAN§¶, SUE J. KIM§, HARDY KORNFELD§, AND RICHARD A. YOUNG*‖

*Whitehead Institute for Biomedical Research, Nine Cambridge Center, and Department of Biology, Massachusetts Institute of Technology, Cambridge, MA 02142; †Infectious Disease Unit, Massachusetts General Hospital, Fruit Street, Boston, MA 02114; §Pulmonary Center, Boston University School of Medicine, 80 East Concord Street, Boston, MA 02188; and ¶Boston Veterans Affairs Medical Center, 150 South Huntington Avenue, Boston, MA 02130

Communicated by Stanley Falkow, Stanford University, Stanford, CA, April 7, 1997 (received for review February 10, 1997)

ABSTRACT **Chronic inflammation and granuloma formation are associated with mononuclear cell infiltrates and are characteristic pathologic responses in tuberculosis. To identify host cell genes involved in tuberculous pathology, we screened macrophage cDNA libraries for genes induced by mycobacterial infection. One gene isolated in this screen, osteopontin (also known as early T lymphocyte activation protein 1 or Eta-1), was of particular interest because it is a cytokine and macrophage chemoattractant. Further study revealed that *Mycobacterium tuberculosis* infection of primary human alveolar macrophages causes a substantial increase in osteopontin gene expression. Osteopontin protein was identified by immunohistochemistry in macrophages, lymphocytes, and the extracellular matrix of pathologic tissue sections of patients with tuberculosis. Increased osteopontin expression also was found to be associated with silicosis, another granulomatous disease. The association of osteopontin with granulomatous pathology, together with the known properties of the protein, suggest that osteopontin may participate in granuloma formation. The strategy of identifying host genes whose expression is altered by infection thus can provide valuable clues to disease mechanisms and will be increasingly valuable as additional human genome sequences become available.**

Mycobacterial infections are among the most numerous in the world, with *Mycobacterium tuberculosis* believed to have infected one-third of the world's population (1). Aggravating the worldwide pandemic have been the emergence of resistant organisms and the concurrent HIV epidemic. These events have renewed interest in understanding the fundamental biology of the interactions between pathogenic mycobacteria and their host.

Exposure to *M. tuberculosis* can lead to a pulmonary infection characterized by macrophage recruitment to the site of infection, followed in many cases by granuloma formation (2–4). *M. tuberculosis* is a facultative intracellular pathogen whose cellular habitat is the macrophage (5–9). Thus, the *M. tuberculosis*–macrophage relationship is of considerable interest. Previous investigations have revealed that interleukin 1, tumor necrosis factor-α, interleukin 6, transforming growth factor-β, and interleukin 8 production by macrophages is increased by exposure to mycobacteria (10–14). Negative effects of mycobacteria on macrophage antigen presentation (15) and responsiveness to cytokines (16, 17) also have been documented. However, little is known about the molecular mechanisms involved in granuloma formation.

To gain insight into the host response to tuberculosis, we used differential screening of cDNA libraries to compare mRNAs of infected and uninfected macrophages. We reasoned that the identification of macrophage genes whose expression is altered after phagocytosis of *M. tuberculosis* might provide clues to pathogenesis. Using a model system that used a macrophage cell line (18, 19), we surveyed the population of macrophage mRNAs for those altered by mycobacterial infection. Genes identified with this strategy then were studied in human cells exposed to *M. tuberculosis* and in tissues from patients with tuberculosis. One gene identified repeatedly in this screen was particularly interesting because its protein product, osteopontin, is a cytokine and macrophage chemoattractant (20, 21). Osteopontin gene expression was induced by mycobacterial infection of human macrophages, and osteopontin protein was found in human tissue specimens from patients with clinical tuberculosis.

METHODS

Bacteria. *Mycobacterium bovis* bacillus Calmette–Guérin (American Type Culture Collection no. 35734) was grown from a frozen stock for 3 days (to OD_{600} ≈1.2) in Middlebrook 7H9 broth with 0.5% glycerol, 0.05% Tween 80, and ADC enrichment (Difco). BCG diluted 1:10 in RPMI medium 1640 with 1% fetal calf serum was added to J774 cells (bacteria:macrophage ratio approximately 10:1). The streptomycin-dependent strain of *Escherichia coli*, sd-4 (American Type Culture Collection no. 11143), was cultured in Luria–Bertani medium with streptomycin at 624 μg/ml. Frozen stocks in 20% glycerol were made from stationary-phase cultures after 2 days growth in Luria–Bertani medium containing 25 μg/ml streptomycin. On the day of infection these bacteria were thawed, were resuspended in 7H9 medium, and were diluted as for BCG (bacteria:macrophage approximately 1:1). These two ratios were required to achieve comparable percentages of infected macrophages; limited growth of the *E. coli* in the absence of streptomycin necessitated a lower ratio. Latex beads (0.8 μm, carboxylate-modified, Sigma no. L-1398) were treated with 70% ethanol before use.

Macrophage Culture and Infection. J774 cells (American Type Culture Collection no. TIB 67) were grown without antibiotics in RPMI medium 1640 with 10% low-endotoxin fetal calf serum (GIBCO/BRL) until infection. These cells were infected by incubation with either bacteria or beads for 4 hr, were washed three times with Hanks' balanced salt solution, and were cultured for an additional 20 hr before RNA harvest. During and after infection, cells were maintained in 1% low-endotoxin fetal calf serum as previously described (18). Alveolar macrophages were obtained from consenting human donors. Bronchoalveolar lavage cells were harvested by bronchoscopy and plated at a density of 500,000 cells/ml. Alveolar macrophages were purified by adherence to plastic after growing 4 days in RPMI medium 1640 with 10% fetal calf serum. Cells were infected as described above except that cultures of *M. tuberculosis* H37Rv and BCG were

The publication costs of this article were defrayed in part by page charge payment. This article must therefore be hereby marked "*advertisement*" in accordance with 18 U.S.C. §1734 solely to indicate this fact.

Abbreviations: BCG, bacillus Calmette–Guérin; MIP-1α, macrophage inflammatory protein 1-α.

‡Present address: Biology Department, Bemidji State University, 1500 Birchmont Drive, NE, Bemidji, MN 56601.
‖To whom reprint requests should be addressed.

passaged through a 25-gauge needle before addition to macrophages.

Library Construction and Screening. RNA was isolated using the guanidinium isothiocyanate/CsCl method (22). Five micrograms of poly(A)$^+$ RNA isolated by oligo(dT) chromatography was used to construct a cDNA library from BCG-infected J774. The Superscript cDNA kit (GIBCO/BRL) was used to generate first-strand cDNA using oligo(dT). Second-strand cDNA was synthesized using a modification of the protocol of Gubler and Hoffman (23). The resulting cDNA was ligated into λgt10 using *Eco*RI–*Not*I linkers. Recombinant phage were selected and amplified using standard techniques. The cDNA library prepared from BCG-infected J774 cells contained 1.1×10^6 independent recombinants with an average insert size of greater than 1 kb. Of six random phage isolates, all contained inserts.

A nonradioactive detection method, the Genius System (Boehringer Mannheim) was used for library screening. Preparation of digoxigenin-labeled cDNA probes from poly(A)$^+$ RNA, hybridization, and detection with Lumi-Phos 530 or NBT/X-phosphate were used as per the manufacturer's protocol. Plaques were screened by incubating duplicate filters with digoxigenin-labeled cDNA from *E. coli* or BCG-infected macrophages.

RNA Analysis. Ten micrograms of total cellular RNA was run per lane of a 1% glyoxal/dimethyl sulfoxide agarose gel and transferred to nylon membranes (Amersham). Hybridization, washing, and probe stripping were as directed by the membrane manufacturer. Probe fragments isolated from agarose gels by using DEAE membrane (Schleicher & Schuell) or by using silica adherence (Geneclean II, SUN Bioscience) were labeled by random priming (PrimeIt II, Stratagene). Relative signals were quantitated with a phosphoimager (Fuji) and were normalized to the actin signals.

Quantitative PCR Analysis. One microgram of total RNA was reverse-transcribed using Superscript reagents (GIBCO/BRL). The PCR used 1/10th of the reverse-transcribed cDNA in a 100-μl volume, and included 10 μl of 10× *Taq* buffer, 4 μl of 5 mM dNTPs, 50 pmol of each primer, 1 μl of competitive template, and 1 μl (5 units) of *Taq* DNA polymerase (Perkin–Elmer). The reaction was incubated for 35 cycles of 94°C for 30 sec, 50°C for 30 sec, and 72°C for 1 min. The competitive template was generated by insertion of a 333-bp DNA fragment from an *Nde*I digest of the yeast *RPB1* gene to the unique *Nde*I site of the human osteopontin gene. The primers used were 5′-CACCTGTGCCATACCAGTTAAACAG-3′ and 5′-CATGGCTGTGAAATTCATGGCTGTG-3′. These primers allowed amplification of an 830-bp cDNA fragment and a 1,163-bp fragment from the competitive template. No product was seen when these primers were used to amplify this fragment from 1 μg of purified genomic DNA. Commercially available actin primers were used (Stratagene).

Immunohistochemical Staining. Tissue sections were obtained from the Gaensler Lung Archive at the Boston University Pulmonary Center and the Boston Veterans Affairs Hospital. These specimens are paraffin-embedded tissue processed using standard clinical techniques. Immunohistochemical staining was done on a Ventanna ES automated stainer (Ventanna, Tucson, AZ). Sections 5 μm thick were baked for 1 hr at 60°C onto positively charged slides and then deparaffinized with xylene and hydrated in graded alcohol washes to water. Slides were then processed with Ventanna's protease I reagent for 4 min and incubated with primary antibodies for 32 min at 42°C. The manufacturer's protocol was used for the diaminobenzidine kit (osteopontin) and the fast red kit (CD68). Images were photographed with Kodak Ektachrome or Ektar film and scanned into Adobe Photoshop to create composite figures.

mAbs MPIIIB10$_1$, specific for rat and human osteopontin, and QH1, specific for quail vascular endothelial cells, were obtained from the Developmental Studies Hybridoma Bank (Iowa City, Iowa) and used at 1:200 dilution of hybridoma supernatant (400 and 500 ng/ml, respectively). mAb KP-1 (24) recognizing human CD68 was obtained from Dako.

RESULTS

Identification of Genes Associated with Infection of Macrophages. The effect of bacterial infection on macrophage gene expression was investigated by differential screening of cDNA libraries. The murine macrophage cell line J774 was used in these initial experiments because previous work has established its usefulness for studying interactions between mycobacteria and macrophages (18, 19). Differential screening of libraries has the advantage of detecting smaller changes in relative mRNA levels than subtractive hybridization.

The screening strategy is summarized in Fig. 1. The J774 cells were exposed to latex beads, or *E. coli,* or *M. bovis* BCG, and recombinant cDNA libraries and probes were prepared from the macrophage poly(A)$^+$ mRNA. The phage library representing mRNAs of macrophages infected with BCG was plated with host bacteria, and duplicate filters were placed on the plaques. These filters then were hybridized with cDNA probes prepared from J774 cells infected with either *E. coli* or BCG, and plaques with different signal strengths were isolated. This screening strategy was designed to identify genes whose expression differed when macrophages were exposed to BCG versus *E. coli.* The library constructed with mRNA from BCG-infected J774 cells was screened to maximize the chance of identifying genes whose expression was specifically increased by BCG.

Approximately 730,000 recombinant phage were screened by probing duplicate filters with labeled cDNA prepared from J774 cells that had phagocytized BCG or *E. coli.* Three clones were isolated that produced stronger signals with cDNA from macrophages infected with *E. coli.* Sequencing of their insert DNAs revealed that one cDNA clone encoded macrophage inflammatory protein 1-α (MIP-1α) (25) and two encoded ferritin (26). Ten clones were isolated that produced stronger signals with cDNA from macrophages infected with BCG. All of these encoded osteopontin (27).

Differential Expression of MIP1α, Ferritin, and Osteopontin mRNAs. To confirm that the three genes represented by the cDNA clones identified by the screening process were indeed differentially expressed, radiolabeled insert DNAs from the clones were used to probe macrophage mRNA immobilized on nylon filters (Fig. 2*A*). The mRNAs of all three genes accumulated to higher levels when macrophages phagocytized the two bacterial species versus the latex beads.

Osteopontin mRNA accumulated to similar levels in macrophages exposed to latex beads or *E. coli*, but accumulated to

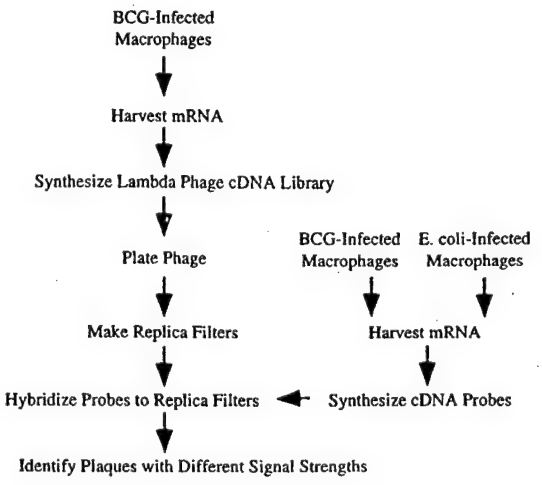

FIG. 1. Screening strategy using lambda phage cDNA library analysis.

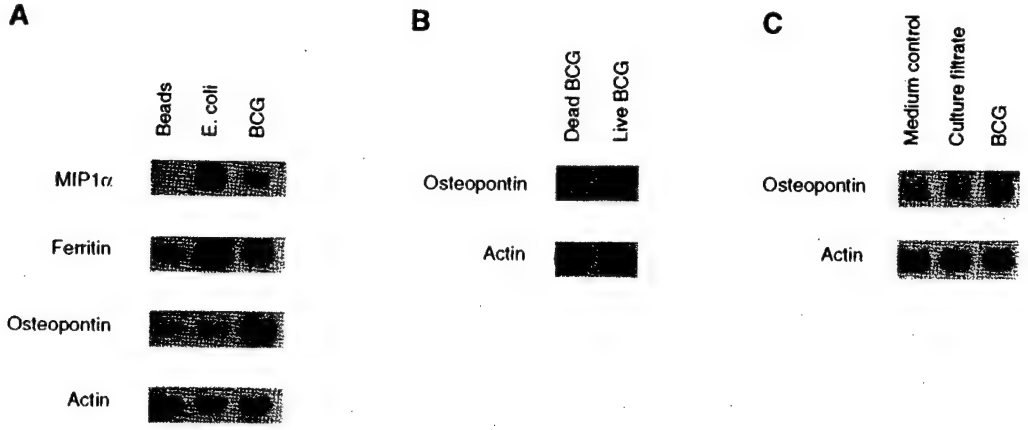

FIG. 2. Analysis of gene expression by Northern hybridization of total cellular RNA prepared from J774 cells stimulated with various agents. (*A*) Confirmation of differential expression of genes identified by phage library screening. J774 macrophages were stimulated with latex beads, *E. coli*, or BCG and RNA was probed with labeled MIP-1α, ferritin, osteopontin, and actin cDNAs. (*B*) Osteopontin mRNA levels are equal in J774 macrophages that have phagocytized dead or live BCG. Heat-killed BCG were prepared by heating a 1-ml culture of BCG in Middlebrook 7H9 broth for 15 min at 65°C. This treatment reduced bacterial viability more than 10,000-fold. (*C*) Osteopontin mRNA is induced in J774 macrophages by the BCG bacillus but not Middlebrook 7H9 medium or a BCG culture filtrate prepared with a 0.2-μm filter.

at least 5-fold higher levels after infection of macrophages with BCG (Fig. 2*A*). There were similar increases in osteopontin mRNA levels in macrophages that had phagocytized live and heat-killed BCG (Fig. 2*B*). As shown in Fig. 2*C*, neither 7H9 medium nor supernatant from a BCG culture was capable of eliciting the increase in osteopontin expression caused by BCG organisms. Thus, osteopontin mRNA levels increase substantially in murine macrophages that phagocytize BCG.

Osteopontin Expression in Human Lung Macrophages. We investigated whether increased osteopontin gene expression occurs in primary human cells in response to phagocytosis of virulent *M. tuberculosis*. Human alveolar macrophages were exposed to latex beads, BCG, and *M. tuberculosis* strain H37Rv. To determine precisely the number of osteopontin mRNA molecules present per cell before and after infection, a reverse transcriptase-PCR assay was used with varying levels of competing template. The results demonstrate that the levels of osteopontin mRNA were higher in alveolar macrophages infected with BCG (Fig. 3, lane B) and virulent *M. tuberculosis* (Fig. 3, lane Rv) than in macrophages that had phagocytized latex beads (Fig. 3, lane L). The human alveolar macrophages that had phagocytized latex beads contained approximately 1 molecule of osteopontin mRNA per cell. In contrast, the alveolar macrophages that had phagocytized BCG and *M. tuberculosis* had about 10 molecules of osteopontin mRNA per cell. This magnitude of increase in osteopontin mRNA after exposure to mycobacteria was similar to that observed with the murine macrophage model.

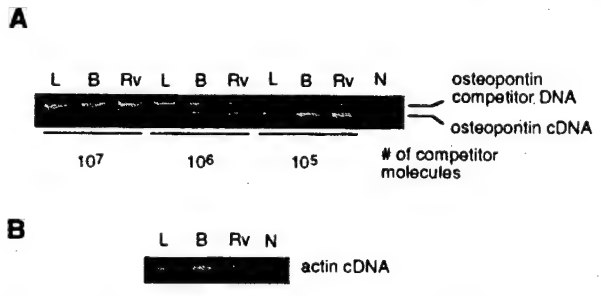

FIG. 3. Quantitative analysis of osteopontin mRNA expression by human alveolar macrophages using competitive reverse transcriptase-PCR. (*A*) Competitive PCR using primers specific for osteopontin cDNA. Osteopontin competitor cDNA had binding sites for the PCR primers but contained an inserted DNA sequence to allow for the generation of a larger-sized PCR product. L, cDNA from human alveolar macrophages that phagocytized latex beads; B, cDNA from human alveolar macrophages that phagocytized BCG; Rv, cDNA from human alveolar macrophages that phagocytized *M. tuberculosis* H37Rv; N, no cDNA added to the PCR. cDNA from approximately 100,000 cells was used in each reaction. (*B*) PCR using primers specific for control actin cDNA.

Osteopontin in Human Granulomatous Diseases. The increase in osteopontin mRNA observed in infected alveolar macrophages predicts that osteopontin protein levels should increase in human tissues infected by *M. tuberculosis*. We therefore investigated whether the presence of osteopontin protein in patient tissues correlated with the histopathology of tuberculosis. Tissue sections from normal and diseased lungs were stained with a mAb specific for osteopontin, MPIIIB10_1, with a mAb specific for the macrophage antigen CD68 (24), or with an isotype control, QH 1 (28). The MPIIIB10_1 mAb has been used extensively to identify osteopontin by immunohistochemistry (29, 30) and immunoprecipitation (31, 32).

Osteopontin was readily identified throughout specimens of tuberculous lung. The architecture of a tuberculosis lesion with necrosis (N) and with a lymphoid aggregate (L) above alveolar air spaces was evident in sections treated with the isotype control antibody and the hematoxylin counterstain (Fig. 4*A*). No staining (brown color) of this specimen was observed with the isotype control (Fig. 4*A*). However, when an adjacent serial section was probed with the MPIIIB10_1 antibody, a strong osteopontin signal was detected in the inflammatory border surrounding the necrosis, and immediately adjacent to and within the areas of caseating necrosis (Fig. 4*B*). At higher power, macrophages were identified in a serial section with anti-CD68 antibody and the fast red reagent (Fig. 4*C*). These cells also expressed osteopontin (Fig. 4*D*). Lymphocytes identified at low power and at high power in Fig. 4 *A* and *C* (L) demonstrated intense osteopontin signal singly and in aggregates (Fig. 4 *B* and *D*). Giant cells expressed CD68 (Fig. 4*E*) but did not universally stain for osteopontin; in general, epithelioid giant cells expressed osteopontin (Fig. 4*F*). Bronchiolar epithelium (Fig. 4*G*) and small blood vessels (Fig. 4*H* and below columnar epithelium in Fig. 4*G*) stained with the MPIIIB10_1 antibody though they have not been known to express osteopontin in normal adult tissue (33–36). In addition, osteopontin appeared in layers near caseation (Fig. 4*B*) and was intimately associated with fibroblast-like cells in a number of views (Fig. 4 *F, G, H*). In summary, osteopontin was identified in a variety of cell types within the tuberculosis specimens.

Specimens from normal lung, an acute inflammatory condition (bacterial bronchopneumonia), and two chronic inflammatory conditions (silicosis and granulation tissue of a pilonidal cyst) were studied to assess the variety of situations in

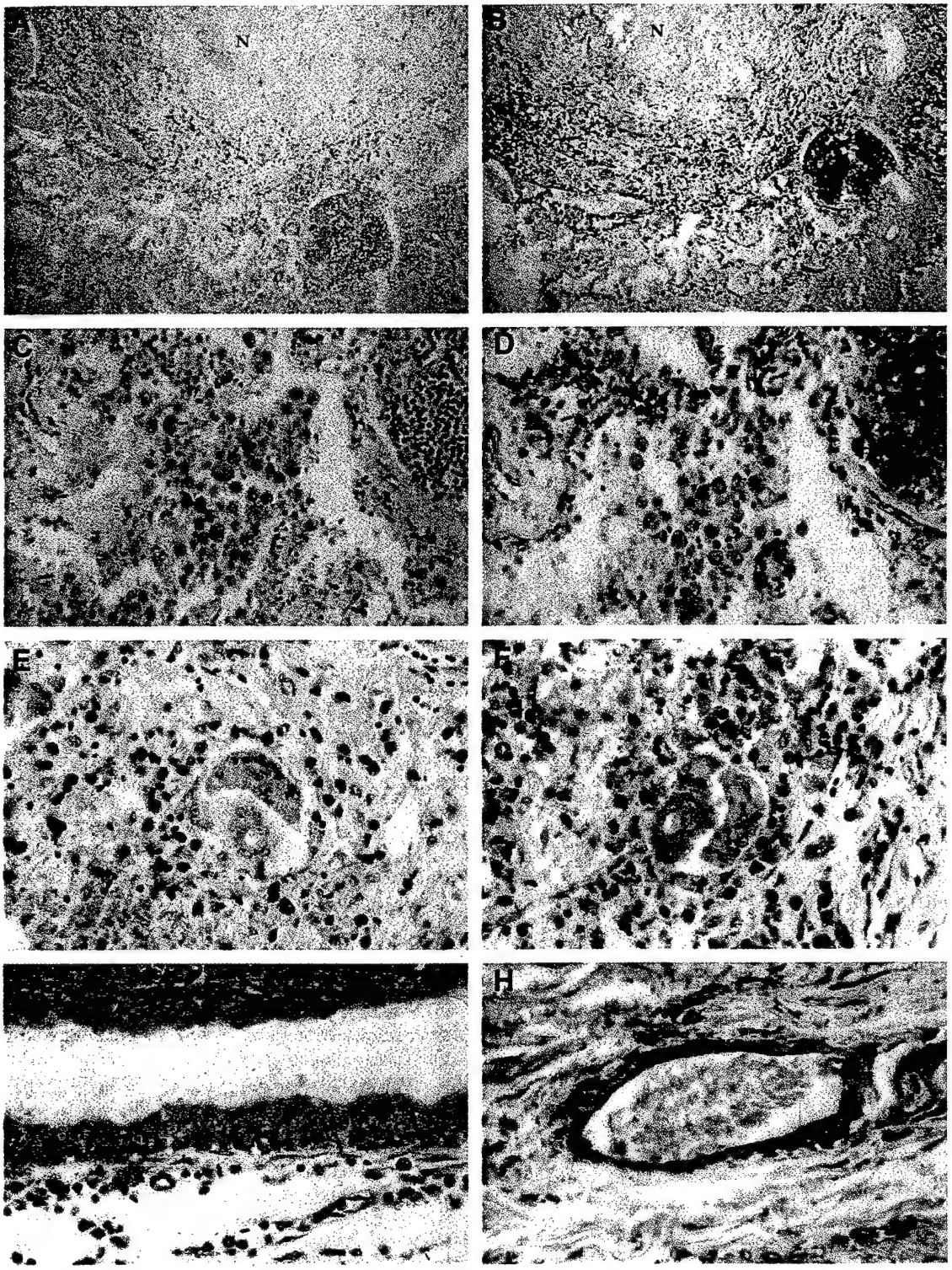

FIG. 4. Immunohistochemical stain of human tuberculosis specimen. (*A*) Tuberculosis granuloma stained with isotype control antibody showing hematoxylin counterstaining of nuclei, ×90. Area of caseating necrosis (N), lymphoid aggregate (L). (*B*) Serial section of granuloma in *A*, stained for osteopontin with mAb MPIIIB10$_1$, ×90. (*C*) Serial section of same specimen stained with anti-CD68 first-step antibody demonstrating macrophage aggregate, ×360. (*D*) Higher power view of *B* showing same macrophage aggregate staining for osteopontin, ×360. (*E*) Giant cells in specimen stained for CD68, ×900. (*F*) Higher power view of *B* showing osteopontin staining of epithelioid, but not Langhans, giant cell, ×900. (*G*) Small airway respiratory epithelium stained for osteopontin; same section though different field of *B*, ×900. (*H*) Small vessel staining with MPIIIB10$_1$, ×900. Similar results were obtained with sections from multiple specimens and patients.

which osteopontin could be detected. Normal lung did not show significant staining for osteopontin either in alveolar networks (Fig. 5*A*) or in airways (not shown). The bronchopneumonia specimen had scattered cells of macrophage and lymphocyte morphology that produced some signal with MPIIIB10$_1$ (Fig. 5*B*). Lymphoid aggregations associated with the pneumonia were also positive for osteopontin (not shown). The two chronic inflammatory conditions showed dichotomous results for the presence of osteopontin. Silicosis is a noninfectious granulomatous disease (37). The silicotic nodule

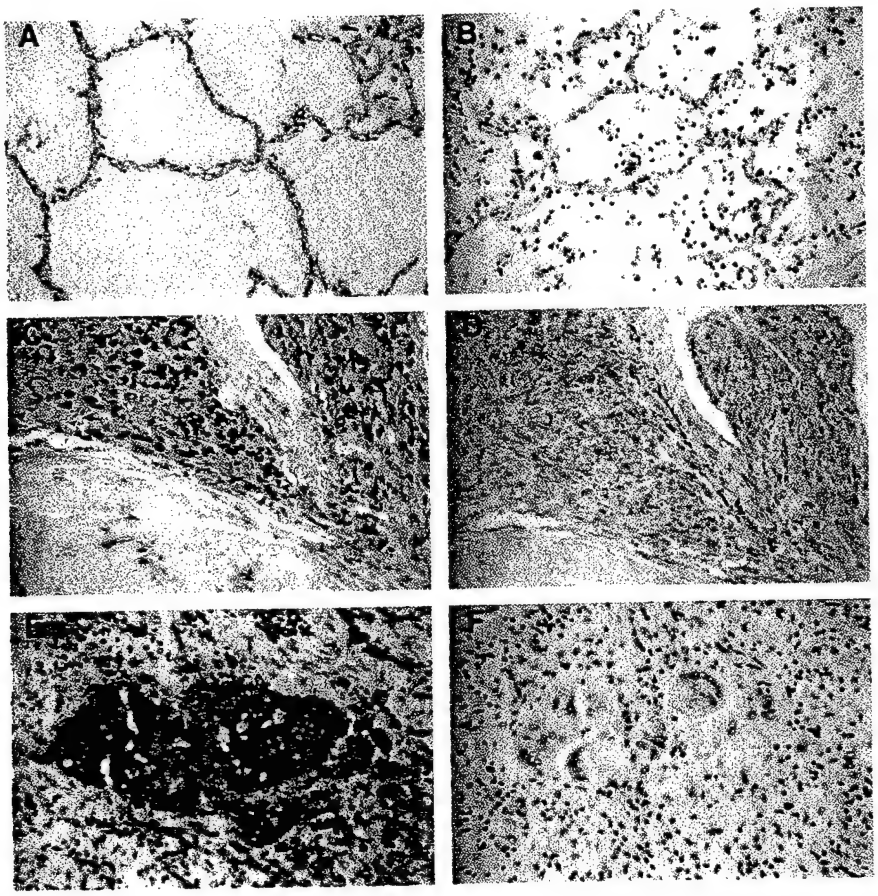

FIG. 5. Immunohistochemical stain for osteopontin in other clinical states. (*A*) Normal lung alveoli stained for osteopontin with mAb MPIIIB10$_1$. (*B*) Bacterial bronchopneumonia stained with MPIIIB10$_1$. (*C*) Lung section from silicosis patient stained for CD68. Intense red color corresponds to fast red color substrate. (*D*) Silicosis specimen stained with MPIIIB10$_1$. (*E*) Granulation tissue stained for CD68. (*F*) Granulation tissue from pilonidal cyst stained for osteopontin. (All images ×260.)

with its characteristic fibrosis showed an abundance of macrophages that stained with CD68 (Fig. 5*C*). These cells, and presumably some of the extracellular matrix, showed heavy signal for osteopontin on immunohistochemical staining (Fig. 5*D*). Granulation tissue is another pathologic process characterized by mononuclear cell infiltration but is distinct from granulomatous inflammation (37). While the granulation tissue of the pilonidal cyst showed a large aggregation of giant cells and numerous macrophages based on CD68 staining (Fig. 5*E*), there was no osteopontin detected (Fig. 5*F*). Thus, only tuberculosis and silicosis, the two granulomatous conditions, expressed high levels of osteopontin in the tissue pathology.

DISCUSSION

The experimental approach used here, employing differential screening of cDNA libraries from infected cell lines, should continue to be useful in future studies of host-pathogen interactions. A model system using a macrophage cell line was essential to permit infections under controlled conditions and to provide the numbers of cells necessary to generate cDNA libraries and probes. This model system, employing the macrophage cell line used by Rastogi and colleagues (18), had excellent predictive value. Our results agree with previous reports linking MIP-1α and ferritin expression with exposure to lipopolysaccharide and BCG (38–40). The J774 cell line also has been used in a PCR-based strategy to determine gene expression changes after exposure to *Listeria monocytogenes* (41). In contrast to previous work, we have extended the observations made with the *in vitro* model to confirm the presence of elevated levels of osteopontin and MIP-1α (data not shown) in human tissue pathology.

Using this approach we have identified a novel association between osteopontin and two granulomatous diseases, tuberculosis and silicosis. Infection of primary human alveolar macrophages with *M. tuberculosis* causes a substantial increase in osteopontin gene expression. Elevated levels of osteopontin protein are found in macrophages and lymphocytes in pathologic tissue sections from patients with tuberculosis. The association of osteopontin with tuberculosis and granulomatous disease, together with previous evidence that osteopontin is an cytokine and macrophage chemoattractant, implicate osteopontin in granuloma formation.

Though osteopontin gained its name from its presence in bone (42, 43), it is expressed in a variety of cell types (27, 34, 44), including T cells (refs. 45, 46; reviewed in ref. 21), and is likely to be important in host responses to infection. This secreted glycosylated phosphoprotein has been shown to promote macrophage migration and adhesion (47, 48). The discovery of a receptor-ligand interaction between CD44 and osteopontin has led to the proposal that this interaction may mediate migration of activated lymphocytes and monocytes out of the bloodstream into sites of inflammation (49). Osteopontin may enhance intercellular interactions and facilitate binding to the extracellular matrix via CD44 and integrins (21). This interaction could anchor CD44$^+$ cells because osteopontin can be covalently linked to fibronectin by transglutaminase (50).

The accumulation of osteopontin in tissues infected with *M. tuberculosis*, and osteopontin's role in macrophage migration and adhesion, suggests a model for granuloma formation. In this model, phagocytosis of *M. tuberculosis* by alveolar macrophages leads to induction of osteopontin gene expression and protein secretion. The secreted osteopontin stimulates accumulation of

monocytes and macrophages, perhaps by promoting chemotaxis, adhesion, and anchoring of these cells, to initiate granuloma formation. This model is attractive because it can account for the genesis and maintenance of the unusual tissue pathology associated with granulomas. However, granuloma formation appears to require more than the simple expression of osteopontin. Low levels of osteopontin were observed in a subset of cells of bacterial bronchopneumonia tissue sections (Fig. 4*B*) and in certain cell types in normal specimens (34) in the absence of granuloma formation. The duration and level of expression of osteopontin, the specific cells producing the protein, and other factors in the tissue environment, all may determine whether granuloma formation is the histologic outcome of an inflammatory process.

Future studies with differential screening strategies should reveal additional associations between specific gene products and infectious processes. The identification of genes that are differentially expressed in infected host cells might use differential cDNA screening, differential display (41, 51), or high-density oligonucleotide arrays (52). As human genome sequences become more available, these approaches will be even more valuable in identifying important elements of host defenses.

We thank John A. Hayes and Margo Goetschkes for assistance with immunohistochemistry and Anna Aldovini and Peter Murray for helpful discussions. The MPIIIB10$_1$ hybridoma supernatant was obtained from the Developmental Studies Hybridoma Bank maintained by the Department of Pharmacology and Molecular Sciences, John Hopkins University School of Medicine, Baltimore, MD, and the Department of Biological Sciences, University of Iowa, Iowa City, IA, under contract N01-HD-6–2915 from the National Institute of Child Health and Human Development. This work was supported by Public Health Service Grants AI 37869 (R.Y.), HL44846 (H.K.), AI08812 (P.G.), AI01305 (G.J.N.), and HL46563 (J.S.B.). H.K. is a Career Investigator of the American Lung Association. G.L.C. is a recipient of of the American Lung Association Research Training Fellowship Award.

1. Bloom, B. R. & Murray, C. J. (1992) *Science* **257,** 1055–1064.
2. Haas, D. W. & DesPrez, R. M. (1995) in *Mycobacterium tuberculosis* (Churchill Livingstone, New York), Vol. 1, pp. 2213–2243.
3. Shima, K., Dannenberg, A. M., Jr., Ando, M., Chandrasekhar, A. S., Seluzicki, J. A. & Fabrikant, J. I. (1972) *Am. J. Path.* **67,** 159–180.
4. Dannenberg, A. M. & Rook, G. A. W. (1994) in *Pathogenesis of Pulmonary Tuberculosis*, ed. Bloom, B. R. (Am. Soc. Microbiol. Press, Washington, DC), pp. 459–484.
5. Kaufmann, S. H. (1993) *Annu. Rev. Immunol.* **11,** 129–163.
6. Rook, G. A. W. & Bloom, B. R. (1994) in *Mechanisms of Pathogenesis in Tuberculosis*, ed. Bloom, B. R. (Am. Soc. Microbiol. Press, Washington, DC), pp. 485–501.
7. Hart, P. D. & Armstrong, J. A. (1974) *Infect. Immun.* **10,** 742–746.
8. Crowle, A. J., Dahl, R., Ross, E. & May, M. H. (1991) *Infect. Immun.* **59,** 1823–1831.
9. McDonough, K. A., Kress, Y. & Bloom, B. R. (1993) *Infect. Immun.* **61,** 2763–2773.
10. Valone, S. E., Rich, E. A., Wallis, R. S. & Ellner, J. J. (1988) *Infect. Immun.* **56,** 3313–3315.
11. Wallis, R. S., Amir-Tahmasseb, M. & Ellner, J. J. (1990) *Proc. Natl. Acad. Sci. USA* **87,** 3348–3352.
12. Huygen, K., Vandenbussche, P. & Heremans, H. (1991) *Cell. Immunol.* **137,** 224–231.
13. Bermudez, L. E. (1993) *J. Immunol.* **150,** 1838–1845.
14. Friedland, J. S., Remick, D. G., Shattock, R. & Griffin, G. E. (1992) *Eur. J. Immunol.* **22,** 1373–1378.
15. Gercken, J., Pryjma, J., Ernst, M. & Flad, H. D. (1994) *Infect. Immun.* **62,** 3472–3478.
16. Sibley, L. D. & Krahenbuhl, J. L. (1988) *J. Leukococyte Biol.* **43,** 60–66.
17. Sibley, L. D., Hunter, S. W., Brennan, P. J. & Krahenbuhl, J. L. (1988) *Infect. Immun.* **56,** 1232–1236.
18. Rastogi, N., Ptar, M.-C. & David, H. L. (1987) *Curr. Microbiol.* **16,** 79–92.
19. Rastogi, N., Blom-Potar, M. C. & David, H. L. (1989) *Acta Leprol.* **1,** 156–159.
20. Patarca, R., Saavedra, R. A. & Cantor, H. (1993) *Crit. Rev. Immunol.* **13,** 225–246.
21. Denhardt, D. T. & Guo, X. (1993) *FASEB J.* **7,** 1475–1482.
22. Sambrook, J., Fritsch, E. F. & Maniatis, T. (1989) *Molecular Cloning: A Laboratory Manual* (Cold Spring Harbor Lab. Press, Plainview, NY).
23. Gubler, U. & Hoffman, B. J. (1983) *Gene* **25,** 263–269.
24. Pulford, K. A., Rigney, E. M., Micklem, K. J., Jones, M., Stross, W. P., Gatter, K. C. & Mason, D. Y. (1989) *J. Clin. Pathol.* **42,** 414–421.
25. Davatelis, G., Tekamp-Olson, P., Wolpe, S. D., Hermsen, K., Luedke, C., Gallegos, C., Coit, D., Merryweather, J. & Cerami, A. (1988) *J. Exp. Med.* **167,** 1939–1944.
26. Torti, S. V., Kwak, E. L., Miller, S. C., Miller, L. L., Ringold, G. M., Myambo, K. B., Young, A. P. & Torti, F. M. (1988) *J. Biol. Chem.* **263,** 12638–12644.
27. Craig, A. M., Smith, J. H. & Denhardt, D. T. (1989) *J. Biol. Chem.* **264,** 9682–9689.
28. Pardanaud, L., Altmann, C., Kitos, P., Dieterlen-Lievre, F. & Buck, C. A. (1987) *Development (Cambridge, U.K.)* **100,** 339–349.
29. Frank, J. D., Balena, R., Masarachia, P., Seedor, J. G. & Cartwright, M. E. (1993) *Histochemistry* **99,** 295–301.
30. Murry, C. E., Giachelli, C. M., Schwartz, S. M. & Vracko, R. (1994) *Am. J. Pathol.* **145,** 1450–1462.
31. Kasugai, S., Nagata, T. & Sodek, J. (1992) *J. Cell. Physiol.* **152,** 467–477.
32. Yokota, M., Nagata, T., Ishida, H. & Wakano, Y. (1992) *Biochem. Biophys. Res. Commun.* **189,** 892–898.
33. Brown, L. F., Papadopoulos-Sergiou, A., Berse, B., Manseau, E. J., Tognazzi, K., Perruzzi, C. A., Dvorak, H. F. & Senger, D. R. (1994) *Am. J. Pathol.* **145,** 610–623.
34. Brown, L. F., Berse, B., Van de Water, L., Papadopoulos-Sergiou, A., Perruzzi, C. A., Manseau, E. J., Dvorak, H. F. & Senger, D. R. (1992) *Mol. Biol. Cell* **3,** 1169–1180.
35. Giachelli, C. M., Bae, N., Almeida, M., Denhardt, D. T., Alpers, C. E. & Schwartz, S. M. (1993) *J. Clin. Invest.* **92,** 1686–1696.
36. Hirota, S., Imakita, M., Kohri, K., Ito, A., Morii, E., Adachi, S., Kim, H. M., Kitamura, Y., Yutani, C. & Nomura, S. (1993) *Am. J. Pathol.* **143,** 1003–1008.
37. Warren, K. S. (1976) *Ann. N.Y. Acad. Sci.* **278,** 7–18.
38. Driscoll, K. E., Hassenbein, D. G., Carter, J., Poynter, J., Asquith, T. N., Grant, R. A., Whitten, J., Purdon, M. P. & Takigiku, R. (1993) *Am. J. Respir. Cell. Mol. Biol.* **8,** 311–318.
39. Appelberg, R. (1992) *J. Leukococyte Biol.* **52,** 303–306.
40. Kumagai, T., Awai, M. & Okada, S. (1992) *Pathol. Res. Pract.* **188,** 931–941.
41. Schwan, W. R., Kugler, S., Schuller, S., Kopecko, D. J. & Goebel, W. (1996) *Infect. Immun.* **64,** 91–99.
42. Franzen, A. & Heinegard, D. (1985) *Biochem. J.* **232,** 715–724.
43. Oldberg, A., Franzen, A. & Heinegard, D. (1986) *Proc. Natl. Acad. Sci. USA* **83,** 8819–8823.
44. Senger, D. R., Wirth, D. F. & Hynes, R. O. (1979) *Cell* **16,** 885–893.
45. Reinholt, F. P., Hultenby, K., Oldberg, A. & Heinegard, D. (1990) *Proc. Natl. Acad. Sci. USA* **87,** 4473–4475.
46. Patarca, R., Freeman, G. J., Singh, R. P., Wei, F. Y., Durfee, T., Blattner, F., Regnier, D. C., Kozak, C. A., Mock, B. A., Morse, H. C., Jerrells, T. R. & Cantor, H. (1989) *J. Exp. Med.* **170,** 145–161.
47. Singh, R. P., Patarca, R., Schwartz, J., Singh, P. & Cantor, H. (1990) *J. Exp. Med.* **171,** 1931–1942.
48. Yamamoto, S., Nasu, K., Ishida, T., Setoguchi, M., Higuchi, Y., Hijiya, N. & Akizuki, S. (1995) *Ann. N.Y. Acad. Sci.* **760,** 378–380.
49. Weber, G. F., Ashkar, S., Glimcher, M. J. & Cantor, H. (1996) *Science* **271,** 509–512.
50. Beninati, S., Senger, D. R., Cordella-Miele, E., Mukherjee, A. B., Chackalaparampil, I., Shanmugam, V., Singh, K. & Mukherjee, B. B. (1994) *J. Biochem.* **115,** 675–682.
51. Wan, J. S., Sharp, S. J., Poirier, G. M.-C., Wagaman, P. C., Chambers, J., Pyati, J., Hom, Y., Galindo, J. E., Huvar, A., Peterson, P. A., Jackson, M. R. & Erlander, M. G. (1996) *Nat. Biotechnol.* **14,** 1685–1691.
52. Lockhart, D. J., Dong, H., Byrne, M. C., Follettie, M. T., Gallo, M. V., Chee, M. S., Mittmann, M., Wang, C., Kobayashi, M., Horton, H. & Brown, E. L. (1996) *Nat. Biotechnol.* **14,** 1675–1680.

Osteopontin Is Associated with T Cells in Sarcoid Granulomas and Has T Cell Adhesive and Cytokine-Like Properties In Vitro[1]

Anthony W. O'Regan,[2]* Geoffrey L. Chupp,[2,3]* John A. Lowry,* Margo Goetschkes,† Niall Mulligan,† and Jeffrey S. Berman[4]*

Sarcoidosis is a systemic disease characterized by the accumulation of activated T cells and widespread granuloma formation. In addition, individual genetic predisposition appears to be important in this disease. Osteopontin, a noncollagenous matrix protein produced by macrophages and T lymphocytes, is expressed in the granulomas of tuberculosis, and is associated with genetic susceptibility to intracellular infection. The function of osteopontin in these T cell-mediated responses is unknown. We sought to elucidate the role of osteopontin in granulomatous inflammation by characterizing its expression in different stages of sarcoidosis and its effector function on T cells in vitro. Lymphocyte-associated expression of osteopontin in sarcoidosis was demonstrated by immunohistochemistry, and its expression correlated with granuloma maturity. In addition, osteopontin induced T cell chemotaxis, supported T cell adhesion (an effect enhanced by thrombin cleavage of osteopontin), and costimulated T cell proliferation. These results suggest a novel mechanism by which osteopontin and thrombin modulate T cell recruitment and activation in granulomatous inflammation. ***The Journal of Immunology,*** **1999, 162: 1024–1031.**

Sarcoidosis is a chronic T cell-mediated granulomatous disease of unknown cause (1). In the United States the incidence rate in whites is 5 per 100,000 and in African Americans is 50 per 100,000 (1). The etiology and pathogenesis of sarcoidosis is poorly understood. It is generally viewed as a T cell-mediated inflammatory response to unknown antigenic stimuli, and, at least in some cases, genetic predisposition appears to be a determinant of disease susceptibility and severity (2, 3). Previous work has focused on identifying specific Ags associated with sarcoidosis (1). However, it is likely that, regardless of the Ag involved, the intensity of the host granulomatous response contributes significantly to the morbidity and mortality of this disease. Therefore, understanding the host determinants of disease susceptibility and severity in sarcoidosis may facilitate the development of therapeutic and preventive strategies in this disease.

Osteopontin (OPN)[5] is a noncollagenous adhesive matrix protein normally found in bone and at epithelial surfaces that contains the arginine-glycine-aspartate (RGD)-binding motif common to many extracellular matrix (ECM) proteins (4–6). Unlike other matrix proteins, OPN contains a thrombin cleavage site adjacent to the RGD domain which, upon cleavage, alters the adhesive capacity of OPN (7–9). Studies have reported both the augmentation and inhibition of OPN-mediated adhesion by thrombin cleavage (7–9). In vitro, OPN promotes integrin- and CD44-mediated cell adhesion and chemotaxis in osteoclasts, smooth muscle cells, monocytes, and B lymphocytes (10–15). These findings have led to research identifying a role for OPN in bone resorption, neoplastic transformation, atheromatous plaque formation, and dystrophic calcification of inflamed and damaged tissues (5, 16–19).

Recent data suggest a role for OPN in the immune response. It is produced in a regulated fashion by macrophages, T cells, and NK cells (20, 21). OPN injected s.c. induces macrophage migration, and in vitro it supports monocyte adhesion and migration (13, 22). In addition, the expression of OPN by macrophages and T cells in heavily calcified prosthetic heart valves suggests that OPN may play a role in the cell-mediated process of dystrophic calcification (19).

OPN is also important in the genetic resistance to intracellular pathogens (20). In mice, the OPN gene maps to the same locus as the immune mediator of natural resistance to the intracellular pathogen *Rickettsia tsutsugamushi*. Alleles of this gene that result in deficient early production of OPN in response to *R. tsutsugamushi* are associated with disease susceptibility (20). We and others have recently described the expression of OPN at sites of granuloma formation in tuberculosis and silicosis and its up-regulation in alveolar macrophages infected with mycobacteria (23, 24). The function of OPN in granulomatous inflammation is unknown. In view of these data, we sought to characterize the in vivo expression of OPN in the granulomas of sarcoidosis and to define the in vitro effects of OPN on T cell function.

In this report, we demonstrate the expression of OPN in granulomas of pulmonary sarcoidosis and note a characteristic pattern of prominent lymphocyte staining. Based on these observations, we characterize the effects of OPN on human T lymphocyte function in vitro. OPN binds to T cells, supports T cell adhesion and

*Pulmonary Center and †Department of Pathology, Boston University School of Medicine, Boston, MA 02188; and Boston Veterans Affairs Medical Center, Boston, MA 02130

Received for publication July 9, 1998. Accepted for publication September 25, 1998.

The costs of publication of this article were defrayed in part by the payment of page charges. This article must therefore be hereby marked *advertisement* in accordance with 18 U.S.C. Section 1734 solely to indicate this fact.

[1] This work was supported in part by National Institutes of Health Specialized Center of Research Grant P5O HL56386 and an American Lung Association research training fellowship award.

[2] These authors contributed equally to the work.

[3] Present address: Section of Pulmonary and Critical Care Medicine, Yale University School of Medicine, 333 Cedar Street, New Haven, CT 06510-8040.

[4] Address correspondence and reprint requests to Dr. Jeffrey S. Berman, Pulmonary Center, Boston University School of Medicine, 715 Albany Street, Boston, MA 02118-2394. E-mail address: jberman@bupula.bu.edu

[5] Abbreviations used in this paper: OPN, osteopontin; ECM, extracellular matrix; RGD, arginine-glycine-aspartate; FN, fibronectin; hpf, high power field; ARDS, acute respiratory distress syndrome; NWNT, nylon wool nonadherent T cell(s).

0022-1767/99/$02.00

chemotaxis, and costimulates resting T cell proliferation in response to ligation of the Ag receptor. Adhesion is modulated by thrombin cleavage of OPN. These data show that OPN is a T cell-associated, RGD-containing protein with cytokine/chemokine-like functions and that its T cell interactions are regulated by thrombin cleavage. The juxtaposition of OPN between the cell-mediated response and the coagulation cascade suggests a novel role by which matrix proteins regulate the immune response. In view of these findings it is possible that OPN may regulate the intensity of sarcoid granulomatous inflammation by recruitment and immobilization of T lymphocytes and by modulating T cell function.

Materials and Methods

Cells

Human PBMC from normal donors were separated by Ficoll-Hypaque density gradient centrifugation. Monocytes and B cells were removed on nylon wool columns as previously described (25). Resting CD3-positive T cells were isolated by immunomagnetic negative selection with Dynabeads M-450 (Dynal, Great Neck, NY) (26, 27). Negative selection using a mixture of mAbs including HLA DR on activated T cells, B cells, and monocytes; CD20 on B cells; CD16 on NK cells; and CD14 on monocytes resulted in cell populations that were >95% $CD3^+$ and were completely depleted of monocytes as determined by FACS analysis and the lack of a proliferative response to optimal concentrations of PHA (PHA-L form; Sigma, St. Louis, MO) (28).

Abs and reagents

The following Abs were used. Anti-OPN Abs, OP148APA (kindly donated by D. Senger, Boston, MA), a polyclonal Ab directed to human milk OPN, MPIIIB10 (specific for rat and human OPN), and its isotype control, QH1 (specific for quail vascular endothelial cells), purchased from the Developmental Studies Hybridoma Bank (Iowa City, IA), were used for immunohistochemistry; polyclonal rabbit anti-fibronectin (FN) Ab (No. A0245; DAKO, Carpinteria, CA) for immunohistochemistry; anti-CD3 Abs, monoclonal anti-CD3 (Clone HIT3a, PharMingen, San Diego, CA) for T cell proliferation, and polyclonal anti-CD3 (No. A0452; DAKO) for immunohistochemistry.

For all experiments we used endotoxin-free OPN, purified from human milk over an Ab column (kindly donated by D. Senger, Boston MA) (29). Human FN and thrombin (3000 National Institute of Health units/mg protein) were purchased from Sigma, and rat tail collagen was purchased from Life Technologies (Grand Island, NY).

Thrombin cleavage of OPN

In the indicated experiments, OPN was cleaved in the manner described by Senger et al. (29). Purified OPN was incubated with purified human thrombin at a concentration of 18 units thrombin/ml for 60 min at 37°C. Protein cleavage was confirmed by SDS-PAGE and Western blot with OP148APA Ab.

Immunohistochemical staining

Lung biopsies from six patients with pulmonary sarcoidosis were obtained from the Gaensler Lung Archive at the Boston University Pulmonary Center and the Boston Veterans Affairs Hospital. These specimens were paraffin embedded using standard techniques. Immunohistochemical staining was facilitated with a Ventana ES automated stainer (Ventana, Tuscon, AZ). Serial sections 5 μm thick were cut and baked for 1 h at 60°C onto positively charged slides and then deparaffinized with xylene and hydrated in graded alcohol washes to water. Slides were then processed with Ventana's protease I reagent for 4 min and incubated with primary Abs for 32 min at 42°C. Staining was detected with a diaminobenzidine kit. Images were photographed with Kodak Ektachrome film and scanned into Adobe Photoshop to create composite figures.

Primary Abs, anti-OPN mAb, MPIIIB10, and isotype control QH1 were used at 1:150 dilution of hybridoma supernatant (500 and 625 ng/ml, respectively). Polyclonal rabbit anti-human FN and anti-human CD3 Abs were used at a concentration of 1:200 and 1:150, respectively. Isotype control rabbit anti-IgG polyclonal Ab (Organo Teknika, Durham, NC) was used at similar concentrations. The above concentrations were selected based on characteristic and selective staining patterns of positive control paraffin-embedded tissue samples (human kidney for OPN and human tonsil for FN and CD3). All slides were read by a blinded pathologist who graded the intensity of staining as follows: 0 = no staining; 1 = weak staining; 2 = strong staining.

Migration assay

T cell migration was assayed using a modified 48-well Boyden chemotaxis chamber (30). Fifty microliters of a T lymphocyte suspension containing 10×10^6 cells/ml of M199-HPS with 0.4% BSA was added to the upper chambers, separated from various concentrations of human milk OPN by an 8-μm pore size nitrocellulose filter, and incubated at 37°C for 3 h. The filters were fixed, stained, dehydrated, and mounted using standard histologic methods. Lymphocyte migration was quantitated by counting the total number of cells migrating beyond a certain depth, with that depth set to give a baseline migration under control conditions of 5–15 cells per high power field (hpf). Five hpf were counted for each of duplicate wells, and results were calculated as mean cells/hpf ± SD; for purposes of comparison data are expressed as mean percentage of control migration ± SEM. Gradient dependence was determined by a checkerboard technique (30). OPN was placed only below the filter (chemoattractant present with concentration gradient), both above and below the filter (chemoattractant present without concentration gradient), or only above the filter (reverse gradient).

Adhesion assay

The adhesion of T cells to OPN was assessed utilizing a fluorometric adhesion assay (31, 32). Briefly, 96-well, non-tissue culture-treated plates were incubated overnight with various concentrations of either OPN, FN, or rat collagen in PBS at 4°C. OPN adhesion was confirmed by Ab detection ELISA using OP148APA mAb. The plates were washed, and the nonspecific binding sites were blocked by incubation with 2.5% BSA/PBS for 2 h at 37°C. T cells were labeled with the acetoxymethyl fluorescein ester Calcein AM (Molecular Probes, Eugene, OR), by incubation at room temperature for 30 min. The cells were washed, activated with PMA (Sigma) at a concentration of 5ng/ml, and then 75,000 cells were added to each well. The cells were allowed to settle at 4°C for 1 h and then were rapidly warmed in a water bath to 37°C for 10 min, a time previously determined to give maximal adhesion. The wells were washed five times, and the fluorescence of the remaining adherent cells was counted on a plate fluorometer (Flostar, BMG, Offenburg, Germany). The percentage of adherent cells was calculated using a standard curve derived for each adhesion assay. The results are expressed as the mean ± SD percentage of cells binding from triplicate wells.

Proliferation assay

Proliferation assays to demonstrate costimulation were performed as previously described (26). Ninety-six-well, non-tissue culture-treated microtiter plates were prepared by incubating the indicated concentrations of anti-CD3 mAb overnight at 4°C in PBS. Unbound Ab was removed, and various concentrations of ECM proteins were incubated overnight at 4°C. OPN adhesion was confirmed by ELISA. Human T cells, 50,000 in 200 μl of RPMI 1640 supplemented with glutamine, 10% heat inactivated FCS, penicillin, and streptomycin, were added to each well and cultured for 72 h at 37°C. [^{3}H]thymidine (1 μCi/well) was added for the last 12 h of the assay, and the cells were harvested onto filters using an automated cell harvester. Where indicated, PMA was added at a concentration of 1 ng/ml of cells and incubated either with immobilized anti-CD3 or alone in a similar manner as outlined. Results are expressed as the arithmetic mean cpm ± SD of triplicate cultures.

Statistical analysis

Data are expressed as mean ± SD. Results were compared for significance using Student's paired two-tailed t test. P values ≤ 0.05 were considered significant.

Results

Lymphocyte-associated expression of OPN in sarcoid granulomas

OPN expression was studied in open lung biopsies from six patients with pulmonary sarcoidosis (Table I). These patients varied in demographics, clinical indices of disease activity, and chest x-ray findings and represent stages in the spectrum of pulmonary sarcoidosis from early active to advanced end-stage disease. Tissue sections were stained with anti-OPN (clone MPIIIB10) or isotype control (clone QH1) mAb as previously described (21, 23). Widespread OPN expression was seen in sarcoid granulomas (Fig. 1, *a*

Table I. *Clinical features and immunohistochemical staining of lung biopsies in six cases of sarcoidosis*[a]

	Clinical Features			Investigations				Immunohistochemistry[b]					
								OPN granuloma expression			FN granuloma expression		
Patient No.	Age and sex	Symptoms	Physical exam	CXR stage[c]	TLC (%)	FEV1/ FVC	DLCO (%)	Lymphocyte	Histiocyte	Matrix	Lymphocyte	Histiocyte	Matrix
1	35 M	Cough	Bilat rales	2	94	71	67	2	1	0	0	1	2
2	58 F	Dyspnea/cough	Bilat rales	2	76	74	65	2	1	0	1	2	2
3	42 F	Dyspnea/cough	Bilat rales	NA	72	93	79	2	1	0	1	1	2
4	35 M	Chest pain	Normal	2	77	80	80	–	1	0	–	1–2	1–2
5	23 F	Asymptomatic	Normal	nod	89	74	NA	2	1	0	1	1	1–2
6	66 F	Dyspnea/cough	Bilat rales	4	50	79	75	1–2	1–2	0	0	1	2

[a] CXR, chest x-ray; FEV1, forced expiratory volume in 1 sec; FVC, forced vital capacity; DLCO, diffusion capacity of the lung for carbon monoxide; NA, not available; TLC, total lung capacity.
[b] Staining as graded by a blinded pathologist: 0 = none; 1 = weak; 2 = strong; – = no lymphocytes present.
[c] Siltzbach Stage/nod: nodular sarcoid.

and *b*). A pattern showing predominant staining of the peripheral lymphocyte rich component of granulomas was a characteristic observation in all patients (Fig. 1*b*). Using serial sections, we demonstrated intense OPN staining of CD3-positive cells (T lymphocytes) (Fig. 1, *e* and *f*). The central core of the granulomas containing macrophages, epithelioid cells, and multinucleated giant cells also exhibited OPN staining; however, this was less than that seen in lymphocytes (Fig. 1*b*). The ECM did not stain for OPN (Fig. 1*a*). No staining was seen with the isotype control Ab (Fig. 1*c*). To determine the specificity of OPN expression in inflammatory lung disease, we stained lung biopsies from four patients with acute respiratory distress syndrome (ARDS), a neutrophil-mediated disease. In contrast to the widespread expression of OPN in sarcoidosis, OPN was seen only in airway epithelium and scattered macrophages in ARDS (Fig. 1*d*). As we have previously reported, this staining of airway epithelium is seen in inflamed but not normal lung (23). In summary, sarcoid granulomas exhibit a characteristic pattern of strong lymphocyte-associated OPN staining.

OPN expression correlates with granuloma maturity in sarcoidosis

OPN expression was determined in granulomas of varying cellularity and maturity (Table I; Fig. 2, *a–f*). The early cellular granulomas (Fig. 2*a*) and intermediate granulomas expressing both cellular and matrix elements (Fig. 2*b*) showed OPN staining (Fig. 2, *d* and *e*) of lymphocytes and histiocytes but not matrix. The late fibrotic granulomas (Fig. 2*c*) exhibited significantly less OPN expression, which was limited to multinucleated giant cells (Fig. 2*f*). This pattern was in contrast to that seen with staining for FN, another matrix protein with immunomodulatory functions that is expressed in sarcoidosis (Table I; Fig. 2, *g–i*) (26, 33). FN was present in cellular and stromal elements within and surrounding granulomas with relative sparing of lymphocyte rich areas (Fig 2, *g–i*). In addition, diffuse matrix-associated staining for FN was seen in all granulomas, irrespective of cellularity and maturity (Table I; Fig. 2, *g–i*). Again, no staining was seen with isotype control (Fig 2, *j–l*). These data demonstrate that OPN expression is more pronounced in the early cellular granulomas of sarcoidosis and that this pattern of expression is distinct from that seen with FN.

OPN induces chemotaxis in T cells

Matrix proteins can modulate lymphocyte function (34). Based on OPN immunoreactivity in T cell areas of granulomas and its known ability to induce migration in monocytes and a murine T cell hybridoma, we postulated that OPN would modulate human T cell migration (12, 13). The ability of OPN to induce T cell chemotaxis was analyzed using a modified Boyden chamber. OPN induced chemotaxis in monocyte-depleted nylon wool nonadherent T cells (NWNTs) at OPN concentrations between 150 ng/ml and 16 μg/ml (2.5–250 nM). The experiment was repeated three times with similar results, and a representative experiment is shown in Fig. 3. In all experiments, peak migration was seen between 2–4 μg/ml (30–60 nM), although in two experiments significant migration was noted at concentrations as low as 150 ng/ml. Although it is possible that this represents chemotaxis mediated by different receptors, it is more likely due to intrinsic variation in the bioassay. The magnitude of chemotaxis seen with OPN (200–300% over migration under control conditions), was similar to that seen in this assay with other lymphocyte chemoattractants such as RANTES and IL-16.

Checkerboard analysis (Table II) was employed to determine whether this migration was chemotactic (gradient dependent) or chemokinetic in nature (random migration induced by chemoattractants in zero gradient, obtained by adding equal amounts of OPN to the upper and lower chambers) (30). By this analysis, the response of T cells to OPN was present solely when a gradient existed (OPN in the bottom well only). Chemokinetic activity was absent, and, in fact, high concentrations of OPN in the upper chamber significantly reduced migration below that seen with control. Identical results were obtained in two separate experiments. Thus, OPN induces chemotactic migration in human T cells.

Activated T cells, but not resting T cells, adhere to OPN-coated surfaces

Coordinated migration and adhesion is essential to the recruitment of T cells to inflammatory sites. Having demonstrated OPN-induced T cell chemotaxis, we tested the ability of OPN to support T cell adhesion using a fluorometric adhesion assay. Although resting T cells did not adhere to immobilized OPN, PMA activation resulted in significant T cell:OPN adhesion. Results from three experiments showed that, at a concentration of 5 μg/ml of OPN, 27 ± 6% (mean ± SD) of PMA-activated T lymphocytes adhered to OPN. This was significantly ($p < 0.05$) greater than lymphocyte adhesion to control wells (mean ± SD, 11 ± 1%) but less than adhesion to FN (mean ± SD, 57 ± 15%). A representative experiment is shown in Fig. 4. The requirement for PMA activation is a recognized phenomenon common to integrin receptors and facilitates adhesion by clustering or altering the affinity of cell surface adhesion molecules (35, 36).

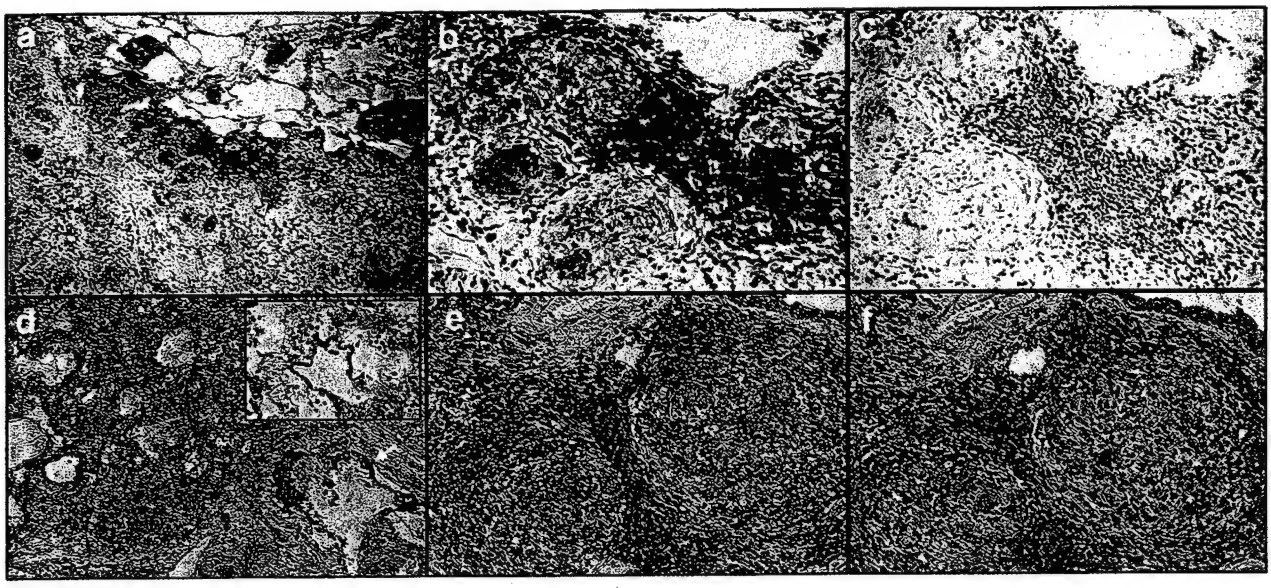

FIGURE 1. Expression of OPN in pulmonary sarcoid granulomas and ARDS. *a* and *b*, OPN staining (brown) of sarcoid granulomas. Magnification (*a*) ×100 (*b*) ×200. *c*, Isotype control. Note strong lymphocyte-associated and weak histiocyte-associated staining for OPN with sparing of matrix. *d*, ARDS stained for OPN. Note OPN stains airway epithelium (arrow) and scattered macrophages. *Inset*, No detectable OPN signal in hyaline membranes or neutrophils. *e* and *f*, Serial sections of sarcoid granuloma stained for OPN (*e*) and CD3 (*f*). Note the strong concordance of detection of OPN with $CD3^+$ T lymphocytes.

Thrombin cleavage enhances T cell adhesion to OPN

In view of the ability of T cells to adhere to OPN, and the known modulatory effect of thrombin cleavage on tumor cell adhesion to OPN, we tested the hypothesis that thrombin-cleaved OPN would support increased T cell adhesion compared with uncleaved OPN. OPN was cleaved by thrombin and immobilized on microtiter plates, and adhesion was compared with uncleaved OPN (Fig. 5). Results from four experiments demonstrated that the cleaved fragments of OPN supported adhesion of a greater percentage of T cells (mean ± SD, 60 ± 15%, $p < 0.05$) than uncleaved OPN (mean ± SD, 35 ± 5%) and a similar percentage to that seen with FN (mean ± SD, 70 ± 20%). T cell adhesion to thrombin-treated rat collagen did not significantly increase. Therefore, OPN is a potent substrate for T cell adhesion, and this adhesion is positively modulated by thrombin cleavage.

Costimulation of CD3-mediated T cell proliferation by OPN

Having demonstrated that OPN is widely expressed in T cells of sarcoidosis, a disease characterized by chronic T cell activation and proliferation, we postulated that OPN would modulate T cell proliferation. Immobilized anti-CD3 mAb ligates the TCR and

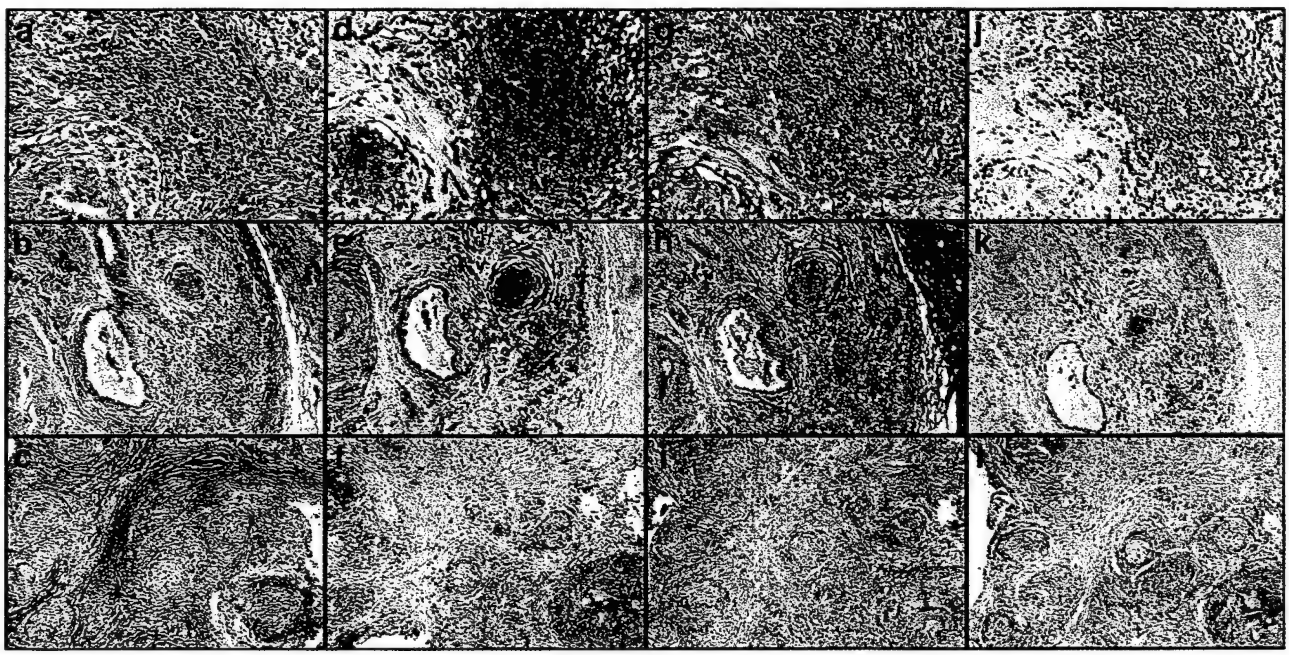

FIGURE 2. Expression of OPN and FN in sarcoid granulomas of varying maturity. *a*, *d*, *g*, and *j*, Early cellular granuloma. *b*, *e*, *h*, and *k*, Intermediate granuloma expressing both cellular and matrix elements. *c*, *f*, *i*, and *l*, Late fibrotic acellular granuloma. Serial sections of these granulomas are stained for hematoxylin and eosin (H&E) (*a–c*), OPN (*d–f*), FN (*g–i*), and isotype control (*j–l*). Note intense lymphocyte immunoreactivity for OPN with sparing of matrix (*d–f*); diffuse immunoreactivity for FN is seen without prominent lymphocyte associated staining (*g–i*); no staining with isotype control (*j–l*).

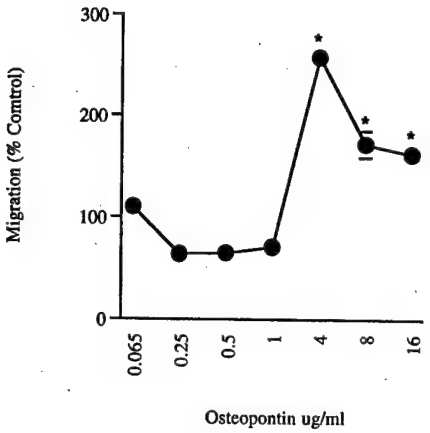

FIGURE 3. OPN induces dose-dependent T cell migration. Using modified Boyden chemotaxis chambers, OPN at various concentrations was added to the lower wells to attract lymphocytes from the upper chambers. Results are expressed as mean percentage (± SEM) of migration seen under control conditions (no OPN in the lower chamber), in which control migration was 15.5 ± 4 (mean ± SD) cells/hpf. Peak migration was seen at an OPN concentration of 4 μg/ml (60 nM). *, $p < 0.05$).

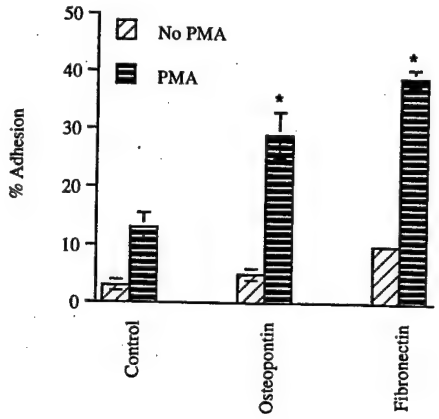

FIGURE 4. T Cell adhesion to OPN. The substrates were BSA 2.5% (control), OPN (5 μg/ml), and FN (10 μg/ml). Monocyte-depleted NWNTs were labeled with Calcein AM and activated with PMA (5ng/ml), and adhesion was measured using a fluorometric adhesion assay. The results are expressed as the mean percentage adhesion ± SD of triplicate wells. PMA activation significantly increased T cell adhesion to OPN and FN. *, $p < 0.05$.

provides a partial, but submaximal, signal for T cell proliferation that is enhanced by an appropriate costimulus. We observed that OPN markedly amplified this CD3-mediated proliferative response in monocyte-depleted NWNTs (Fig. 6). Although high concentrations of anti-CD3 mAb engaged the TCR sufficiently to trigger some T cell proliferation, at lower or suboptimal doses the proliferation was negligible (Fig. 6). At all concentrations of anti-CD3 mAb, the presence of immobilized OPN resulted in significant T cell proliferation (Fig. 6). Despite significant donor variation in the absolute degree of proliferation as measured by [^{3}H]thymidine incorporation, over several experiments the T cell proliferative response in the presence of coimmobilized OPN was two- to sevenfold greater than that seen with anti-CD3 mAb alone ($n = 10$, mean ± SD, 4.5 ± 2.5-fold). Although variability in the magnitude of proliferation between experiments makes it impossible to compare the potency of various costimuli in vitro, OPN-mediated costimulation was similar to the response observed with anti-CD3 mAb combined with either FN or PMA, both known costimulants (Fig. 7) (26, 28).

Since OPN supports monocyte adhesion and chemotaxis, it was possible that OPN directly activated the few remaining monocytes rather than lymphocytes and thereby induced monocyte-dependent T cell proliferation (22). We demonstrated that OPN is a direct costimulant of resting T cell proliferation by vigorously removing all accessory cells using magnetic bead negative depletion. The resultant cells were >95% CD3 positive T cells by FACS and completely depleted of all accessory cells as determined by lack of a proliferative response to PHA. Under these circumstances OPN costimulation resulted in significant amplification of anti-CD3-induced T cell proliferation ([^{3}H]thymidine incorporation three- to ninefold greater with OPN plus anti-CD3 vs anti-CD3 alone, $n = 2$, $p < 0.05$).

Table II. *Checkerboard analysis of the chemoattractant effect of osteopontin on T cells*[a]

OPN Below Filter (ng/ml)	OPN Above Filter (ng/ml)					
	0	6	32	160	800	4000
0	100 ± 16	132 ± 13	128 ± 8	96 ± 1	123 ± 12	64 ± 6*
6	86 ± 27	83 ± 10				
32	120 ± 16		150 ± 27			
160	200 ± 24*			133 ± 12		
800	182 ± 17*				104 ± 10	
4000	293 ± 32*					40 ± 7*

[a] OPN-induced T cell migration was assessed by adding OPN at various concentrations to the lower or upper wells of a modified Boyden chamber. Data are expressed as mean percentage migration (100% is migration under control conditions) ± SEM in which control was 5.8 ± 2.8 (mean ± SD) cells/hpf. OPN induces dose-dependent T cell migration. Two separate experiments produced identical results. *, Significantly different from migration under control conditions ($p < 0.05$).

Discussion

OPN has been considered a matrix protein because of its RGD motif (5). However, it has many other novel properties, relevant to inflammation and the cell-mediated immune response, that suggest that it may behave more as a cytokine in these situations (20, 21,

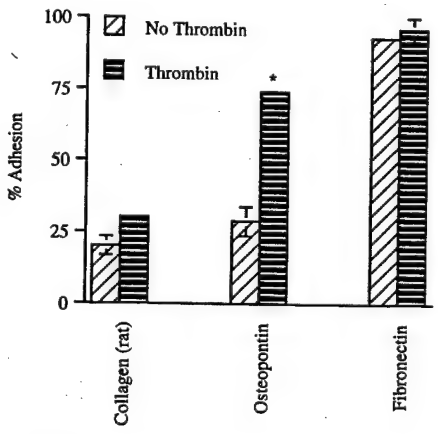

FIGURE 5. Effect of thrombin cleavage on T cell adhesion to OPN. The substrates were rat collagen (5 μg/ml), OPN (5 μg/ml), and FN (10 μg/ml). Each substrate was incubated with thrombin 18 IU/ml for 1 h. Thrombin cleavage significantly augmented the adhesive capacity of OPN in comparison with intact OPN but did not significantly alter that seen with collagen substrate. *, $p < 0.05$.

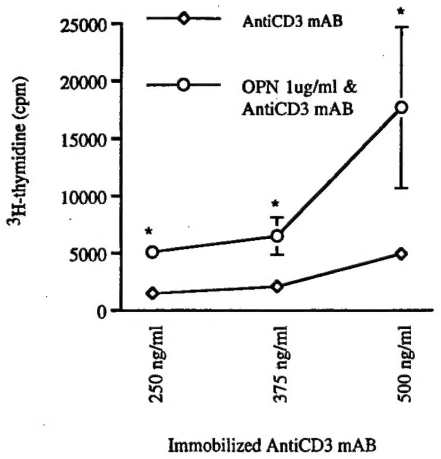

FIGURE 6. T cell costimulation by OPN coimmobilized with anti-CD3 mAb. Anti-CD3 mAb was coimmobilized at various concentrations with OPN (1 μg/ml). Monocyte-depleted NWNT proliferation was measured by [^{3}H]thymidine incorporation. Results are expressed as mean ± SD of triplicate cultures. Anti-CD3 mAb alone induced T cell proliferation, which was minimal at concentrations below 375 ng/ml. OPN significantly costimulated proliferation at all doses of ant-CD3 mAb. *, $p < 0.05$.

23, 37). In this paper, we have demonstrated widespread T cell-associated OPN immunoreactivity in sarcoid granulomas. In addition we have characterized its modulatory effects on T cell function in vitro relevant to T cell accumulation and activation in sarcoidosis.

In sarcoidosis the initial granulomatous response involves the coordinated recruitment and focused adhesion of both macrophages and activated T cells (38). Later, possibly as the Ag inducing the response is cleared or contained, granulomas become acellular and fibrotic. The coordinated expression, both in time and space, of different components of the ECM may influence and regulate this response. In this regard, we identified OPN predominantly in the T cell-rich areas of sarcoid granulomas and noted that its expression was limited or absent in acellular fibrotic granulomas. Since both macrophages and activated T cells can produce OPN, it is unclear whether this lymphocyte-associated staining represents T cell adhesion to macrophage-derived OPN or de novo expression of OPN by T lymphocytes (20, 21). These findings suggest that OPN may interact with and modulate the function of T cells in sarcoidosis. Furthermore, the more pronounced expression of OPN in active cellular granulomas supports a potential role for OPN early in granuloma formation.

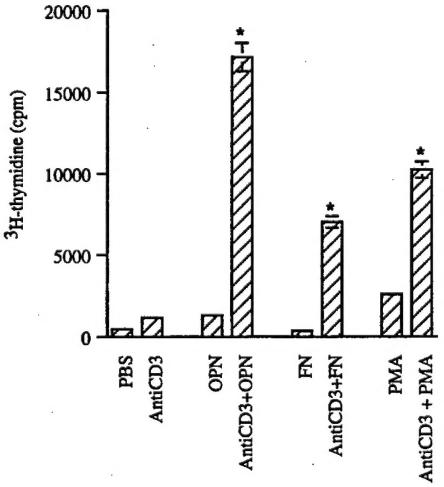

FIGURE 7. The T cell costimulatory signal delivered by OPN is comparable to that of FN or phorbol ester. The proliferation experiment was performed as described. Concentrations of reagents were: Anti-CD3 mAb (anti-CD3) 500 ng/ml (100 μl/well), OPN 1 μg/ml (100 μl/well), FN 10 μg/ml (100 μl/well), and PMA 1 ng/ml of cells. Proliferation of monocyte-depleted NWNTs was measured and expressed as the arithmetic mean ± SD of triplicate cultures. Results show significant proliferation in response to OPN coimmobilized with anti-CD3 mAb but not to either stimulus alone. Anti-CD3 immobilized with FN or in the presence of PMA also resulted in significant proliferation. *, $p < 0.05$.

The expression of OPN in granulomas differed from that of FN, another matrix protein known to support T cell adhesion and proliferation (26). In contrast to the cell-associated expression of OPN, FN was predominantly associated with the ECM. Furthermore, unlike OPN, FN was found in the matrix of both highly cellular inflammatory granulomas as well as acellular fibrotic granulomas. This dissociation of FN and OPN expression suggests that OPN may function differently from FN in the granulomatous response.

Our immunohistochemical findings differ from those of Carlson et al., who found OPN immunoreactivity restricted to histiocytes in granulomas of diverse etiology (24). Using Carlson's Ab, a mAb against human OPN, we found a similar result in granulomas of sarcoidosis. However, strong lymphocyte-associated OPN immunoreactivity, in a pattern identical to that of MPBIII10 mAb, was detected with a second Ab directed against an epitope adjacent to the thrombin cleavage site on human OPN (not shown). Whether this disparity is due to differences in Ab affinity or expression of variant epitopes or forms of OPN is not yet clear. Based on the concordance of our findings using two distinct Abs and the extensive prior use of MPBIII10 mAb for immunohistochemistry in human tissue, our data demonstrate widespread association of OPN with T cells in sarcoidosis (21, 23).

While OPN may be beneficial to the host early in the granulomatous response, persistent OPN expression may contribute to disease morbidity and mortality. OPN, along with other bone matrix proteins, is known to regulate skeletal mineralization (16). In fact, OPN has been reported to exert both positive and negative influences on tissue calcification (19). Dystrophic calcification, the process by which inflamed or damaged tissues become calcified, is thought to be a coordinated cell-mediated response regulated by noncollagenous ECM components (19). It has been shown that, in this response, OPN expression correlates with macrophage and T cell infiltration and subsequent tissue calcification (19). Dystrophic calcification occurs in some chronic granulomatous lung diseases and is associated with significant tissue dysfunction. Although dystrophic calcification is uncommon in sarcoidosis, it is possible that persisting OPN expression may be a determinant of lung tissue mineralization in granulomatous inflammation. An improved understanding of the role of OPN in this response may offer a therapeutic approach to inhibit an aggressive and persistent host granulomatous response that is ultimately detrimental to disease outcome.

We have shown that OPN supports the chemotaxis and adhesion of human T cells. Taken with the known adhesive and chemotactic effects of OPN for monocytes and a murine T cell hybridoma, our data suggest that OPN could act in the recruitment and focused adhesion of T cells and monocytes in early granuloma formation and may promote cell-cell interactions important to T cell activation (13, 14, 22). Our immunohistochemical findings suggest that OPN may be important early in granuloma formation. This is further supported by other studies that show that lack of an early OPN response is associated with host susceptibility to *R. tsutsugamushi* in mice, that macrophages respond to *Mycobacterium tuberculosis*

infection by prominent early production of OPN, and that OPN (or early T lymphocyte activation 1 (eta-1) protein) is a major early protein produced by activated T cells (20, 23, 37).

The adhesion of T cells to OPN is increased by thrombin cleavage of OPN. A number of previous studies evaluating the regulation of OPN activity by thrombin cleavage have reported conflicting results. One report demonstrated that thrombin treatment reduced RGD-mediated adhesion to recombinant human and native bovine OPN (9). Conversely, it has been shown that cleavage of native human OPN augments adhesion to a variety of human cell lines including fibroblasts, smooth muscle cells, and tumor cells (7). In addition, by generating peptides corresponding to the cleaved fragments of OPN, it was shown that the N-terminal fragment, which contains the RGD domain, supports adhesion of a human melanoma cell line that is unable to adhere to the C-terminal fragment or native OPN (8). Our data concur with the latter two studies and support a role for thrombin in the augmentation of T cell adhesion to OPN. These conflicting studies do not represent mutually exclusive results. OPN contains another potential thrombin cleavage site within the RGD domain, and it is possible that different thrombin cleavage conditions or variable access to this thrombin cleavage site could disrupt the RGD sequence and RGD-mediated adhesion (8). Furthermore, since OPN can bind a number of receptors that are differentially expressed on different cells and cell lines, it is possible that some interactions are augmented while others are inhibited by thrombin cleavage, depending on the cell tested. Based on our data, thrombin serves to up-regulate T cell adhesion to OPN in vitro.

The expression of OPN in granulomatous diseases and the role of thrombin in regulating OPN adhesion have interesting implications in the pathogenesis of granuloma formation. There is ample data suggesting that active thrombin and "procoagulant activity" follow granuloma formation. Increased bronchoalveolar lavage procoagulant activity and the presence of circulating D-dimers have been demonstrated in pulmonary sarcoidosis (39, 40). Moreover, Perez reported that mice susceptible to granuloma-inducing Ags from *M. tuberculosis* have increased procoagulant activity while nonsusceptible mice have increased plasminogen activator activity (41). Taken together with our data, this suggests that activation of the T cell-adhesive properties of OPN represents a novel role for thrombin in granuloma formation and that the immunomodulatory effects of the coagulation system may, in part, be delivered through its interaction with OPN. The impact of inhibition of coagulation on granulomatous inflammation is unknown, although heparin treatment has been shown to inhibit delayed-type hypersensitivity reactions (42).

Costimulation of proliferation by OPN is a property shared with other matrix proteins (34). The ability of FN, laminin, and hyaluronic acid to costimulate T cell proliferation through distinct receptors, both RGD-dependent and -independent, suggests that different components of the ECM may have specific immune modulatory effects (26, 43). Chronic T cell activation and proliferation is an essential component of sarcoid granulomatous inflammation (38). The lymphocyte-associated expression of OPN in sarcoidosis and its ability to costimulate T cells suggest another mechanism by which T cell proliferation is augmented within the sarcoid granuloma.

In the sarcoid lung and in models of sarcoid granuloma formation, the earliest pathologic finding is a mononuclear infiltration of T lymphocytes and monocyte-macrophages followed by the formation of distinct granulomas (38). Elaboration of specific granulomagenic factors is thought to coordinate this process (38). While granuloma formation likely reflects a complex interaction of cytokines, cell-cell, and cell-matrix interactions, an ideal granulomagenic factor would be produced in large amounts early in granuloma formation, persist during inflammation, and be cleared when inflammation wanes; and it would support the chemotaxis and subsequent adhesion, activation, and proliferation of recruited inflammatory cells. Our data show that OPN possesses many of the properties of an ideal granuloma-forming matrix. In addition, the known association of genetically determined OPN expression and susceptibility to intracellular infection in mice suggests that different alleles of the OPN gene may determine genetic susceptibility and pathogenesis of granulomatous immune responses, including sarcoidosis. Finally, the link between the coagulation cascade and OPN activity suggests a novel therapeutic approach to sarcoidosis using anticoagulant inhibitors of thrombin generation and activation.

Acknowledgments

We thank Dr. Donald Senger, Beth Israel Hospital, Boston, MA for generously donating the OP174 and OP148 Abs used in the above experiments and for his frequent helpful advice, and Dr. David Center and Dr. Hardy Kornfeld for their thoughtful review of the manuscript.

References

1. Newman, L. S., C. S. Rose, and L. A. Maier. 1997. Sarcoidosis. *N. Engl. J. Med. 336:1224.*
2. Coultas, D. B., H. Gong, R. Grad, A. Handler, S. McCurdy, S. Player, E. R. Rhoades, J. M. Samet, A. Thomas, and M. Westley. 1994. Respiratory diease in minorities of the United States. *Am. J. Respir. Crit. Care Med. 149:S93.*
3. Rybicki, B. A., M. J. Maliarik, M. Major, J. Popovich, and M. C. Iannuzzi. 1997. Genetics of sarcoidosis. *Clin. Chest Med. 18:707.*
4. Brown, L. F., B. Berse, L. Van de Water, S. A. Papadopoulos, C. A. Perruzzi, E. J. Manseau, H. F. Dvorak, and D. R. Senger. 1992. Expression and distribution of osteopontin in human tissues: widespread association with luminal epithelial surfaces. *Mol. Biol. Cell 3:1169.*
5. Oldberg, A., A. Franzen, and D. Heinegard. 1986. Cloning and sequence analysis of rat bone sialoprotein (osteopontin) cDNA reveals an Arg-Gly-Asp cell-binding sequence. *Proc. Natl. Acad. Sci. USA 83:8819.*
6. Senger, D. R., and C. A. Perruzzi. 1985. Secreted phosphoprotein markers for neoplastic transformation of human epithelial and fibroblastic cells. *Cancer Res. 45:5818.*
7. Senger, D. R., C. A. Perruzzi, S. A. Papadopoulos, and L. Van de Water. 1994. Adhesive properties of osteopontin: regulation by a naturally occurring thrombin-cleavage in close proximity to the GRGDS cell-binding domain. *Mol. Biol. Cell 5:565.*
8. Smith, L. L., H. K. Cheung, L. E. Ling, J. Chen, D. Sheppard, R. Pytela, and C. M. Giachelli. 1996. Osteopontin N-terminal domain contains a cryptic adhesive sequence recognized by $\alpha_9\beta_1$ integrin. *J. Biol. Chem. 271:28485.*
9. Xuan, J.W., C. Hota, and A.F. Chambers. 1994. Recombinant GST-human osteopontin fusion protein is functional in RGD-dependent cell adhesion. *J. Cell. Biochem. 54:247.*
10. Reinholt, F. P., K. Hultenby, A. Oldberg, and D. Heinengard. 1990. Osteopontin: a possible anchor of osteoclasts to bone. *Proc. Natl. Acad. Sci. USA 87:4473.*
11. Somerman, M. J., C. W. Prince, W. T. Butler, R. A. Foster, J. M. Moehring, and J. J. Sauk. 1989. Cell attachment activity of the 44-kilodalton bone phosphoprotein is not restricted to bone cells. *Matrix 9:49.*
12. Liaw, L., M. Almeida, C. E. Hart, S. M. Schwartz, and C. M. Giachelli. 1994. Osteopontin promotes vascular cell adhesion and spreading and is chemotactic for smooth muscle cells in vitro. *Circ. Res. 74:214.*
13. Yamamoto, S., K. Nasu, T. Ishida, M. Setoguchi, Y. Higuchi, N. Hijiya, and S. Akizuki. 1995. Effect of recombinant osteopontin on adhesion and migration of P388D1 cells. *Ann. NY Acad. Sci. 760:378.*
14. Weber, G. F., S. Ashkar, M. J. Glimcher, and H. Cantor. 1996. Receptor-ligand interaction between CD44 and osteopontin (Eta-1). *Science 271:509.*
15. Bennett, J. S., C. Chan, G. Vilaire, S. A. Mousa, and W. F. DeGrado. 1997. Agonist-activated $\alpha_v\beta_3$ on platelets and lymphocytes binds to the matrix protein osteopontin. *J. Biol. Chem. 272:8137.*
16. Ross, F. P., J. Chappel, J. I. Alverez, D. Sander, W. T. Butler, M. C. Farach-Carson, K. A. Mintz, P. G. Robey, S. L. Teitelbaum, and D. A. Cheresh. 1993. Interactions between the bone matrix proteins osteopontin and bone sialoprotein and the osteoclast integrin $\alpha_v\beta_3$ potentiate bone resorption. *J. Biol. Chem. 268:9901.*
17. Giachelli, C. M., L. Liaw, C. E. Murry, S. M. Schwartz, and M. Almeida. 1995. Osteopontin expression in cardiovascular diseases. *Ann. NY Acad. Sci. 760:109.*
18. Senger, D. R., B. B. Asch, B. D. Smith, C. A. Perruzzi, and H. F. Dvorak. 1983. A secreted phosphoprotein marker for neoplastic transformation of both epithelial and fibroblastic cells. *Nature 302:714.*
19. Srivatsa, S. S., P. J. Harrity, P. B. Maercklein, L. Kleppe, J. Veinot, W. D. Edwards, C. M. Johnson, and L. A. Fitzpatrick. 1997. Increased cellular

expression of matrix proteins that regulate mineralization is associated with calcification of native human and porcine xenograft bioprosthetic heart valves. *J. Clin. Invest. 99:996.*

20. Patarca, R., R. A. Saavedra, and H. Cantor. 1993. Molecular and cellular basis of genetic resistance to bacterial infection: the role of the early T-lymphocyte activation-1/osteopontin gene. *Crit. Rev. Immunol. 13:225.*
21. Murry, C. E., C. M. Giachelli, S. M. Schwartz, and R. Vracko. 1994. Macrophages express osteopontin during repair of myocardial necrosis. *Am. J. Pathol. 145:1450.*
22. Singh, R. P., R. Patarca, J. Schwartz, and H. Cantor. 1990. Definition of the specific interaction between the early T lymphocyte activation 1 (Eta-1) protein and the murine macrophages in vitro and its effect upon macrophages in vivo. *J. Exp. Med. 171:1931.*
23. Nau, G. J., P. Guilfoile, G. L. Chupp, J. S. Berman, S. J. Kim, H. Kornfeld, and R. A. Young. 1997. A chemoattractant cytokine associated with granulomas in tuberculosis and silicosis. *Proc. Natl. Acad. Sci. USA 94:6414.*
24. Carlson, I., K. Tognazzi, E. J. Manseau, H. F. Dvorak, and L. F. Brown. 1997. Osteopontin is strongly expressed by histiocytes in granulomas of diverse etiology. *Lab. Invest. 77:103.*
25. Kanof, M. E., and P. D. Smith. 1991. Preparation of the human mononuclear cell populations and subpopulations. In *Current Protocols in Immunology*, Vol. 2. J. E. Coligan, A. M. Kruisbeek, D. H. Marguiles, E. M. Shevach, and W. Strober, eds. John Wiley and Sons, New York, p. 7.1.1.
26. Shimizu, Y., G. A. van Seventer, K. J. Horgan, and S. Shaw. 1990. Costimulation of proliferative responses of resting $CD4^+$ T cells by the interaction of VLA-4 and VLA-5 with fibronectin or VLA-6 with laminin. *J. Immunol. 145:59.*
27. Horgan, K. J., and S. Shaw. 1989. Immuno-magnetic negative selection of lymphocyte subsets. In *Current Protocols in Immunology*, Vol. 2. J. E. Coligan, A. M. Kruisbeek, D. H. Margulies, E. M. Shevach, and W. Strober, eds. 7.4.1.
28. Davis, L., and P. E. Lipsky. 1986. Signals involved in T cell activation. *J. Immunol. 136:3588.*
29. Senger, D. R., C. A. Perruzzi, A. Papadopoulos, and D. G. Tenen. 1989. Purification of a human milk protein closely similar to tumor-secreted phosphoproteins and osteopontin. *J. Biol. Chem. 262:9702.*
30. Berman, J. S., and D. M. Center. 1987. Chemotactic activity of porcine insulin for human T lymphocytes in vitro. *J. Immunol. 138:2100.*
31. Pai, J., R. W. Bond, and J. A. Pachter. 1992. Approaches for the discovery of cell adhesion antagonists: characterization of adhesion to fibronectin and ELAM-1. *J. Biochem. Res. 2:53.*
32. Mobley, J. L., and Y. Shimizu. 1991. Measurement of cellular adhesion under static conditions. In *Current Protocols in Immunology*, Vol. 2. J. E. Coligan, A. M. Kruisbeek, D. H. Marguiles, E. M. Shevach, and W. Strober, eds. John Wiley and Sons, New York, p. 7.28.1.
33. Roman, J., J. Young-June, A. Gal, and R. L. Perez. 1995. Distribution of extracellular matrices, matrix receptors, and transforming growth factor-β1 in human and experimental lung granulomatous inflammation. *Am. J. Med. Sci. 309:124.*
34. Shimizu, Y., and S. Shaw. 1991. Lymphocyte interactions with the extracellular matrix. *FASEB J. 5:2292.*
35. Seki, J., N. Koyama, N. L. Kovach, T. Yednock, A. W. Clowes, and J. M. Harlan. 1996. Regulation of β_1-integrin function in cultured human vascular smooth muscle cells. *Circ. Res. 78:596.*
36. Stewart, M. P., C. Cabanas, and N. Hogg. 1996. T cell adhesion to intercellular adhesion molecule-1 (ICAM-1) is controlled by cell spreading and the activation of integrin LFA-1. *J. Immunol. 156:1810.*
37. Weber, G. F., and H. Cantor. 1996. The immunology of ETA-1/osteopontin. *Cytokine Growth Factor Rev. 7:241.*
38. Kataria, Y. P., and J. F. Holter. 1997. Immunology of sarcoidosis. *Clin. Chest Med. 18:719.*
39. Hasday, J. D., P. R. Bachwich, J. D. Lynch, and R. G. Sitrin. 1988. Procoagulant and plasminogen activator activities of bronchoalveolar fluid in patients with pulmonary sarcoidosis. *Exp. Lung Res. 14:261.*
40. Perez, R. L., A. Duncan, R. L. Hunter, and G. J. Staton. 1993. Elevated D dimer in the lungs and blood of patients with sarcoidosis. *Chest 103:1100.*
41. Perez, R. L., J. Roman, G. J. Staton, and R. L. Hunter. 1994. Extravascular coagulation and fibrinolysis in murine lung inflammation induced by the mycobacterial cord factor trehalose-6,6′-dimycolate. *Am. J. Respir. Crit. Care Med. 149:510.*
42. Cohen, S., B. Benacerraf, R. T. McCluskey, and Z. Ovary. 1967. Effect of anticoagulants on delayed hypersensitivity reactions. *J. Immunol. 98:351.*
43. Galandrini, R., E. Galluzzo, N. Albi, C. E. Grossi, and A. Velardi. 1994. Hyaluronate is costimulatory for human T cell effector functions and binds to CD44 on activated T cells. *J. Immunol. 153:21.*

Experimental interstitial pneumonia mediated by CD8$^+$ cytotoxic T cells does not require perforin or Fas: Importance of TNF-α expressed by T cells

Ashraf Z. Mohammed*, Dana Fiedeldey¶, Ward R. Rice¶, and Richard I. Enelow†
†University of Virginia School of Medicine, Charlottesville, VA, USA; *Assiut University, Egypt; and ¶Children's Hospital Medical Center, Cincinnati, OH, USA.

CD8$^+$ T cells appear to play an important role in many inflammatory lung diseases. The primary function of this T cell subset is cytolysis of virus-infected cells, and there are two accepted mechanisms by which this occurs: the perforin/granzyme-mediated pathway of cytolysis and the Fas ligand-Fas pathway of induction of target cell apoptosis. This is based primarily upon data obtained using hematopoetic cell lines as targets. We have used a transgenic murine model of T cell-mediated interstitial pneumonia, and a novel in vitro assay, to directly assess the mechanisms involved in alveolar injury caused by cytotoxic CD8$^+$ T cells. We show that FasL-induced Fas-mediated apoptosis does not directly contribute to T cell mediated alveolar cell injury, though Fas is expressed and functional on alveolar epithelial cells. We have also demonstrated that the perforin-independent cytolytic activity of CD8$^+$ T cells on alveolar epithelial cells is accounted for exclusively and entirely by tumor necrosis factor-alpha (TNF-α) which is expressed on T cells. Furthermore, lung injury mediated by cytolytic CD8$^+$ T cells in vivo does not require perforin or Fas, but is dependent upon TNF-α expression on the T cells, and TNF receptor expression on the alveolar epithelial cell. These results suggest that alveolar epithelial cells are unusually sensitive to T cell-triggered TNF-α-mediated apoptosis, and resistant to FasL-induced apoptosis. We further propose that, in the absence of virus infection, perforin-mediated cytolysis does not contribute significantly to alveolar injury by T cells. These results may have important ramifications in the pathophysiology of interstitial lung disease.

This abstract is funded by: NIH/NHLBI; ALA-Virginia

ALLOREACTIVE CLONED TH1 CELLS THAT INDUCE LUNG INJURY LOCALIZE IN LUNG BY A MECHANISM INVOLVING LFA-1.

A.E.Dixon, J.B.Mandac, P.J.Martin, D.K.Madtes, R.K.Hackman & J.G.Clark. Fred Hutchinson Cancer Research Center & University of Washington, Seattle, WA.

Acute lung injury is a common complication of bone marrow transplantation. Graft versus host disease (GVHD) is a major risk factor for this form of lung injury. Th1 cells have been implicated in the generation of GVHD. We previously described a mouse model of acute lung injury induced by Th1 cell clones (JI, 161: 1913, 1998). These clones recognize one of the two forms of Ly5 (CD45), Ly5a or Ly5b, expressed on murine hematopoetic cells. Injection of alloreactive cells produces lung injury, no other major organs are injured. To investigate mechanisms that result in selective injury to lung, we studied the in vivo distribution of T cells after i.v. injection. ^{51}Cr labeled anti-Ly5a cells were administered by tail vein injection into Ly5a and Ly5b animals. After 1 hour greater than 85% of radioactivity was detected in lung, and the level of radioactivity in lung was approximately 18 fold higher than any other organ. At 24 hours, 40% of radioactivity was still localized in lung. Lung injury was observed in Ly5a, but not Ly5b mice, indicating that localization of Th1 cells is not sufficient to induce lung injury. We then studied the role of adhesion molecules by co-administering ^{51}Cr labeled cells with neutralizing antibody to LFA-1 (Fab fragment of MK17/4). Radioactivity in lung was reduced by approximately 50% at 24 hours compared with isotype control. Animals deficient in ICAM-1 (PNAS, 90: 8529, 1993) also had reduced localization of T cells at 24 hours. These studies suggest that lung localization of these T cells is partially dependent on the interaction between LFA-1 and ICAM-1. Further studies are required to delineate the interaction between T cell localization and the development of lung injury.

This abstract is funded by: HL55200

ESSENTIAL ROLES OF THE FAS-FAS LIGAND PATHWAY IN THE DEVELOPMENT OF PULMONARY FIBROSIS.

N.Hagimoto[1], K. Kuwano[1], M. Kawasaki[1], T. Yatomi[2], N. Nakamura[2], S. Nagata[3], R. Kunitake[1], T. Maeyama[1], H. Miyazaki[1], N. Hara[1]
[1]Research Institute for Diseases of the Chest, Faculty of Medicine, Kyushu University, Fukuoka [2]Biosciences Research Laboratory, Mochida Pharmaceutical Co., Tokyo [3]Department of Genetics, Osaka University Medical School, Osaka, JAPAN

Fas ligand (FasL) is predominantly expressed in activated T cells and one of the major effector molecules of cytotoxic T lymphocytes, which can transduce apoptotic signals to Fas bearing cells. We previously demonstrated that the excessive apoptosis of lung epithelial cells and the overexpression of FasL mRNA in infiltrating lymphocytes in bleomycin-induced pulmonary fibrosis in mice. To investigate the roles of Fas-FasL pathway in bleomycin-induced pulmonary fibrosis, we first investigated whether Fas (*lpr*) or FasL-deficient (*gld*) mice are resistant to development of this model. Compared with wild-type mice, *gld*-and *lpr*-mice were relatively resistant. Secondary, administration of hFas-Fc prevented epithelial cells apoptosis and pulmonary fibrosis in this model. These results indicate that Fas-FasL pathway has essential roles in the development of pulmonary fibrosis, and that preventing this pathway would have therapeutic value in lung injury and fibrosis.

This abstract is funded by:

OSTEOPONTIN, A NOVEL EARLY T CELL ASSOCIATED CYTOKINE IN GRANULOMATOUS DISEASE, AUGMENTS A TH1 CYTOKINE RESPONSE

A.W. O'Regan, E.A. Wright, J.S. Berman. The Pulmonary Center, Boston University School of Medicine, Boston, MA, USA.

IL12 and Interferon (IFN)γ production are central to Th1 granulomatous responses like sarcoidosis and tuberculosis. Osteopontin (OPN) is an RGD containing cytokine expressed by macrophages and T cells, and is associated with early host responses to mycobacteria. We have previously shown that OPN is associated with T cells in the granulomas of tuberculosis and sarcoidosis, and can function as a pro-inflammatory T cell cytokine/chemokine in vitro. In view of these data, we hypothesized that OPN would support a Th1 cytokine response. **Methods**: Human nylon wool non-adherent T cells were stimulated with anti-CD3 mAb with and without co-immobilized human OPN (1ug/ml). IFNγ and IL12 were measured in the supernatants and by intracellular FACS analysis at 24 and 48 hours. **Results**: By ELISA, the production of IFNγ by T cells was 1.7 fold greater in the presence of OPN co-immobilized with anti-CD3 mAb as compared to anti-CD3 mAb alone (n=7, 1.7+/-0.6 fold increase, $p<0.05$). OPN alone did not induce IFNγ. By FACS analysis, OPN with anti-CD3 mAb induced 15% of CD3+ T cells to produce IFNγ, as compared to 5% of T cells stimulated with anti-CD3 alone. IL12 production was similarly augmented by stimulation with OPN (n=7, 1.9+/-0.6 fold increase, $p<0.05$). OPN augmentation of both IFNγ and IL12 was RGD dependent. OPN co-stimulation did not increase IL4 production. **Conclusions:** OPN augments early Th1 cytokine production in vitro via an RGD dependent interaction. As OPN is associated with early events in granulomatous disease and intracellular infection, our data suggest that OPN dependent IL12 and IFNγ production represents an early cytokine pathway modulating Th1 granulomatous diseases.

This abstract is funded by: ALA Fellowship Award / Scor PSO HL56386

PULMONARY ALVEOLAR ADHERENT CELLS REGULATE T CELL RESPONSES IN THE LUNG

J. Zhang-Hoover and Joan Stein-Streilein. Schepens Eye Research Institute and Pulmonary and Critical Care Division, Dept. of Medicine, Brigham and Women's Hospital, Harvard Medical School, Boston, MA 02114, USA

The hapten immune pulmonary interstitial fibrosis (HIPIF) is induced by priming mice for contact hypersensitivity response to hapten (2,4,6-Trinitrobenzenesulfonic acid, TNBS) followed by a single intratrachael challenge (IT) with the hapten. IT challenged-only mice do not develop fibrosis and heal the pulmonary lesion induced by the hapten exposure. Mice that are only challenged (IT) with TNBS downregulate MHC II and B7.2 on bronchoalveolar lavage (BAL) adherent cells compared to cells from naive mice. However, sensitized mice that are IT challenged express MHC II and upregulate MAC-1 and B7.1 on BAL adherent cells compared to challenged-only mice. Cells from sensitized and challenged mice also, uniquely, express more intracellular TNFα (flow cytometric analysis). Moreover, BAL adherent cells from challenged-only mice suppress T cell proliferation, while BAL adherent cells from sensitized and challenged mice promote both mitogen (Concanavalin A) and antigen (TNP) specific T cell proliferation *in vitro*. These results show that prior sensitization releases the BAL adherent cells from their immunosuppressive mode to support T cell activation and chronic inflammation leading to fibrosis. The phenotype of the alveolar adherent cells and cytokine profile determine whether T cell responses occur in the lung.

This abstract is funded by: